

**ROAD ENVIRONMENT  
AND  
TRAFFIC CRASHES**

**Transfund New Zealand Research Report No. 79**



# **ROAD ENVIRONMENT AND TRAFFIC CRASHES**

**P.D. CENEK, R.B. DAVIES, M.W. MCLARIN,  
G. GRIFFITH-JONES & N.J. LOCKE**  
Opus Central Laboratories,  
Lower Hutt

**Transfund New Zealand Research Report No. 79**

ISBN 0-478-10537-1

ISSN 1174-0574

- © 1997, Transfund New Zealand  
P O Box 2331, Lambton Quay, Wellington New Zealand  
Telephone (04) 473-0220; Facsimile (04) 499-0733

P.D. Cenek, R.B. Davies, M.W. McLarin, G Griffith-Jones, N.J. Locke 1997. Road environment and traffic crashes. *Transfund New Zealand Research Report No. 79*. 132 pp.

**Keywords:** crash risk, geometry, highway, models, RAMM, RGDAS, road, TAR

## AN IMPORTANT NOTE FOR THE READER

The research detailed in this report was commissioned by Transit New Zealand when it had responsibility for funding roading in New Zealand. This is now the responsibility of Transfund New Zealand.

While this report is believed to be correct at the time of publication, neither Transit New Zealand or Transfund New Zealand, their employees and agents involved in preparation and publication accept any contractual, tortious or other liability for its content or for any consequences arising from its use and make no warranties or representations of any kind whatsoever in relation to any of its contents.

The report is only made available on the basis that all users of it, whether direct or indirect, must take appropriate legal or other expert advice in relation to their own circumstances and must rely solely on their own judgement and seek their own legal or other expert advice.

*The material contained in this report is the output of research and should not be construed in any way as policy adopted by Transit New Zealand nor Transfund New Zealand but may form the basis of future policy.*



## CONTENTS

<b>EXECUTIVE SUMMARY</b>	9
<b>ABSTRACT</b>	13
<b>1. INTRODUCTION</b>	13
<b>2. THE ARRB ROAD GEOMETRY INSTRUMENTED VEHICLE</b>	15
<b>3. PREPARATION OF DATABASE</b>	16
3.1 RGDAS Data	16
3.1.1 Rubberbanding	16
3.1.2 Segmenting	16
3.1.3 Advisory Speeds	17
3.2 RAMM Data	18
3.3 TAR Data	18
3.4 Data Integrity	19
<b>4. VALIDATION OF RGDAS ROAD GEOMETRY DATA</b>	21
4.1 Distance Measurement	22
4.2 Horizontal Curvature	23
4.3 Superelevation	24
4.4 Gradient	27
4.5 Vertical Curvature	29
4.6 Mapping Ability	32
4.7 Transit New Zealand's Pulsar	34
4.8 Summary	36
<b>5. STATISTICAL ANALYSIS</b>	37
5.1 The Tables	38
5.1.1 One Way Tables	38
5.1.2 Two Way Tables	40
5.2 Poisson Regression Analysis	41
5.3 Additional Analyses	44
<b>6. DISCUSSION OF RESULTS</b>	45
6.1 Comparison with a Previous New Zealand Study of Crash Curve Geometry Relationships	45
6.2 Effects of Prior Highway Geometry	46
6.3 Curve Severity	46
6.4 Gradient	47
6.5 Direction of Travel	47
6.6 AADT	47
6.7 Sealed Carriageway Width	48

<b>7.</b>	<b>EFFECT OF SHAPE CORRECTION ON CRASH RISK</b>	<b>48</b>
7.1	Statistical Study of Crash Sites	49
7.1.1	Statistical Analysis	50
7.1.2	Results	50
7.1.3	Discussion	50
7.2	Road Curvature and Superelevation	51
7.2.1	State Highway 58	52
<b>8.</b>	<b>CONCLUSIONS</b>	<b>59</b>
8.1	Measurement of Highway Geometry	59
8.2	Accuracy of RGDAS Data	59
8.3	Poisson Generalised Linear Model	59
8.4	Shape Correction and Crash Risk	60
8.5	Prediction of Mid-Curve Speeds	60
8.6	Road Design Guide	61
<b>9.</b>	<b>REFERENCES</b>	<b>62</b>
<b>APPENDIX 1</b>	<b>DATABASE FIELDS</b>	<b>63</b>
<b>APPENDIX 2</b>	<b>STATISTICAL CRASH RISK ANALYSIS</b>	<b>67</b>



## EXECUTIVE SUMMARY

The economic assessment of geometric improvements to roads relies on being able to predict crash risk before and after modification. It is thought that the subjective nature of the methods used for crash risk estimation in the past may have had significant impact on how road maintenance decisions have been made. This study seeks to establish, through statistical analysis, the contribution of key geometric variables to the relative crash risk.

### **Measurement of Highway Geometry**

In 1992 a road geometry survey of the New Zealand highway system was carried out using the Australian Road Research Board's Road Geometry Data Acquisition System (RGDAS). This survey covered virtually all sealed highways in New Zealand, some 22 000 km, and provided information on the vertical and horizontal curvature, superelevation and gradient. A combined database was constructed using this data together with information from the Transit New Zealand Road Asset Maintenance Management (RAMM) database and the Land Transport Safety Authority (LTSA) Traffic Accident Report (TAR) system, to enable investigation of the relationship between highway geometry and crash risk.

### **Accuracy of RGDAS Data**

The integrity and accuracy of the RGDAS data was investigated. The RGDAS road survey vehicle provided a useful measure of superelevation, gradient and radius of curvature. However, the moving average over 56 m applied to data compromises accuracy particularly for short arc length, small radius bends. In addition, distance measurements by the RGDAS often showed errors of the order of hundreds of metres with respect to Transit New Zealand's reference stations. Hence in order to extract data for a particular feature (e.g. curve) a labour-intensive manual feature-matching process had to be used, as opposed to directly indexing the database by distance.

### **Recommendation**

The main limitation of the RGDAS was the inaccuracy of distance measurement, which made extraction of data for a particular geographical point inefficient. The addition of differential Global Positioning System (GPS) data to future surveys would remove the 'dead reckoning' component inherent in the coordinate data, providing an accurate mapping function and solving the problem of position location within the road geometry data files.

### **Poisson Generalised Linear Model**

Because road crashes are comparatively isolated events in New Zealand, a relatively new statistical technique called Poission regression analysis was applied to a specially constructed database comprising 200 m road segments of New Zealand's sealed state highway network classified as rural, two lane, not divided. This statistical technique enables the risk of a crash occurring to be related to explanatory variables. Emphasis was placed on crashes where road geometry factors were identified as the primary contributory cause as opposed to human and vehicle factors. Crashes that occurred at intersections or where alcohol or drugs were suspected to be the primary causal factor were also excluded. As a result, the analysis was confined to a subset (approximately 15%) of all reported injury crashes on the state highway network.

The model developed by performing a Poisson regression analysis on the RGDAS, RAMM and TAR data goes some way toward providing a rational quantitative method for evaluating, and hence reducing, the crash risk associated with various geometric elements of highway design. The model gives the relative crash risk for changes in the road geometry and environment parameters. The model allows formal significance tests to be carried out.

As in past studies, turn severity was found to be the major factor of road geometry affecting crash rates. More severe turns resulted in greater crash rates. A secondary effect was direction of turn, with left turns being riskier than right turns. Low values of calculated advisory speed (indicative of severe turns) in the 400 m prior to a severe turn was found to reduce the crash rate on such a turn. A reverse interaction was found, where severe turns prior to a straight increased the risk of a crash on the straight section.

The gradient of the highway was found to be significant, with increasing absolute values giving an increase in crash rate. A secondary effect showed ascending grades to be safer than descending grades.

The consistency of the main effects found, when compared with those reported independently by Matthews and Barnes (1988), encouraged confidence in the findings. However, there were some peculiar effects seen in the data, such as the significance of direction of travel (northwest-southeast) to crash rate.

### **Recommendation**

Further validation and expansion to include other road features not yet investigated is suggested. Examples of such features which may yield useful results are the forward sight distance, clear formation width and the roadside hazard rating.

### **Shape Correction and Crash Risk**

The quality of shape correction work could not be gauged by crash rates as there was insufficient numbers of crashes for any degree of statistical significance. Whilst no definite conclusions could be reached, crash rates appeared to reduce after shape correction. However, as both traffic characteristics and crash reporting systems change with time, and roadmarkings and signage may well change after shape correction, it is very hard to reach any definitive conclusions.

### **Prediction of Mid-Curve Speeds**

The relationship between road geometry and vehicle speed was investigated by comparing the RGDAS calculated advisory speed with the 85th percentile mid-curve vehicle speeds measured at a selection of curves. A clear linear relationship was found between the calculated and measured cornering speeds. This indicates that the RGDAS calculated advisory speed may provide a useful alternative, or addition, to the traditional ball-bank indicator in selecting the signposted advisory speeds for curves. A further use may be to search the database to find curves that have no advisory speed posted yet have low RGDAS calculated advisory speed.

### **Road Design Assessment**

In New Zealand many roads pass over "difficult terrain". These roads have tended to "evolve" and consequently vary considerably in alignment standard. The Project Evaluation Manual (PEM) which is used for roading improvements considers typical crash rates for roads classified into just three categories - flat, rolling and mountainous. The Poisson generalised linear model developed in this study, relating crash risk to a number of road geometry variables, provided a vast improvement to the economic cost/benefit analysis of a proposed road modification. Crash risk and therefore economic cost can now be estimated for existing and proposed road designs, hence providing a valuable tool for road design engineers.

### **Recommendations**

1. Consideration should be given to revising the way the PEM quantifies crash risk as the contribution to overall relative risk from each road environment variable, such as bendiness (curvature), superelevation, gradient, and vertical curvature, can now be estimated. This would represent a major improvement over the previously used three category classification system which classified all rural highway environments simply as flat, rolling or mountainous.
2. More accurate recording of crash location (possibly using GPS) and an integrated database linking road geometry, surface characteristics, road condition, traffic data and the TAR database, would be of

considerable help for future studies aimed at refining the statistical crash risk models and reducing traffic crashes.

3. The generalised description of terrain and the crash risk relationships developed in this research should be refined to allow the impact of adopting different design standards to be identified and an economically appropriate improvement strategy to be developed.

## ABSTRACT

This report presents a road geometry survey of the New Zealand highway system and the subsequent use of the data to model the relationship between highway features and relative crash risk. The Australian Road Research Board's RGDAS (Road Geometry Data Acquisition System) survey vehicle was used in 1992, to survey the geometry of all of New Zealand's highways (excluding unsealed sections) totalling some 22 000 km. A database was constructed containing the survey data. This data was used together with data from Transit New Zealand's Road Asset Maintenance Management (RAMM) database and the Land Transport Safety Authority's Traffic Accident Report (TAR) database to develop a statistical model relating relative crash risk to road geometry. An attempt was made to investigate the effect of shape correction operations upon crash risk, although results were inconclusive due to the small number of crashes.

### 1. INTRODUCTION

Because of the manner in which New Zealand's roading system has evolved, not all road sections are of the same geometric design standard. An instrumented road survey vehicle developed by the Australian Road Research Board, named RGDAS (Road Geometry Data Acquisition System), was therefore brought to New Zealand to investigate relationships between road geometry and motor vehicle crashes occurring on sealed two-lane rural highways. Emphasis was placed on crashes where road geometry factors were identified as the primary contributory cause, as opposed to human and vehicle factors. Crashes that occurred at intersections or where alcohol or drugs were suspected to be the primary causal factor were also excluded. As a result, the research was confined to a subset (approximately 15%) of all reported injury crashes on the state highway network.

The primary objective of the work reported herein was to develop a crash prediction model which describes the relationship between rural road geometry and crashes. Such a model would allow a quantitative determination of the relative risk of a section of road, for example before and after realignment, providing a powerful tool to help highway designers reduce the risk of crashes. The previous development of such a model had not been possible because of the lack of detailed information on road geometry including grade, superelevation, vertical curvature and horizontal curvature over the roading network. To address this, Transit New Zealand commissioned Central Laboratories to:

- (1) Survey the state highway network (using RGDAS);
- (2) Construct a database containing the survey data; and

- (3) Carry out statistical analyses on this database in association with Transit New Zealand's Road Asset Maintenance Management (RAMM) database and the Land Transport Safety Authorities' (LTSA) Traffic Accident Report Database (TAR) in order to develop risk prediction models.

A further objective that arose during the course of the project was to investigate the effect of shape correction operations on crash risk. This required the use of road maintenance information in addition to the TAR database.

The report is structured as follows:

**Chapter 1**

Introduction.

**Chapter 2**

The Australian Road Research Board's RGDAS vehicle is described. The instrumentation and measurements available are discussed, and limitations of the equipment are investigated.

**Chapter 3**

The collection and subsequent manipulation of data from the RGDAS vehicle is described. Extraction of data from both the RAMM and the TAR databases is also described, and the integrity of the data is investigated.

**Chapter 4**

Samples of the RGDAS data collected during the survey are used in conjunction with data from manual surveys and measurements from Transit New Zealand's instrumented test vehicle (Nissan Pulsar) in order to evaluate the accuracy of the RGDAS data.

**Chapter 5**

The development of the statistical risk model utilising Poisson regression analysis on the RGDAS, RAMM and TAR data is described.

**Chapter 6**

Risk factors associated with a variety of road features are investigated and discussed. The results are compared with those from a previous New Zealand crash study.

**Chapter 7**

Following a proposal that shape correction operations may change the relative risk factors associated with particular sites, a statistical method is used with data from the TAR and regional Transit New Zealand offices to investigate whether such an effect is apparent.

**Chapter 8**

Conclusions and further recommendations are presented.

Appendices describe the fields of the database linking RGDAS, RAMM and TAR data. Supplementary material relevant to the development of the mathematical crash risk models is also presented.

## 2. THE ARRB ROAD GEOMETRY INSTRUMENTED VEHICLE

The micro processor based RGDAS was developed in the mid 1980's by the ARRB to automatically measure and record road alignment data in a dedicated vehicle travelling at highway speed. The items recorded by RGDAS are distance, gradient, superelevation, horizontal curvature, vertical curvature, survey speed, route and location information and comments. The recorded road alignment parameters are in turn used to calculate advisory speed, altitude change, direction change and relative mapping coordinates.

The RGDAS measurement system comprises a rate gyroscope and two accelerometers aligned longitudinally and transversely. These transducers are sampled at a rate of 100 samples per second and averaged at the end of each 8 m measurement cycle corresponding to four revolutions of the host vehicle's differential. Direct measures of horizontal curvature and grade are obtained, whereas vertical curvature is calculated from the rate of change of grade.

Post survey, the alignment parameters are smoothed over seven measurement cycles (about 56 m) using a moving average technique. No smoothing is applied to vertical curvature as the least squares procedure used in its derivation has a sufficient smoothing effect. On completion of the smoothing process, all parameters are stored, at 10 m intervals, in a summary table.

Menu driven software is provided to allow the smoothed RGDAS data to be displayed on a personal computer. This software generates displays of road survey data versus distance, plan map (north-south, east-west) of the road path, and altitude versus distance. The latter two plots can display other data, such as advisory speed or grade, as a scaled "comb" plot superimposed on the road path line and altitude profile respectively. There is also a "DRIVE" program which generates a screen display of the view of the road alignment as if driving along the road.

The RGDAS system can only perform relative, dead-reckoning mapping. Therefore it can produce a shape for the path of the road between reference points, but it does not know the correct orientation of the road. It does not know where north is, where sea level is, or where it is on a mapping grid. Software provided with RGDAS allows for map corrections. By giving known east (E) and north (N) coordinate pairs, altitudes and road bearings, at a few sparse identifiable points along the highway surveyed, say at between 20-50 km intervals, the map and vertical profile can be corrected to have a familiar appearance. However, to perform fine corrections of shape details so that a better conformance with the true coordinates results requires very accurate map correction data, i.e. E and N accurate to 10 m, altitude to better than 10 m, and bearing to 1°. Such data can be supplied by conventional survey techniques or by a GPS (geographic positioning satellite) receiver. (A later version of RGDAS, renamed GipsiTrac, incorporates GPS to automatically provide accurate coordinate data.)

No map corrections were made to the RGDAS database used in the traffic crash study which forms the basis of this report as we considered correct orientation of the road to be secondary to accurate definition of the curve geometry.

Despite the 1992 New Zealand survey being the first application of the RGDAS at a network level, covering some 22 000 lane-kms, we experienced no significant system problems or operating difficulties attesting to the robustness of the system and associated graphics software. More complete details of the RGDAS system can be found in Rawlinson (1983).

Chapter 4 describes a detailed investigation into the accuracy, abilities and limitations of the RGDAS system.

### **3. PREPARATION OF DATABASE**

The data used in this crash study were assembled from three source databases: road geometry data from RGDAS, road condition and traffic data from RAMM, and crash data from TAR. In all cases some work was required to bring the data to a compatible condition so that linking of these sources could be conveniently achieved. The time period covered by the database extracts was a compromise to provide data relevant to the highway network at the time of the RGDAS survey while also providing a reasonably large number of crashes. The RAMM data used were current at April 1992 and the TAR data were for the five year period 1 July 1987 to 30 June 1992.

Appendix 1 gives a full listing of the variables stored in the resulting database.

#### **3.1 RGDAS Data**

##### **3.1.1 Rubberbanding**

The smoothed RGDAS data (reported at 10 m intervals for the entire sealed length of the New Zealand state highway system) were found to be imprecise in the spatial location (see Chapter 4). Attempts were made to correct the spatial coordinates but abandoned as unwarranted. However, travel distances in each measurement run were adjusted to the official distances between the start and end reference stations of the run by a process of "duplicating" or removing a record at appropriate intervals.

##### **3.1.2 Segmenting**

To make the total volume of RGDAS geometry data more manageable and to facilitate crash environment matching, the highway network was divided into 200 m segments, with each segment having data for both highway directions. Two geometry databases were constructed on a segment basis, one containing selected data at the rubberbanded 10 m intervals, the other containing selected summary statistics representing the 10 m data (20 data points) of the current 200 m segment, and also some summary data derived from the 10 m data for up to 1 km of the previous highway.



The data selected for the 10 m interval database were the spatial coordinates (x,y,z), the vertical and horizontal curvatures, and the superelevations.

The data selected for the 200 m segment summary statistics were the average, the maximum and the minimum of four parameters - grade, horizontal and vertical curvature, and superelevation. An average compass direction for the segment (resolved to the nearest of the eight primary compass points) was derived from the imprecise bearing data which was considered adequate for this purpose. Also included in the summary statistics were the average and minimum advisory speeds for the current segment and for previous segments as described below.

### 3.1.3 Advisory Speeds

A variable likely to be important is the advisory speed (AS). The advisory speed at each 10 m data point was calculated from the horizontal curvature (H) and superelevation (X) as follows:

$$AS = \sqrt{(bk)^2 + 2k \left( a + \frac{X}{100} \right)} - bk \quad \text{km/h} \quad (1)$$

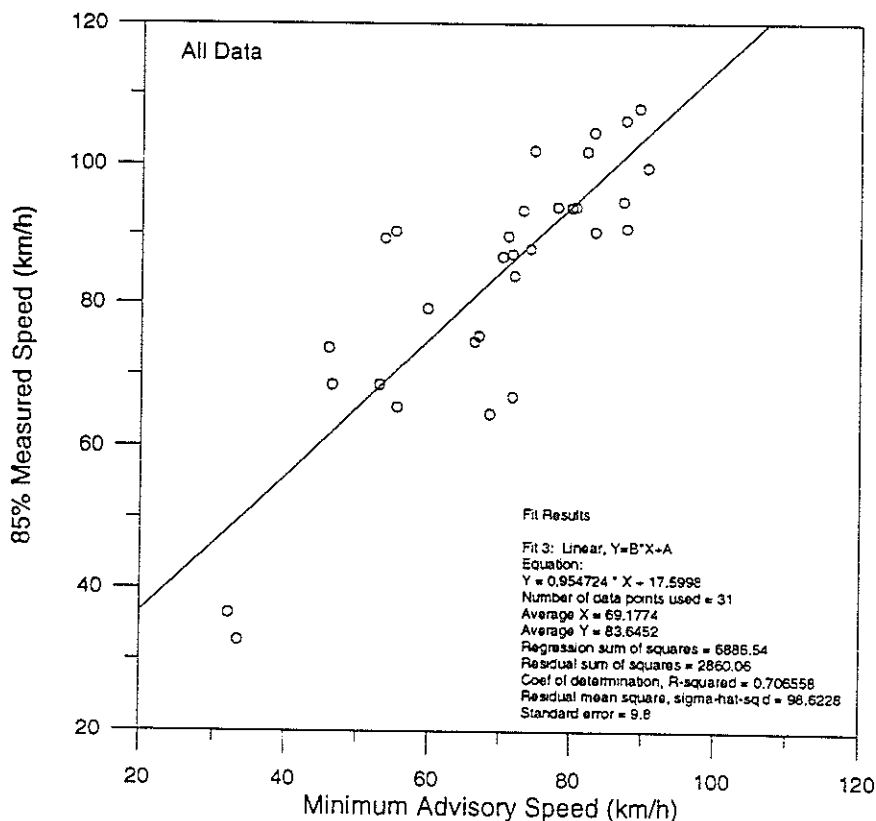
where a = 0.3  
 b = 0.0017  
 k = 63,500/H (km)  
 X = % superelevation  
 H = curvature (radians/km)

A maximum of AS = 200 km/h was set for nearly straight road.

Segment summary data included the minimum advisory speed and average advisory speed for the current 200 m segment, as well as the minimum and average for the previous two segments (0.4 km) and the previous five segments (1 km).

The relationship between road geometry and vehicle speed given by equation (1) was validated by comparing RGDAS advisory speed with 85 percentile mid curve vehicle speeds measured at 31 curve sites, 22 of which were located on the flat. The results are graphically presented in Figure 1 and show a clear linear relationship, with a good coefficient of determination ( $r^2$ ) of about 0.71.

Figure 1. Relationship between RGDAS derived advisory speed and measured 85 percentile mid curve vehicle speeds.



### 3.2 RAMM Data

A tailored RAMM database was extracted from the parent RAMM databases selecting information on road conditions judged to be potentially relevant to traffic crashes. The surface type, date of surface and width of surface were selected as well as the vehicle exposure factors such as the annual average daily traffic volume (AADT), the number of lanes (also if divided or not and if motorway or not), and if the location was urban or rural.

The selected data were assembled in 200 m segments to match the geometry data. Where RAMM factors changed within a segment, the change was transferred to the nearest segment boundary, but the segment was flagged as containing a change in one or more factors.

### 3.3 TAR Data

The complete database of reported injury crashes on the state highway network was used, but crashes in urban areas and crashes unlikely to be related to road geometry or road conditions were excluded. Extreme conditions such as snow and ice were also excluded. The exclusions specifically were as follows:

- Urban crashes (i.e. speed limit less than or equal to 70 km/h plus Limited Speed Zones).

- Crashes at intersections or driveway junctions.
- All vehicle "movement codes" entered in TAR other than overtaking, head-on, loss of control, and cornering related directly or otherwise to a cornering manoeuvre.
- All "contributing factors" unless there were factors of speed, cornering or overtaking.
- All "slippery road" factors other than rain, e.g. oil, mud, snow and ice.

These exclusions reduced the total number of crashes to be considered from about 18 500 to about 3500.

Data for selected crashes was extracted on the location, direction of travel, time and date, movement code and contributing factors, curve severity and wet or dry road.

### 3.4 Data Integrity

There was some concern regarding the accuracy of location of crashes (or at least the geometry feature supposedly contributing to the crashes) and the location reliability of the geometry data. Both were linked back to the state highway network reference stations, but high accuracy in the reporting/linking processes could not be assured. A broad test of positioning accuracy was made by comparing the "curve severity" description in the TAR data with the minimum advisory speed (ASMIN) in the 200 m segment as derived from the RGDAS data. There are four curve severity categories (straight, easy, moderate, severe) but the data showed that the ASMIN were similarly distributed for the "easy" and "moderate" categories, and therefore these two were combined.

Figure 2(a) shows the minimum advisory speed distributions for the three remaining categories and the distribution of all the selected crash data. The total distribution is strongly bimodal (verging on trimodal), and the three component distributions indicate that this arises from "crashes on straight road", "crashes on gentle curves" and, in lower numbers, "crashes on severe curves". Of concern was the substantial number of crashes where the curve severity category and the minimum advisory speed value did not reconcile. There were examples of this in all categories, and it was supposed that many of these could be cases of incorrect crash location/segment location.

A "neighbouring segment" search scheme was implemented to check the possibility that the minimum advisory speed of a nearby segment would give a better match to the curve severity description reported with the crash. In the search a weighting was given to relocating by only  $\pm 1$  segment, but the search was extended up to  $\pm 5$  segments if the original mismatch was substantial. Figure 2(b) shows the distributions of the adjusted data. The number of mismatches has clearly been reduced, and a trimodal "all data" distribution is more pronounced.

Of particular importance to this investigation is the influence of the smoothing procedures (a linear least squares fit applied over seven measurement points, or 56 m) used in producing the \*.TAB data. The smoothing described is expected to have a significant effect on peak readings in the data. A second version of processed data was created by bypassing the smoothing procedure described, in order to gauge the effect of the smoothing.

#### 4.1 Distance Measurement

For the RGDAS data to be of use it is essential that spatially correct values can be selected from the RGDAS files for a particular road feature. If a particular road feature such as a corner is being studied, the accidental selection of RGDAS data from a position just 100 m away (depending on the scale of the feature) may give quite misleading results. This section investigates the use of the RGDAS distance measurements for location of data within RGDAS files.

In the past the distance measurements from RGDAS have been assumed to be correct, and have been used to select data for given highway locations. In order to investigate the accuracy of these distance measurements, a number of data files were looked at and the distance measurements compared with those defined by Transit New Zealand, referred to as reference station (RS) numbers. (It is likely that the position of any road feature, crash site, etc being investigated will be defined using the RS numbering system).

The raw data files (\*.DAT) over the Haywards Junction-Featherston section of State Highway 2 were investigated. These files contain the as-measured data, before spatial averaging and rubberbanding were carried out. The segment lengths between adjacent reference station positions (usually approximately 15 km apart) were compared with the Transit New Zealand measured distance. The mean error for the segment lengths was 0.9%, with a maximum error of 1.3%.

The "rubberbanding" process used on the data is a simple proportional stretching/shrinking of the data so that the overall highway length matches the official Transit New Zealand distance. This means that the distance measurement will be correct at either end of the measurement distance (typically of the order of 140 km), but may not be correct in between (unless the original error was a constant proportional error). Ten highway data files were chosen at random from the North Island, and the positional errors of the reference stations within the measurement distance were calculated.

There appears to be considerable variation from data file to data file. Some files, such as those for State Highways 43, 26 and 10, showed excellent agreement between the RGDAS and RS measurements with distance errors not exceeding 10 m over distances in excess of 100 km. Other files however showed considerable errors. The RS positions in the data for State Highway 30 were out by typically 130 m and up to 190 m. State Highway 16 had positional errors of 310 m for two reference stations, and State Highway 5 had errors up to 240 m. State Highway 1 (North Island section), a 920 km road, had considerable variation within its length with many RS positions lying within 10 m of the correct values although a minority were up to 100 m out. A 95% confidence error bound of 72 m was calculated for this data set.

The positional errors that are present even in the corrected (rubberbanded) data sets throw considerable doubt on any road data analysis that relies solely on the distance measurements from the \*.XYZ RGDAS files. All comparisons of data described in the following sections of this report for the analysis of the accuracy of superelevation, gradient and curvature used a labour intensive process of matching data sets by eye, with respect to positional location. The size of the positional errors that have been found, sometimes 200-300 m, would lead to worthless results if data sets were compared directly using the distance measurements incorporated in the RGDAS system.

## 4.2 Horizontal Curvature

The ability of the RGDAS system to measure the horizontal curvature or corner radius of the road it travels on is of prime importance in determining friction demand and advisory speeds for bends. RGDAS does not measure the horizontal curvature directly, but combines data from two sources, a yaw rate meter and a velocity reading, and calculates the horizontal curvature from these.

In order to investigate the quality of the horizontal curvature data, 25 corners were selected on the Featherston Junction-Haywards Hill turnoff section of State Highway 2. Five of these corners are large radius bends (>500 m) on motorway sections, and good quality survey data is available for the radii. The other 20 curves are a selection of varying radius curves (20-50 m) on the Rimutaka Hill, and the radius for each curve was measured manually from 1:1000 drawings of the road. It is estimated that the manual measurements for these curves resulted in errors not exceeding 2 m on the radii.

The maximum RGDAS derived radius for each curve was selected from the \*.XYZ data. Figure 3 shows the percentage error of the RGDAS derived radius compared with the actual curve radius, with respect to the corner curvature (1/km). A group of data points to the left of the graph, representing the wide radius curves, show a reasonable cluster of points largely within  $\pm 10\%$  of 0. The data points to the right, representing the low radius curves, show more cause for concern with a wide spread of errors from around 0 to over 70% error. (Note that points above the X axis indicate that the RGDAS derived radius is over-estimated compared to the actual radius, and that this is the case for virtually all of the data points.) This effect is thought to be due at least in part to the linear fit smoothing mentioned above, in which a linear least squares fit is applied to the horizontal curvature over 56 m in order to smooth transients and noise. This linear fit process has no effect on the maximum curvature values for the large radius curves, as there is a considerable length of road in the middle of the curve where the radius is constant for at least 56 m and it is from the plateau of readings in the RGDAS data for this region that the curvature is selected. It should be noted, however, that readings near the entry and exit points of curves may be inaccurate due to the smoothing process.

For the tighter curves, the arc length is frequently less than 56 m and in such cases there will always be some part of the transition curve or straight road being included in the linear fit. As can be seen, this tends to give an overestimation of the curve minimum radius by RGDAS. This problem is particularly prevalent where the curve arc length is short due to:

- (a) Small radius; and
- (b) Curves with low deflection (change in direction).

Figure 4 shows the percentage error of the RGDAS derived radius compared with the actual curve radius with respect to the corner curvature (1/km), for the raw (unsmoothed) data. In comparison to Figure 3, it can be seen that the data is now clustered more uniformly about the X axis and the relative errors on the radius measurements now fall largely within 30%. The improvement seen is due to bypassing the smoothing process. The remaining errors are due in part to inaccuracies when radii are measured from maps and the .TAR to .XYZ operation whereby data is crudely converted from a 7.9 m sample interval to a 10 m sample interval using the previously described simple distance matching procedure rather than interpolation. There is also considerable difficulty in selecting measurements from an RGDAS file that contains continually variable values, in a region that is supposed to represent a constant radius curve. It is not possible to distinguish between these error sources and any RGDAS measurement error, although a good indication or upper bound is placed on the RGDAS data.

Hence it can be concluded for the \*.XYZ file data that when the radius remains constant for at least 56 m, the RGDAS system provides a measurement of the minimum radius to within  $\pm 10\%$ . For the small radius bends ( $r < 50$  m), the minimum radii are over-estimated by up to 70%. Some component of this error is due to the linear fit averaging which has a significant smoothing effect on the radius measurements. Marked improvement in the measurement of radius is seen in the unsmoothed RGDAS data files.

### 4.3 Superelevation

The superelevation of the road lane is calculated by RGDAS by taking the difference between the lateral acceleration (measured directly) and the centrifugal acceleration (calculated from the curve radius and vehicle velocity). Whilst it was originally envisaged that survey data including superelevation would be available for sections of State Highway 2, such data was minimal and of dubious quality. Manual survey data for the superelevation and gradient for a selection of highway sites in the Nelson region became available during the course of this project, and it was decided to use this information in the investigation into the quality of data from the RGDAS system.

Figures 5, 6 and 7 show the relationship between the RGDAS and surveyed data at two of the Nelson test sites. (The data sets were matched distancewise by eye as described in Section 4.1.) Figures 6 and 7 show the same site, but travelling in different directions. All three figures show very good agreement between the two sources of data, although the measured data can be seen to be greater than the RGDAS data, particularly at the peak readings. This is thought to be due to the smoothing by the linear least-squares fit employed by RGDAS.

The data from the manual survey was available at 25 m stations, whereas the data from RGDAS is available at 10 m stations. RGDAS data at 25 m intervals was interpolated from the .XYZ files in order to be comparable to the manual measurements on a reading to reading

Figure 3. Radius error vs curvature. 7 point linear least-squares smoothing.

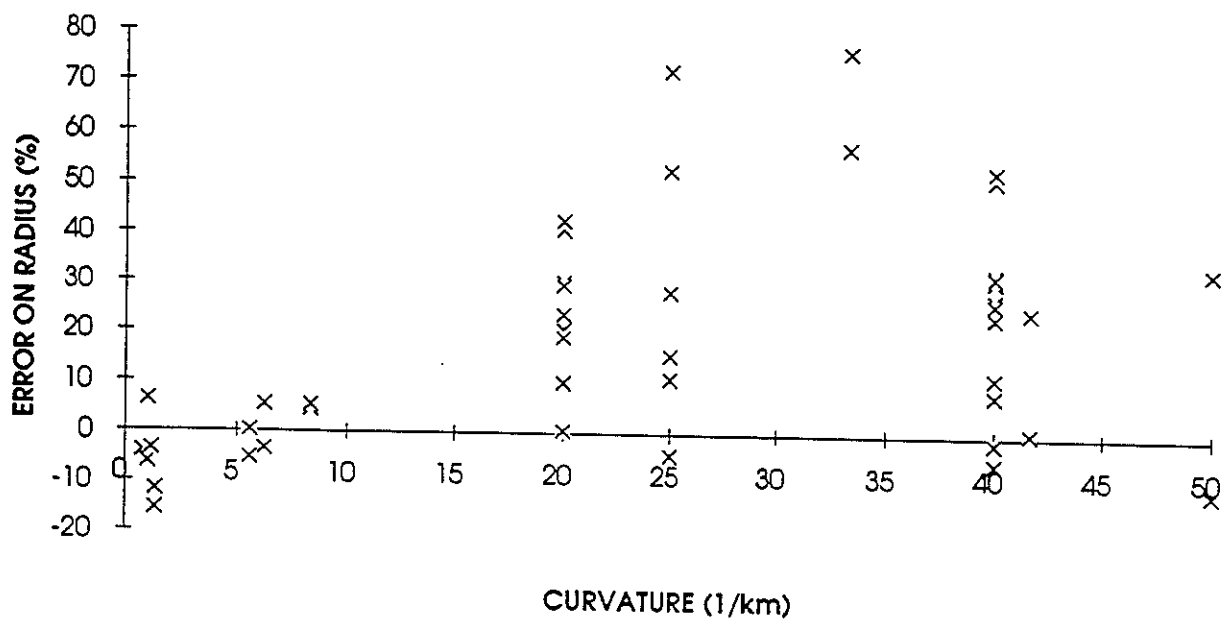
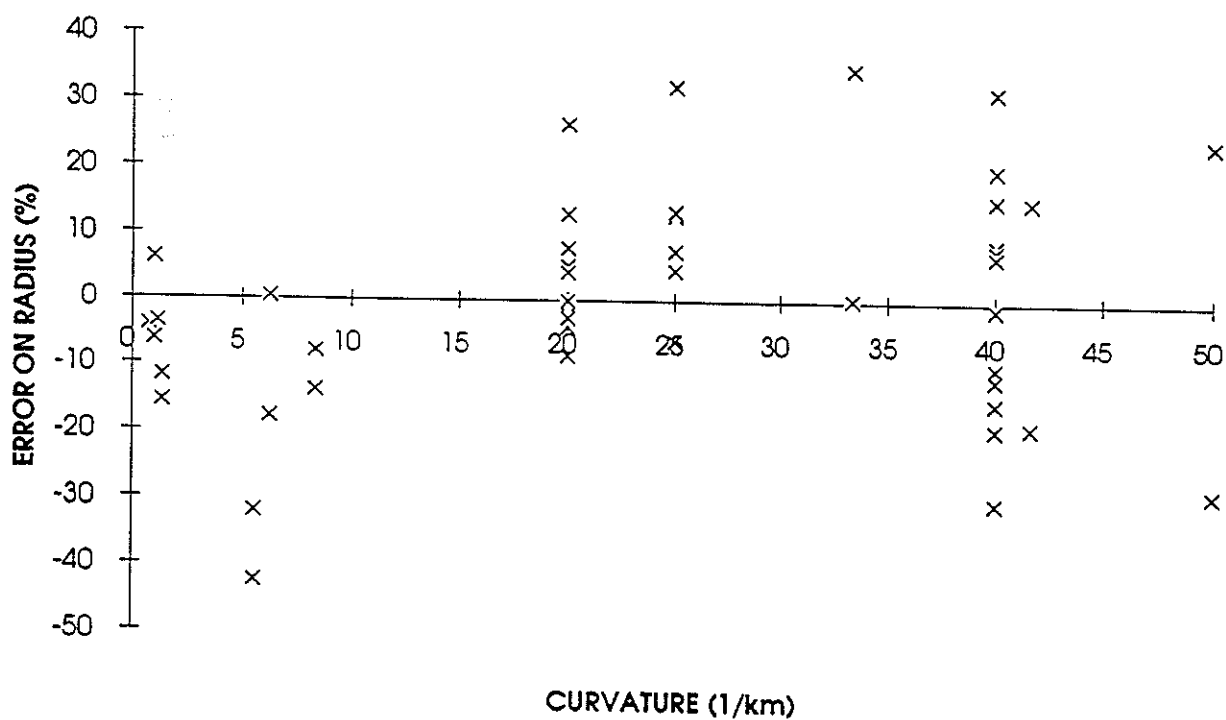


Figure 4. Radius error vs curvature. Raw (unsmoothed) data.



basis. The absolute errors were then derived by subtracting the manual survey readings from the RGDAS readings at each point. Listing the absolute values of the errors gave a mean error of 1.0%, with a 95 percentile value of  $\pm 2.1\%$  of superelevation.

In conclusion, it can be stated that the superelevation values given by RGDAS are in good agreement with the actual values and an error bound of 2.1% (gradient) will encompass 95% of RGDAS superelevation measurement errors.

Figure 5. Superelevation : RGDAS vs measured at RP 201/4.4.

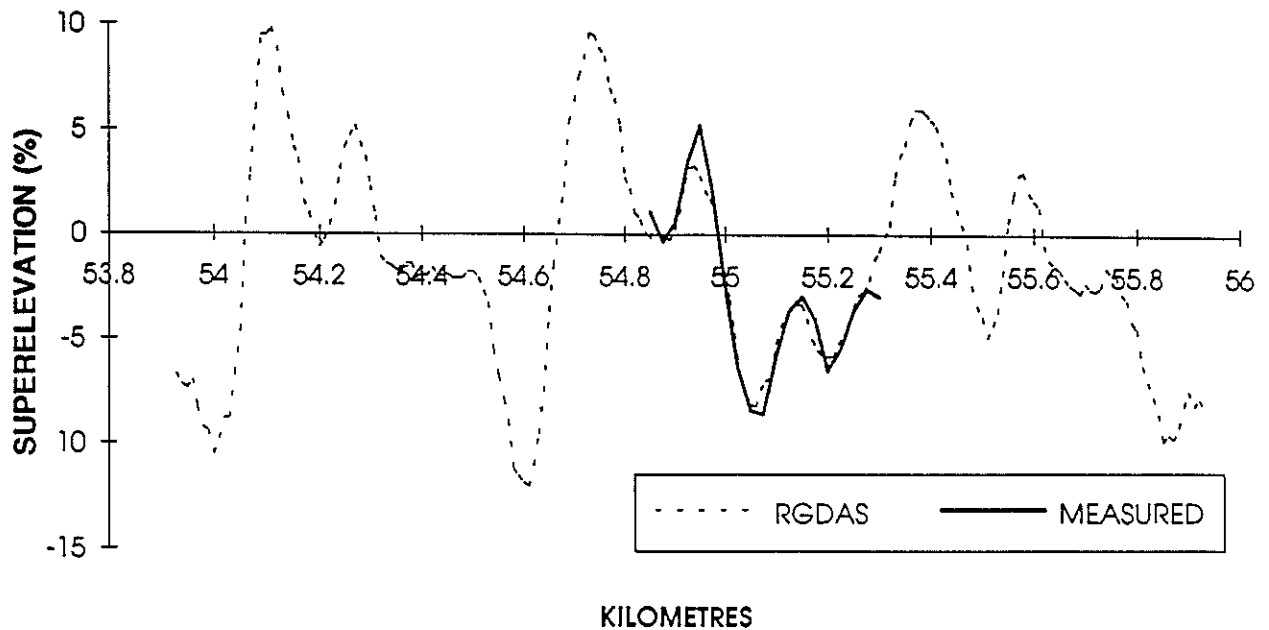


Figure 6. Superelevation : RGDAS vs measured (RP 239/3.1 and 3.3, increasing).

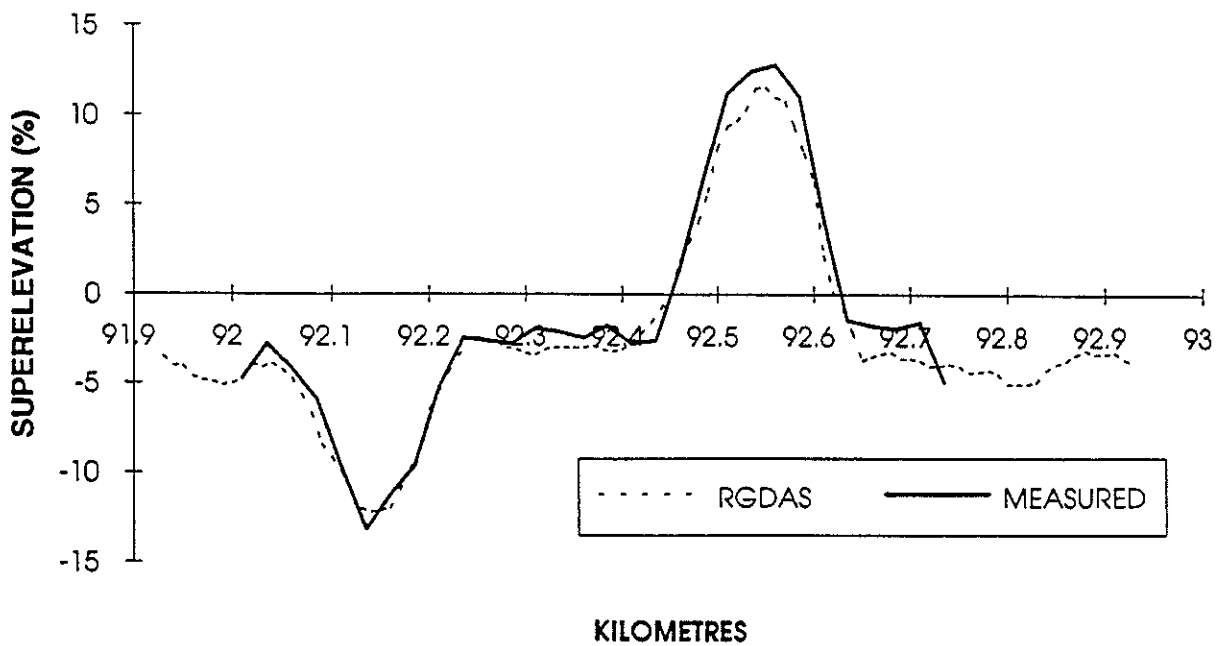
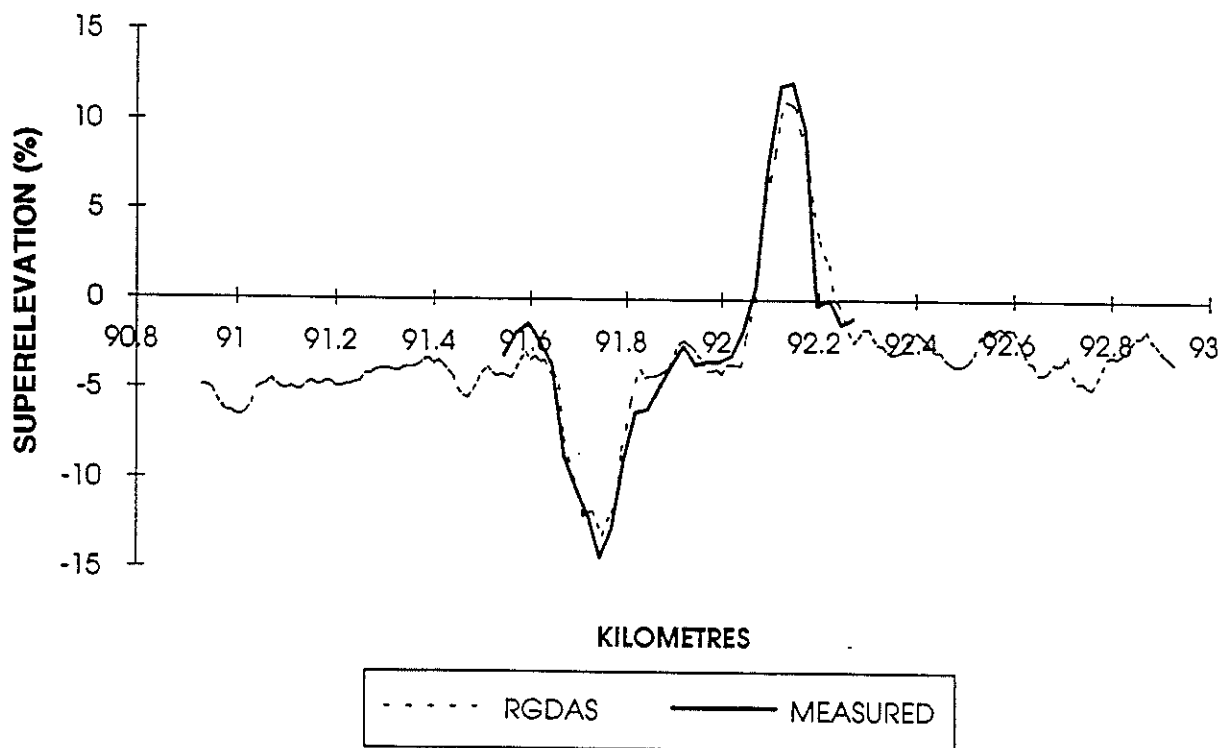




Figure 7. Superelevation : RGDAS vs measured (RP 239/3.1 and 3.3, decreasing).



#### 4.4 Gradient

The gradient of the road is calculated by RGDAS from the longitudinal accelerometer and the acceleration of the vehicle, the latter being derived from the velocity readings.

Road gradient data for the investigation into the accuracy of the RGDAS data was taken from the same locations as described in section 4.3. Figures 8, 9 and 10 illustrate the relationship between the RGDAS data and the survey data. Figure 8 shows the results for a site with considerable variation in gradient, and can be seen to show a very good correlation between the two data sets. Figures 9 and 10 appear to be somewhat more random although when viewing these it must be kept in mind that this site has little variation in gradient and is virtually flat, and the fine vertical scale exaggerates the errors present.

The gradient data for these sites was processed in a similar manner to that described in Section 4.3, giving an average absolute error of 0.59% and a 95% limit of 1.1%.

Figure 8. Gradient : RGDAS vs measured at RP 201/4.4.

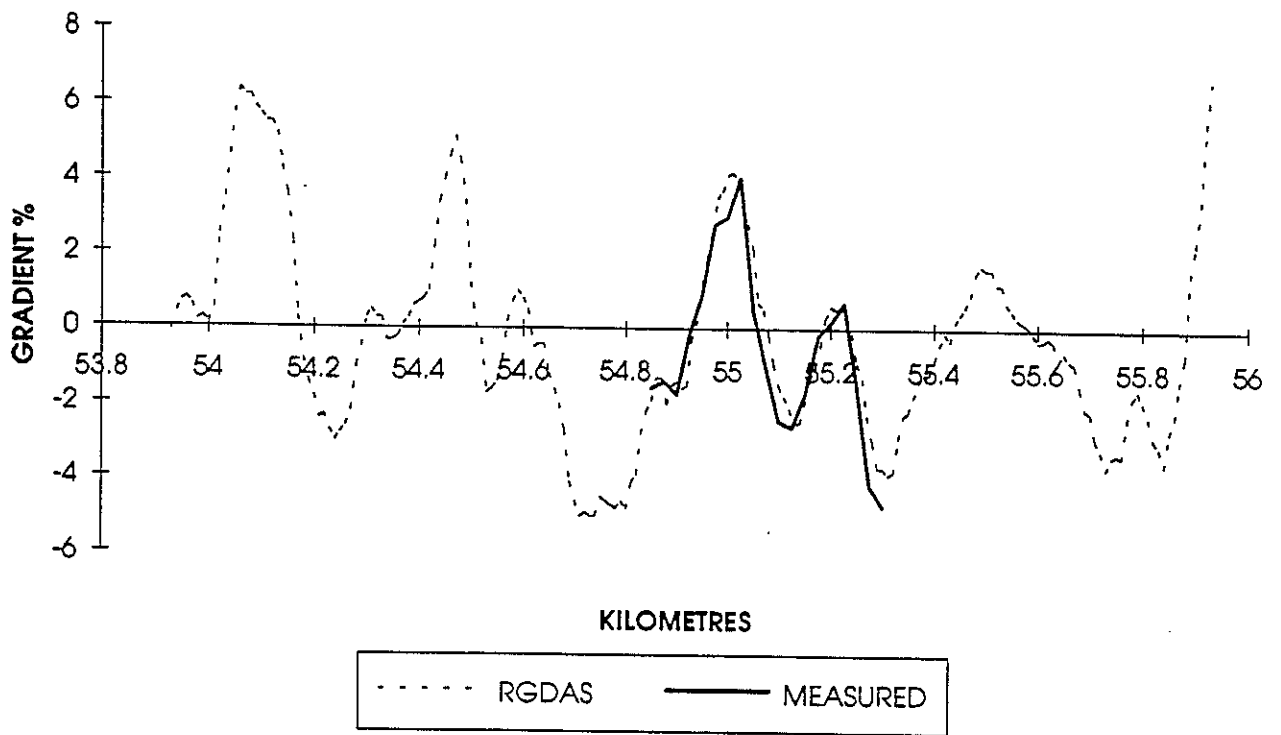


Figure 9. Gradient : RGDAS vs measured (RP 239/3.1 and 3.3, increasing).

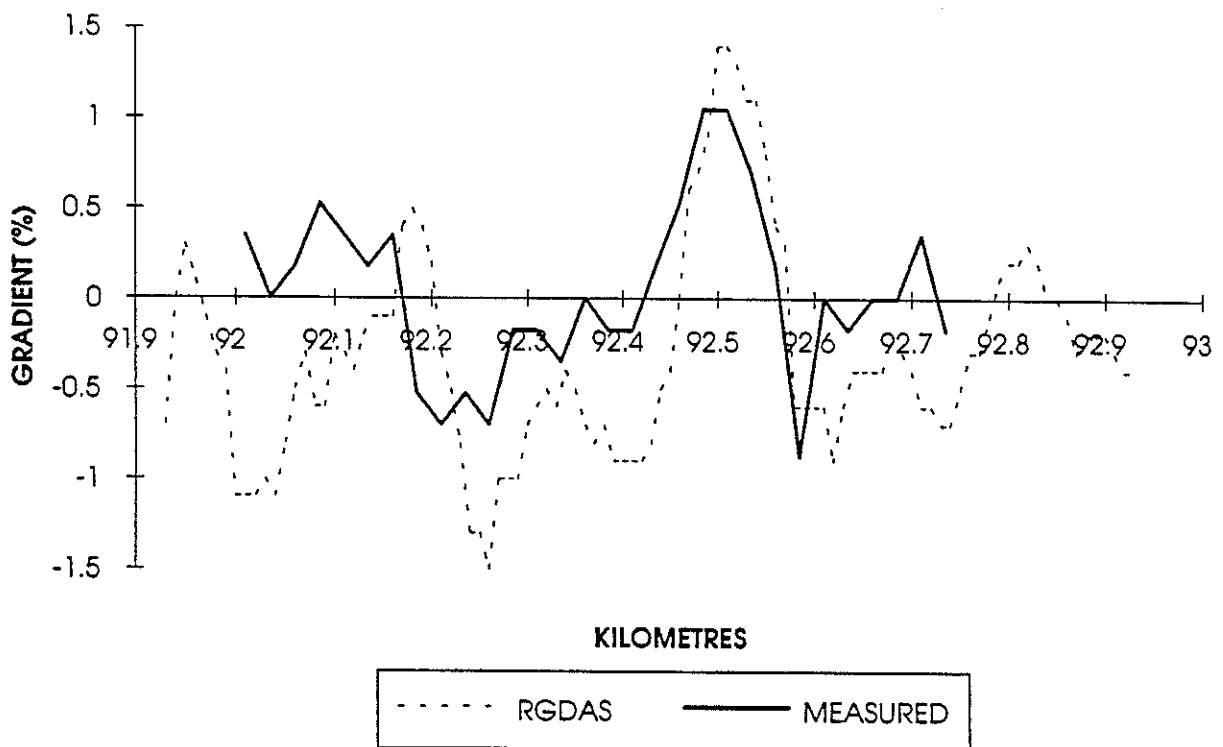
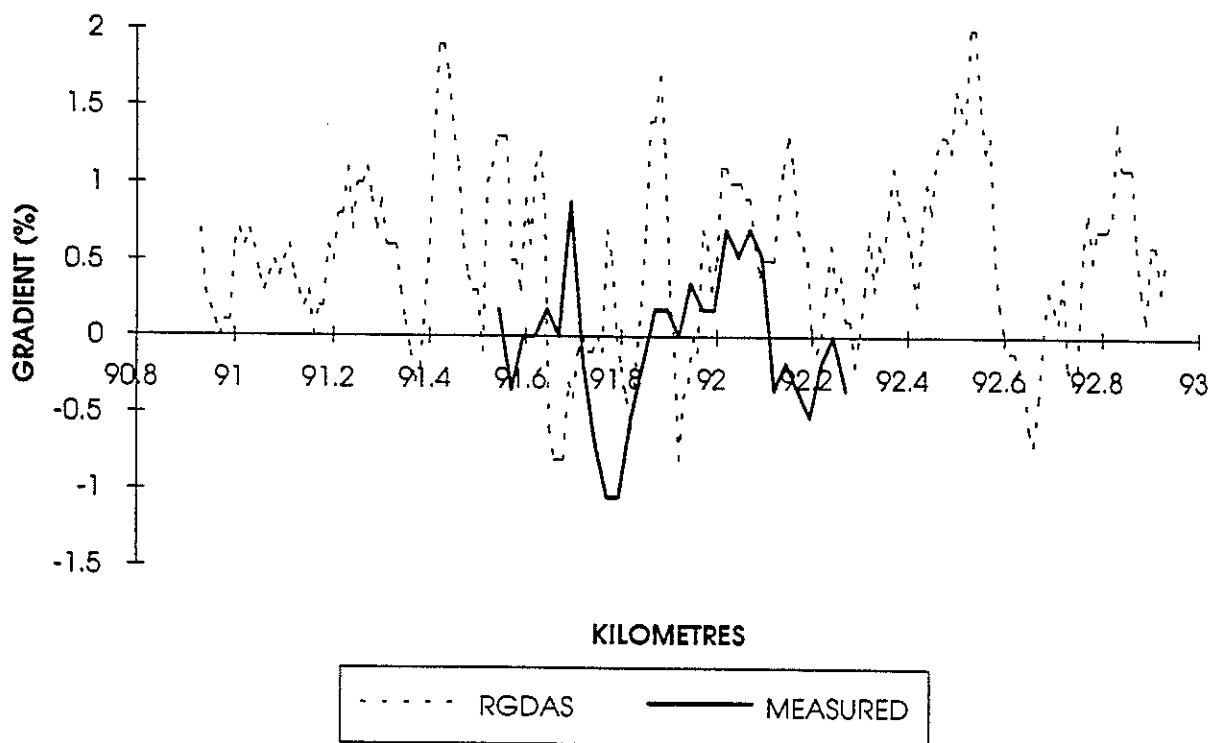


Figure 10. Gradient : RGDAS vs measured (RP 239/3.1 and 3.3, decreasing).



#### 4.5 Vertical Curvature

RGDAS obtains estimates of the gradient of the road at about 8 m intervals. A vertical curve occurs when the gradient is progressively changing. RGDAS calculates a least-squares best fit to the rate of change of gradient with respect to distance, over seven measurement cycles (56 m), yielding the vertical curvature. Whilst this process is similar to that used to calculate the horizontal curvature, the resulting values are less robust as the gradient is derived from other variables and is unlikely to be as accurate as the directly measured yaw.

Survey data from a 1900 m highway site near Whangamata was selected to provide data for comparison with the RGDAS data. The survey data was available in the form of horizontal (20 m spacing) and vertical coordinates. The curve radius was found by taking groups of three points and calculating the position of a fourth point that was equal in distance from each of the other three points. The radius and curvature could then easily be found.

Figure 11 shows the RGDAS vertical curvature data (in both increasing and decreasing highway directions) and surveyed curvature data for a 1900 m stretch of highway near Whangamata. Large variations can be seen in the RGDAS traces, although the trend is similar to the surveyed values.

Figure 12 shows smoothed data, with a 56 m moving average applied to both the RGDAS and surveyed data. The RGDAS values can clearly be seen to follow the surveyed data. An estimated error of 0.2/km would appear to cover most of the errors, although this is of the

Figure 11. Vertical curvature : surveyed vs RGDAS (unsmoothed).

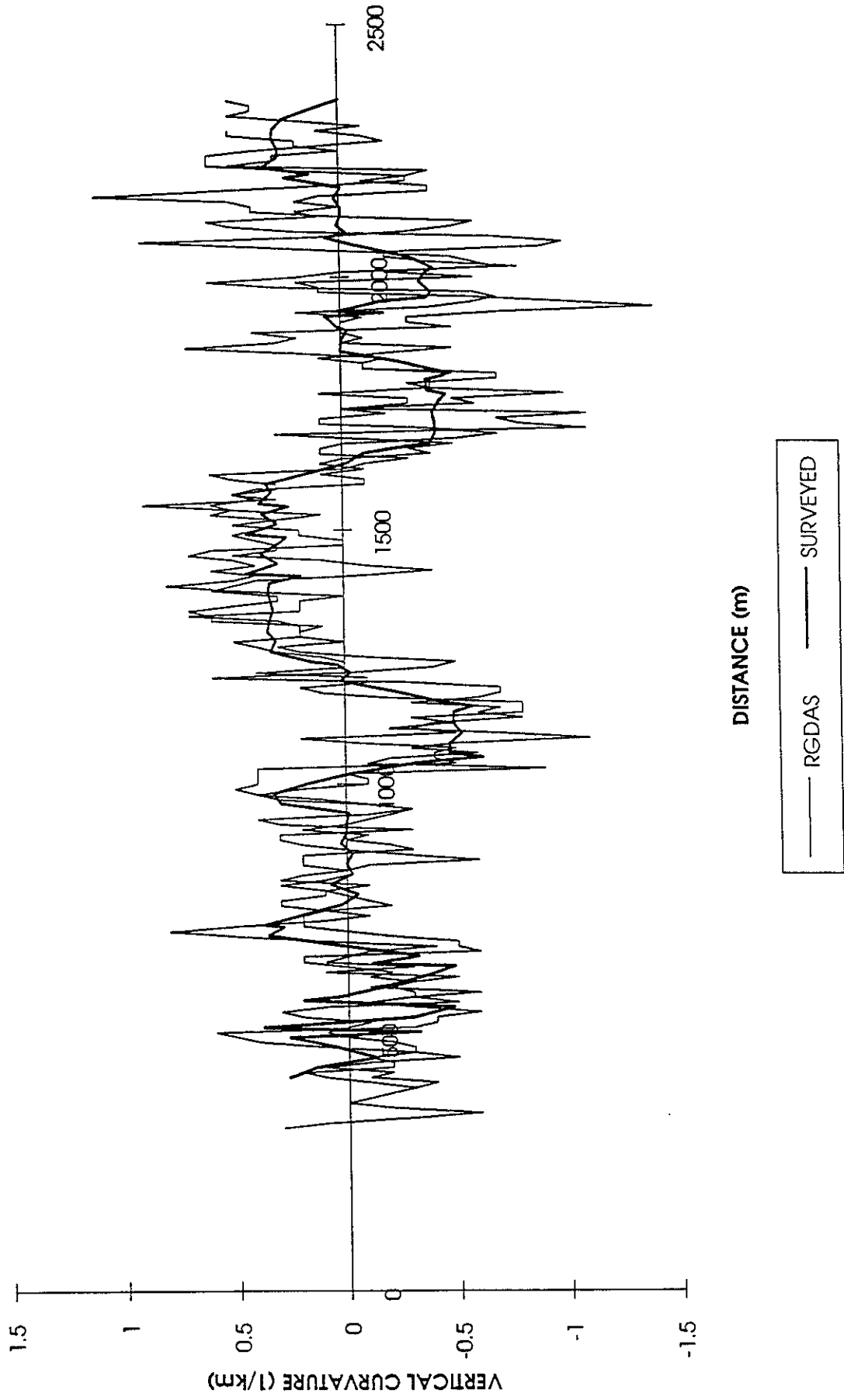
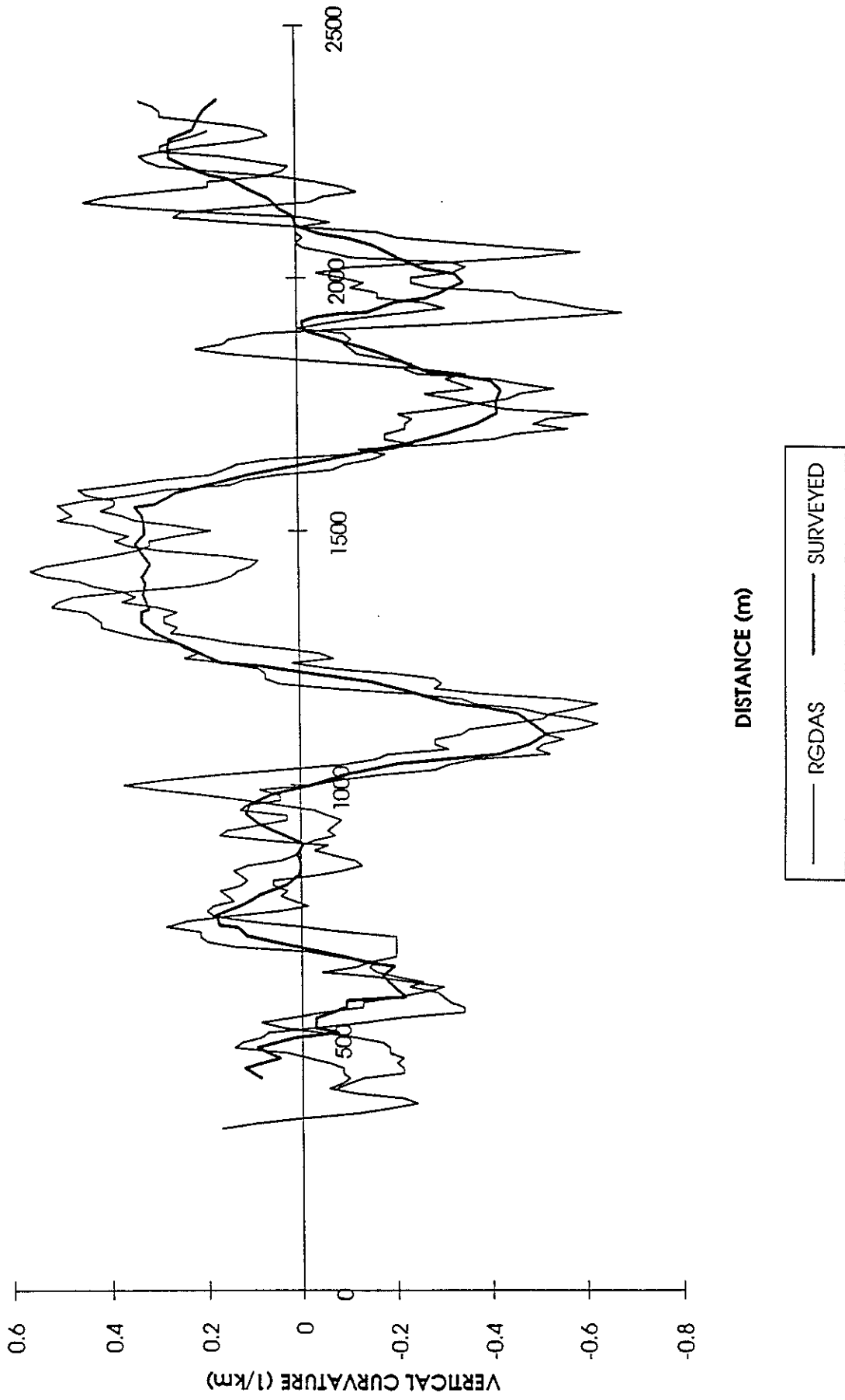


Figure 12. Vertical curvature : surveyed vs RGDAS (smoothed).



same order of magnitude as the reported curvature. The large size of the errors with respect to the values is thought to be due to two sources:

- (a) The errors seen in the RGDAS road gradient data are a significant proportion of the typical gradient values (see Section 4.4). These errors, typically 1% gradient for gradient values that rarely exceed a few percent, are passed on to the vertical curvature values.
- (b) Vertical curvature values are inherently low. Highway design favours relatively constant gradient, sometimes at the cost of many tight curves. (A good example of this is the Rimutaka Hill road, data from which was used in Section 4.2 of this report, which has many tight curves yet near constant gradient.) Accordingly, whereas horizontal curvature may exceed 40/km (curve radius 25 m), vertical curvature is typically of the order 0.4/km (curve radius 2500 m). The measurement errors have a large impact due to the low curvature values normally found.

In conclusion, it can be stated that trends in vertical curvature are shown in RGDAS, with typical measurement accuracy of 0.2/km (around half a typical vertical curvature value). A 56 m moving average clearly adds to the value and usefulness of the data, by smoothing out some of the 'noise' that is present in the RGDAS data.

#### 4.6 Mapping Ability

It has been suggested that the RGDAS system could be used as a road mapping system. Figure 13 shows superimposed X-Y plots from three data collection runs over the same stretch of highway. It can be seen that small scale features such as bends are preserved well and can be seen to remain very similar from one run to the next, although the overall picture shows the three traces diverging due to transducer drift and slight inaccuracies in calibration. This would indicate that whilst the RGDAS data is useful for quantitative data on individual highway features, at least to the accuracies discussed in Sections 4.1 to 4.5, the RGDAS system is no substitute for mapping or surveying on a large scale.

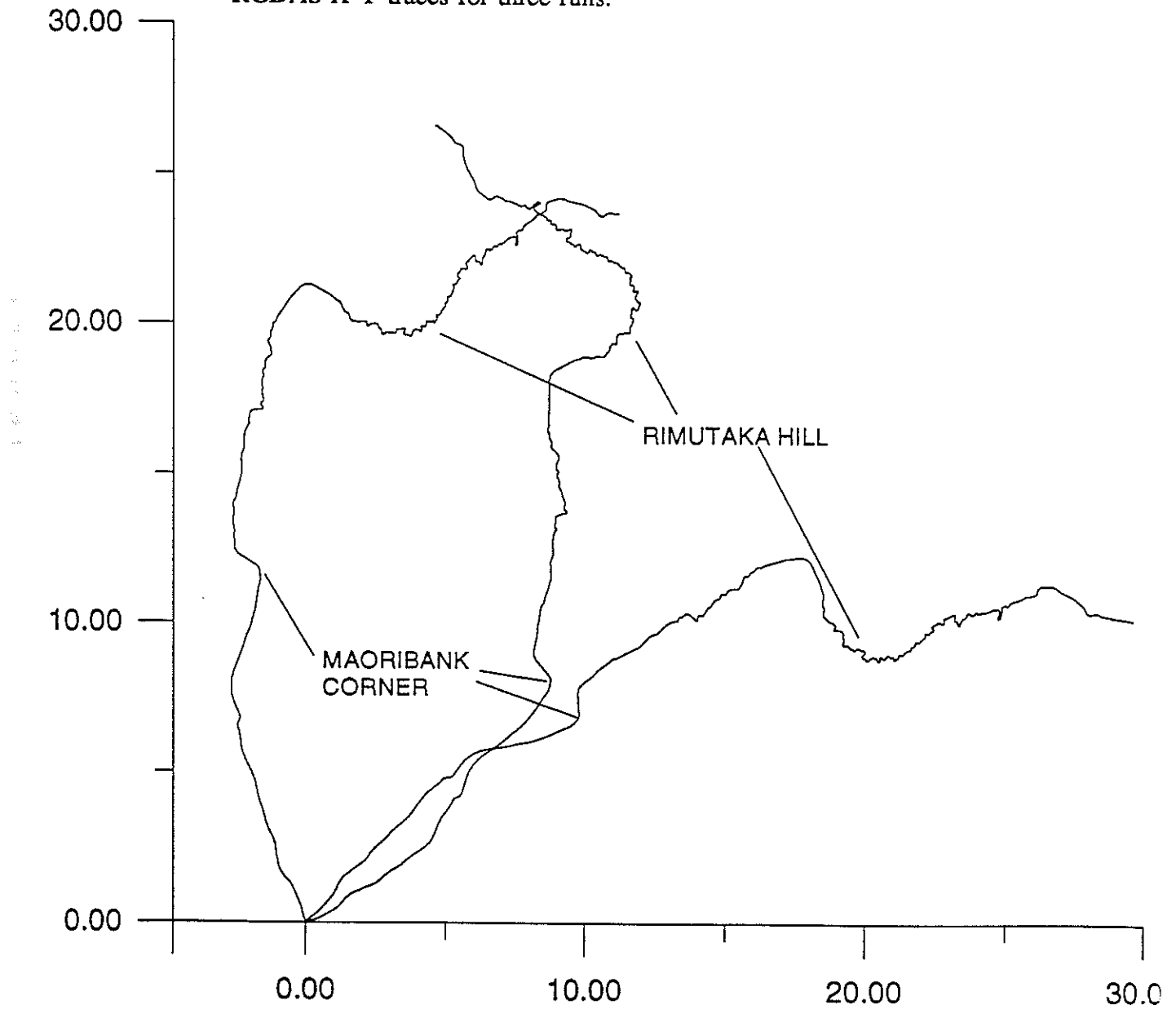
The data smoothing process (as described at the start of this chapter) will have some effect on the shape of the curves seen in the X-Y plots of the RGDAS data. The smoothing will tend to smear or spread the RGDAS variables, for example curvature, leading to a spreading of the curves particularly near the transition points (entry and exit). The smoothing procedure is thought to conserve the integral of a variable over a distance, so that whilst in the case of horizontal curvature the curve shape will be distorted (more spread out than the actual shape) the smoothing process should not give any errors in the road bearing over long distances. It is thought that RGDAS data more suitable to mapping purposes would result if the smoothing process was bypassed.

A further problem with the data is the accuracy of the distance measurement. Even if the odometer were completely accurate, variations in individual driving style, tyre temperature and pressure, etc can still give rise to small but significant errors in distance measurement as discussed in Section 4.1. The distance measurements in the RGDAS data were found to be not accurate enough to allow direct comparison with data from other sources, and all the data

comparison described in this report required that data from different sources be matched (with respect to distance) by eye.

The RGDAS data processing software does have a facility for entering the coordinates of known reference points. The data is then stretched and forced to fit these points. Wanty *et al* (1995) discusses this approach, and state that the sparse identifiable points currently used to correct the RGDAS data (typically every 20-50 km) serve only to give the map a familiar appearance. Very accurate map correction data would be required (i.e. frequent datum positions with east and north accurate to 10 m, altitude to better than 10 m, and bearing to 1°) to give good conformance with the true road shape, and it is suggested that such performance may be achieved by the latest version of RGDAS (renamed GIPSITRAC) which incorporates a GPS (Global Positioning System) receiver. These conclusions from Wanty *et al* (1995) are in good agreement with the results found from this investigation.

Figure 13. State Highway 2, Haywards intersection to Featherston.  
RGDAS X-Y traces for three runs.



#### 4.7 Transit New Zealand's Pulsar

Transit New Zealand's instrumented Nissan Pulsar, which has been employed in on-road determination of tyre rolling resistance (Cenek and Shaw 1989), can provide limited data for comparison with the RGDAS data. The Pulsar does not provide as complete a set of information as RGDAS, although the gradient and side acceleration are relevant to this investigation.

Figures 14 and 15 show the gradient over the first 17 km of the Haywards-Featherston section of State Highway 2, for the RGDAS and Pulsar respectively. The Pulsar data has been smoothed using a 60 m moving average, for compatibility with the smoothed RGDAS data. Comparison of the two plots shows excellent agreement between the two sets of data, with slightly higher peak values being recorded by the Pulsar.

Figure 16 shows the side acceleration for both systems. A moving average was again applied to the Pulsar data. The side acceleration is dependent on vehicle speed as well as road geometry, so it was necessary to use the Pulsar velocity data as well as the RGDAS-derived superelevation and curvature in order to calculate the RGDAS side acceleration in a manner that would allow direct comparison with the Pulsar data. Equation (2) shows the relationship between these parameters:

$$\text{Lateral acceleration (m/s}^2\text{)} = \frac{\text{VSS}^2}{\text{RC}} - g \text{ SP} \quad (2)$$

where VSS = steady state speed (m/s)  
RC = radius of curvature (m)  
SP = superelevation = cross-fall (%) / 100  
g = acceleration due to gravity

A calibration offset is evident and allowed both sets of data to be shown on the same graph without confusion. Besides from the offset there is excellent agreement between the two sources of data, although a large negative spike is evident in the RGDAS data. This was found to have been caused by a very high curvature reading in the RGDAS data due to the test vehicle pulling off the road. The high curvature reading was accompanied by a low velocity in the RGDAS data; as the PULSAR velocity values (which did not include a vehicle stop) were used with the RGDAS geometry data to calculate the values shown on Figure 16, an absurdly high side acceleration resulted.

The appearance of such a tight radius curve in the RGDAS data due to the test vehicle pulling off the road presents some concern. A check through the national RGDAS database showed at least 10 sites where the reported radius was less than 10 m. The RGDAS data showed very low velocity (<1 m/s) at each of these sites and some (but not all) were labelled 'C:STOP', 'C:COMPASS BRG', etc. It must therefore be noted that there are a number of very tight radius curves seen in the RGDAS data that do not represent a real curve.



Figure 14. RGDAS gradient data, State Highway 2.

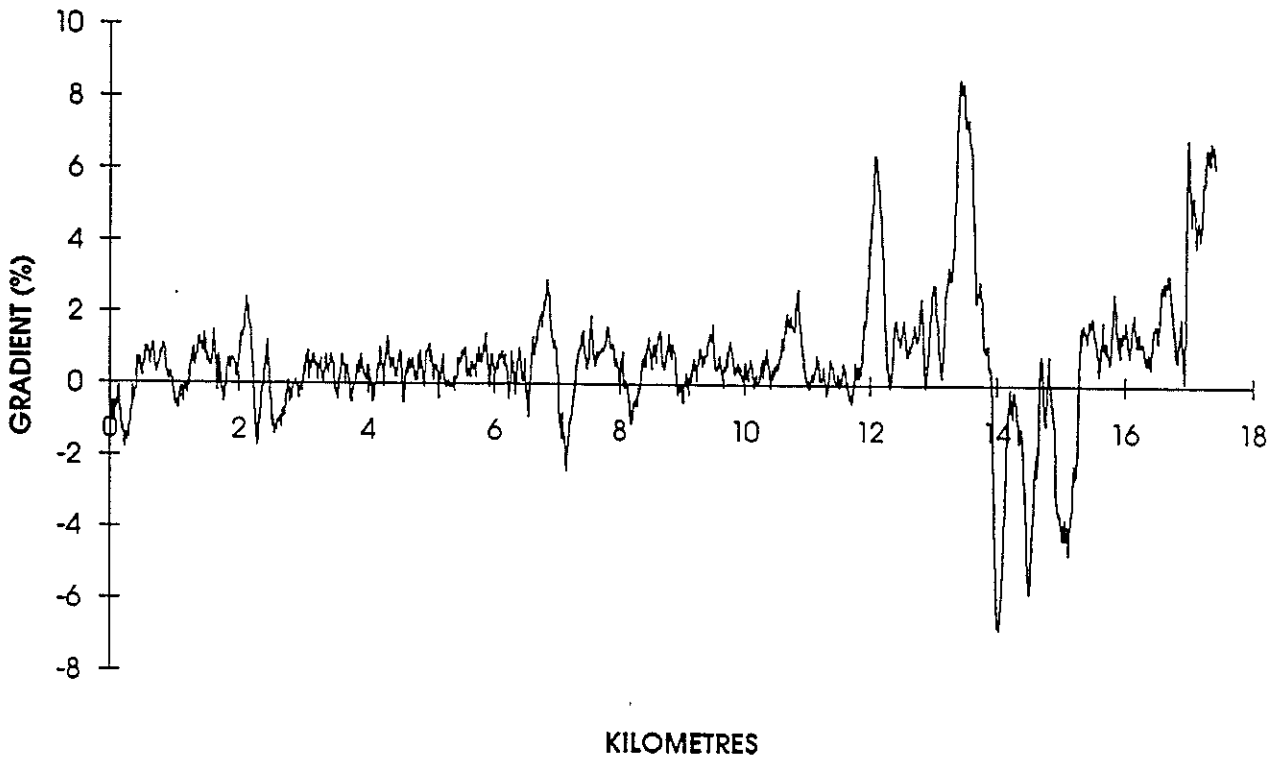


Figure 15. Pulsar gradient data, State Highway 2.

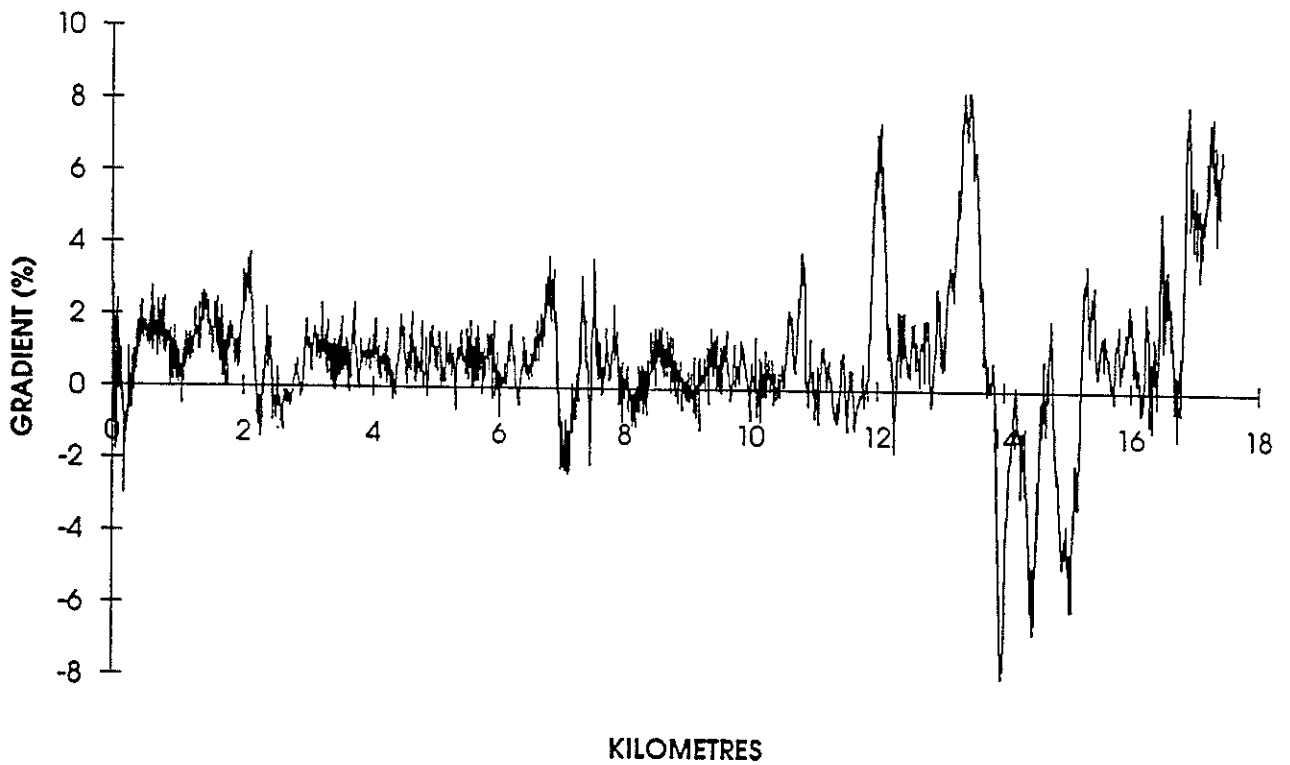
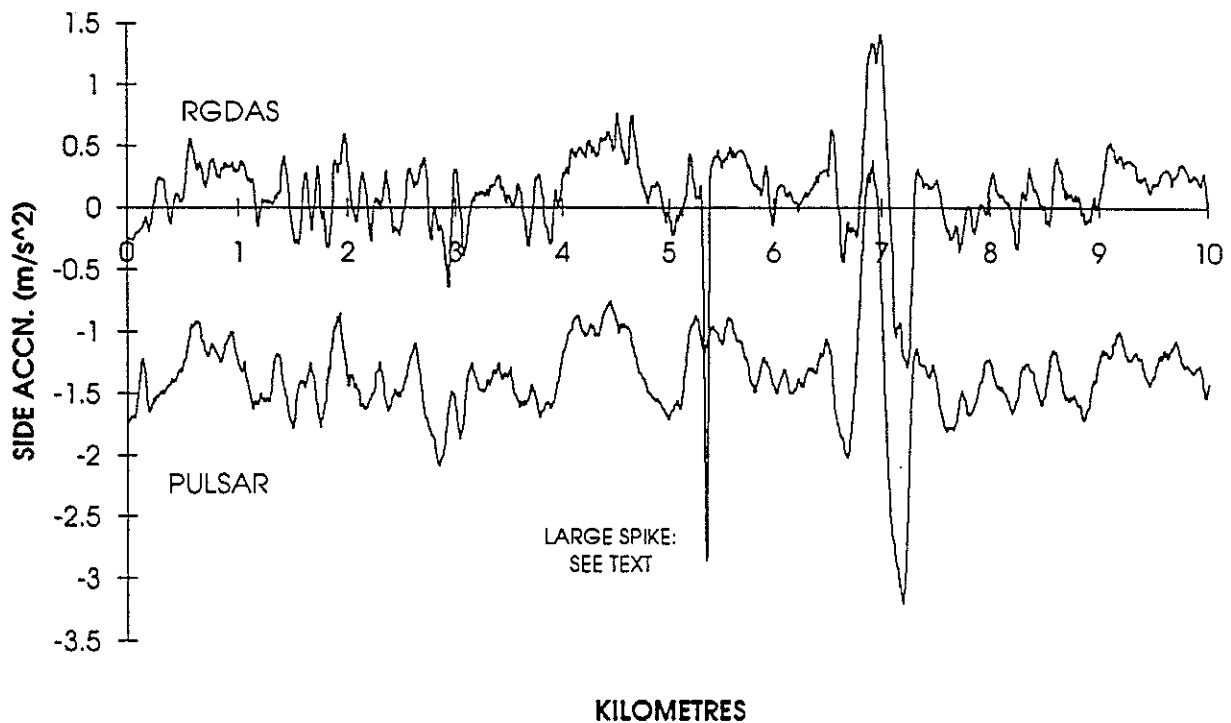


Figure 16. Side acceleration data, State Highway 2.



The accuracy of the Pulsar data is not known, so can not be used to set error limits on the RGDAS data although the excellent agreement that can be seen between the two sets of data does go some way towards increasing the level of confidence in which we can apply to both data sources.

#### 4.8 Summary

The RGDAS data has been compared with data from maps, road surveys and Transit New Zealand's instrumented Nissan Pulsar in order to gauge its accuracy and usefulness for tasks that require quantitative highway information. The principal findings from this study are summarised below for ready reference.

- (1) The distance measurements from RGDAS contain errors of the order of hundreds of metres with respect to Transit New Zealand's reference station distance measurements, even in the length adjusted (rubberbanded) data sets. When these errors are larger than the road features being studied, it is clearly unacceptable to simply read off data from the files using the RGDAS distance measurements. The best way to accurately match RGDAS data with road features is by plotting the RGDAS data, normally in an X-Y plot, and visually picking out identifiable features. This process is labour intensive and not easily automated. This is a major limitation of the RGDAS data.
- (2) The fundamental curvature measurement process is sound, and produces curvature or radius measurements that are within 30% (relative error) of the correct value. The data smoothing process that the RGDAS applies to the raw data necessarily smooths and

blurs the data where the data values are changing. This becomes apparent where the arc length of a corner is shorter than the 56 m averaging length, due to either a tight radius or low deflection corner. In these cases, radius measurements are regularly over-estimated by up to 70%. RGDAS measurements for the longer arc length curves show better agreement with the actual radius, with the radius at gentle curves ( $R > 100$  m) being reported to 10% (relative error).

- (3) Gradient measurements accurately reflect the actual (surveyed) gradient, with 95% confidence limits on the absolute error of 1.1%.
- (4) Similarly, RGDAS superelevation measurements show good agreement with the surveyed values and a 95% limit on the absolute error was found to be 2.1% (gradient).
- (5) The RGDAS data gives a reasonable quantitative description of the individual road features, subject to limitations already described. The data does contain small inaccuracies due to data smoothing, transducer drift and other error sources, and owing to these is not at present capable of replacing mapping surveys.
- (6) The RGDAS data contains 'curves' of very high curvature ( $>100/\text{km}$ ) which were caused not by actual curves in the road but by the test vehicle pulling over to stop for various reasons. It is unfortunate that the test procedure was not designed to eliminate these. Post-processing may be able to filter them out automatically, although it is probably impossible to distinguish between a legitimate tight curve and a pullover (not all pullovers were labelled).
- (7) Trends in vertical curvature are shown in RGDAS, with typical measurement accuracy of 0.2/km (around half a typical vertical curvature value). A 56 m moving average adds to the value and usefulness of the data, by smoothing out some of the 'noise' that is present in the RGDAS data.

## 5. STATISTICAL ANALYSIS

A detailed description of the data and methods used in the statistical analysis and the results of the analysis are given in Dr Robert Davies' paper, provided in full in Appendix 2.

Two database files were used in the analysis. A highway file was assembled from the RGDAS (stats) and RAMM extracts described in the previous section. This gives geometry and road conditions for each 200 m segment of the state highway network.

In addition, we have a crash file which gives the segment identifier of each crash that occurred during the period of the study and some details of the crash. Crashes were limited to those for which road geometry may have been a factor.

Preliminary analysis using location-adjusted data described in the previous section seemed to produce seriously anomalous results, suggesting that the adjustments made were too severe. Consequently, unadjusted data were used for the analysis. Undoubtedly some crashes have been assigned to wrong segments, so probably the effects we find in the present analysis are somewhat less than is really the case.

In the present study we restricted attention to road segments classified as rural, two lane, not divided, not motorway, and with no missing values in the data. Also roads with unusually wide or narrow sealed carriageways were omitted, as were a few road segments with obviously incorrect data. This remaining data set has 87 196 road segments (each direction counted separately) and 2365 crashes.

Prior to analysis, scatter plots of variable pairs were prepared and inspected for strong variable correlations, and cumulative distributions of Average Annual Daily Traffic (AADT) were checked for data distortions. No unexpected correlations were found and AADT distributions showed no data distortions of concern. The latter did illustrate that extreme values of AADT could be omitted without substantial loss of total vehicle travel from the data.

The following list summarises the data, and abbreviations used, that are available for each segment and direction.

- Horizontal curvature maximum, minimum and average (HMAX, HMIN, HAV)
- Cross-section slope maximum, minimum and average (XMAX, XMIN, XAV)
- Gradient maximum, minimum and average (GMAX, GMIN, GAV)
- Vertical curvature maximum, minimum and average (VMAX, VMIN, VAV)
- Advisory speed minimum and average (ASMIN, ASAV)
- Advisory speed over previous 400 m, minimum and average (PASMIN2, PASAV2)
- Advisory speed over previous kilometre, minimum and average (PASMIN5, PASAV5)
- Average compass direction (DIR).

## 5.1 The Tables

Road segments were classified by ranges of each of a number of explanatory variables and then the crash rate calculated for each of the ranges, and the results expressed in a table.

Each table gives the ranges of the classifying variable, the observed number of crashes in each of the ranges, the total AADT in that range, and the crash rate in crashes per  $10^9$  VKT (vehicle-kilometres travelled)<sup>(1)</sup>.

### 5.1.1 One Way Tables

Table 1 probably under-estimates the crash rate for the low AADT roads because minor crashes are less likely to be reported on these roads than on the higher AADT roads. Nevertheless the table shows a somewhat higher crash rate for the low AADT roads.

---

(1) The accident rates may need some interpretation. An isolated curve in a road is essentially a point on a road, and vehicle-kilometres travelled over it is not a meaningful concept. More appropriate would simply be total vehicles travelled. However, if we think of the risk item being a 200 m section of road, including a bend, then VKT does make sense.

The rate for roads with AADT at least 20 000 is exceptionally low. These road segments are sections of State Highways 1 and 2 and a section of State Highway 30 in the tourist area of Rotorua. Most likely they should be thought of as essentially urban roads and should be excluded from the study.

Table 1. Classification by AADT.

AADT	<500	0.5-1k	1-2k	2-5k	5-10k	10-20k	>20k
Observed	81	254	432	980	447	161	1
AADT (000)	5271	15 721	29 091	68 075	40 328	15 202	2008
Crash Rate (10 <sup>9</sup> VKT)	84	88	81	79	61	58	3

Minimum advisory speed gives a better relationship with crash rates than average advisory speed, so that is what is considered here in Table 2. The rates for very low ASMIN are probably under-estimates due to reduced reporting rates.

Table 2. Classification by advisory speed minimum (ASMIN).

ASMIN (km/h)	<60	60-80	80-100	100-120	120-140	140-160	>160
Observed	350	586	612	303	376	124	5
AADT (000)	8321	17 949	35 062	33 438	54 569	24 731	1627
Crash Rate (10 <sup>9</sup> VKT)	230	179	96	50	38	27	17

Table 3 shows a low crash rate for HAV (average horizontal curvature) near to zero and increasing as curvature increases either to the left or right.

Table 3. Classification by horizontal curvature average (HAV).

HAV	<-5	-5 to -3	-3 to -1	-1 to +1	+1 to +3	+3 to +5	>+5
Observed	80	176	444	1081	387	124	64
AADT (000)	1672	4547	21 013	123 464	19 190	4249	1561
Crash Rate (10 <sup>9</sup> VKT)	262	212	116	48	110	160	224

Note: Horizontal curvature is the reciprocal of radius, therefore HAV=5 corresponds to a curve radius of 200 m, whereas HAV=1 corresponds to a curve radius of 1000 m.

HDIFF is the difference between maximum and minimum horizontal curvature (HMAX and HMIN), and captures an aspect of the geometry not completely captured by the average curvature, namely road alignment prior to curve entry. Table 4 shows risk rises with increasing HDIFF.

Table 4. Classification by HDIFF = HMAX – HMIN.

HDIFF	<0.1	0.5 to 1	1 to 2	2 to 3	3 to 5	5 to 10	>10
Observed	276	241	255	251	408	468	457
AADT (000)	51 562	31 086	27 092	18 713	21 301	15 223	10 719
Crash Rate (10 <sup>9</sup> VKT)	29	42	52	73	105	168	233

### 5.1.2 Two Way Tables

When considering only one variable at a time we cannot say if any effect in crash rate is due to the variable in question or is due to some other variable which is correlated with the variable in question. As an example, lower AADT roads have higher crash rates. Probably the major reason for this is that lower AADT is associated with more difficult roads, and it is the nature of the road that is causing the higher crash rates rather than the low AADT. The classification variables are considered two at a time in order to try to disentangle this effect.

The following two way tables correspond to the crash rate line (last line) of the preceding one way tables. Because the number of crashes contained in each cell of the two way tables is much smaller than for the one way tables, the statistical fluctuation in the rates is rather larger. We have put the rates in bold when the corresponding observed number of crashes is at least 25 since there is not much accuracy in the data when the number of crashes is less.

Table 5 shows that generally for a given ASMIN, the crash rate is not highly dependent on AADT.

Table 5. Crash rate - classification by ASMIN and AADT.

AADT	Crashes per 10 <sup>9</sup> VKT						
	<500	0.5-1k	1-2k	2-5k	5-10k	10-20k	>20k
ASMIN<60	155	<b>230</b>	<b>271</b>	<b>247</b>	<b>208</b>	94	
60-80	138	<b>161</b>	<b>146</b>	<b>251</b>	<b>126</b>	<b>132</b>	0
80-100	75	<b>91</b>	<b>87</b>	<b>105</b>	<b>94</b>	<b>102</b>	0
100-120	39	46	<b>45</b>	<b>53</b>	<b>55</b>	<b>43</b>	13
120-140	67	37	<b>42</b>	<b>41</b>	<b>32</b>	<b>34</b>	0
140-160	41	33	22	<b>28</b>	<b>30</b>	23	0
>160	0	0	21	26	0	0	

PASMIN2 is the minimum advisory speed over the previous 400 m (two segments). Table 6 shows some evidence of the risk rising towards the top right hand side of the table corresponding to a sudden transition from a high advisory speed to a low advisory speed.

Table 6. Crash rate - classification by ASMIN and PASMIN2.

PASMIN2 (km/h)	Crashes per 10 <sup>9</sup> VKT						
	<60	60-80	80-100	100-120	120-140	140-160	>160
ASMIN<60	196	328	290	339	147	0	
60-80	142	172	186	245	251	160	
80-100	92	117	92	95	72	124	0
100-120	54	78	55	42	44	31	0
120-140	76	67	49	36	30	28	0
140-160	107	58	35	26	25	22	0
>160	0	0	0	0	19	26	0

## 5.2 Poisson Regression Analysis

This section describes the fitting of the Poisson generalised linear model. Each road segment corresponds to an observation. We suppose the number of crashes on this road segment has a Poisson distribution with expected value depending on the AADT and the road geometry.

Suppose  $Y_i$  denotes the number of crashes in the  $i$ th road segment (where  $i$  runs from 1 to  $n$ ), and  $x_{i,1}, \dots, x_{i,m}$  denote  $m$  explanatory variables (e.g. geometry variables). The generalised linear model for the Poisson distribution with  $\log_{10}$  link function supposes that the  $Y_i$  are independently distributed with Poisson distributions and

$$E(Y_i) = \lambda_i = \gamma_i \exp \left( \beta_0 + \sum_{j=1}^m x_{i,j} \beta_j \right) = \gamma_i e^{\beta_0} \prod_{j=1}^m \exp(x_{i,j} \beta_j) \quad (3)$$

where the  $\beta_j$  are the unknown regression coefficients which need to be estimated. We let  $\gamma_i$  be the AADT for the segment since we expect the number of crashes to be approximately proportional to the AADT. The last expression can be interpreted as expressing the crash risk as a product of risk factors. We used the S-plus statistical package for fitting the Poisson model. S-plus includes this as one of its standard analyses. One can test for the statistical significance of each of the explanatory variables in much the same way as one does in an analysis of variance using a quantity known as the deviance<sup>(2)</sup>.

We cannot expect a generalised linear model to fit over a wide range of values of the explanatory variables, so we removed the data with extreme values of AADT and horizontal

(2) Note that we cannot use the residual deviance for assessing goodness of fit as is commonly done because of the small average number of crashes per segment.

curvature (Table 7). This left 24 896 road segments and 1053 crashes in our analysis using the most restricted set of data (subset I). We carried out two analyses. One used HAV, HDIFF and XAV (average superelevation). The other used ASMIN (minimum advisory speed) and PASMIN2 (minimum advisory speed over the previous two segments). Both also included  $\log_{10}(\text{AADT})$ , gradient, vertical curvature, sealed carriageway width and direction as possible explanatory variables. In the first analysis we found HAV, HDIFF as the most statistically significant explanatory variables, with gradient and direction also being significant. In the second analysis, ASMIN and PASMIN2 were strongly significant, with some interaction. Gradient and direction were also significant as before. We entered most of the variables as polynomial functions to allow for non-linearity in the relationship.

Table 7. Key variables in Poisson generalised linear model.

	Data numbers		Using raw geometry	Using derived advisory speeds
	Road segments	Crashes		
<u>Subset I</u> 2000 ≤ AADT < 20 000 HDIFF ≤ 10 ASMIN ≥ 80	24 896	1053	HAV (quadratic) HDIFF (quadratic) DIR (discrete) GAV (quadratic) AADT* (logarithmic)	ASMIN, PASMIN2 (bivariate quadratic) DIR (discrete) GAV (quadratic) AADT* (logarithmic)
<u>Subset II</u> 500 ≤ AADT < 20 000 HDIFF ≤ 20 ASMIN ≥ 60	66 711	1944	HAV (quartic) HDIFF (cubic) DIR (discrete) GAV (quadratic) AADT* (quadratic logarithm) SCW (quadratic)	ASMIN, PASMIN2 (bivariate quadratic) DIR (discrete) GAV (quadratic) AADT* (logarithmic) SCW (quadratic)

\* For AADT effects other than direct proportionality - not quite significant at the 95% level for subset I.

These two analyses were repeated on the less restricted set of data (subset II) and gave similar results, except that now  $\log_{10}(\text{AADT})$  and SCW (sealed carriageway width) were also found to be significant. The higher order polynomials needed for subset II and the interaction of the advisory speed variables are more complex models to interpret, as shown in Appendix 2. In further discussion here only the first analysis of subset I is considered in detail.

The relative risk due to each factor can be derived from equation (3). They are easiest to understand when expressed graphically. We have done this for the first analysis in Figure 17. In each case, the middle line is the estimate and the outer lines are confidence intervals corresponding to two standard errors so they are about 95% confidence intervals.

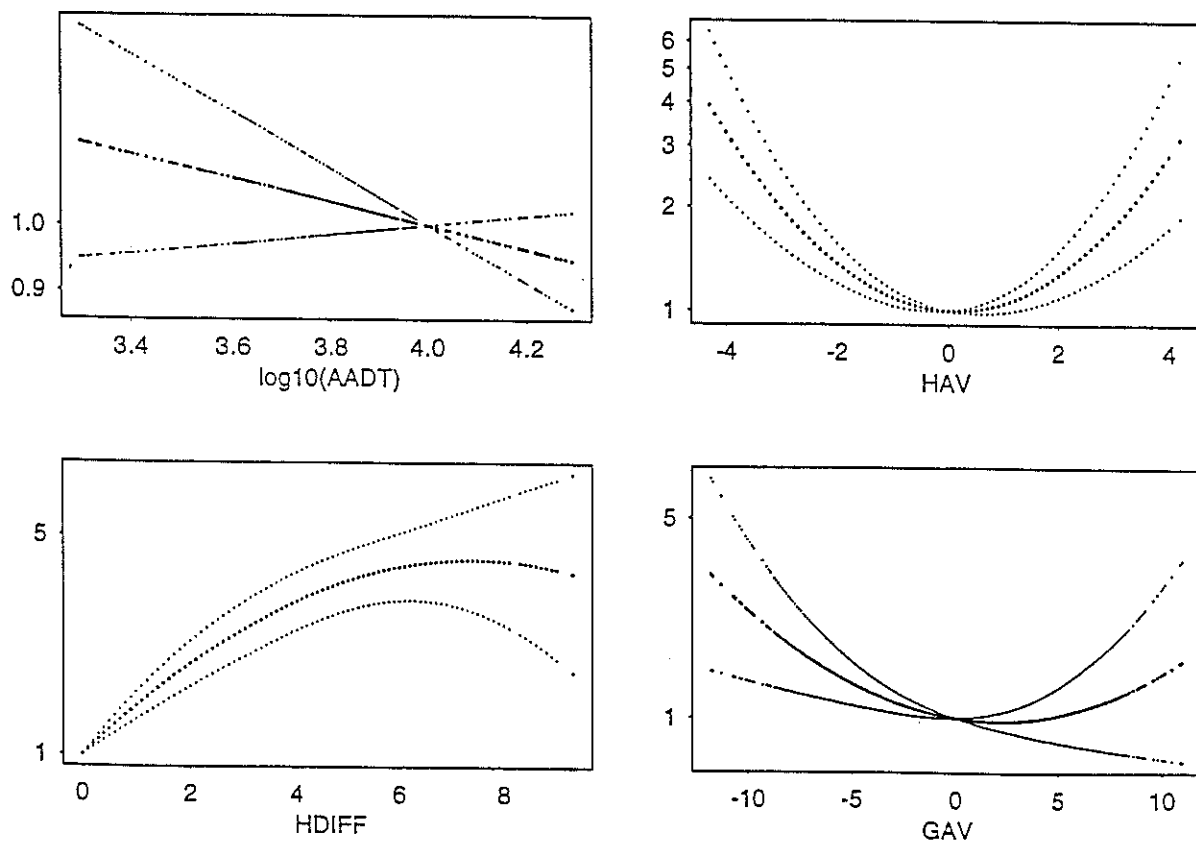
In order to illustrate the use of these graphs, consider a 200 m road segment with average horizontal curvature (HAV) equal to 3 (i.e. 333 m radius), and difference between the maximum and minimum curvature (HDIFF) equal to 4 (say corresponding to a 250 m radius curve and a straight). Now suppose the road is realigned so that HAV is equal to 2 (i.e. 500 m radius) and HDIFF also equal to 2 (e.g. 500 m radius curve and a straight). The change in relative risk is calculated in Table 8.



Table 8. Example of change in crash risk.

	Before Realignment		After Realignment	
	Value	Relative Risk (from Figure 17)	Value	Relative Risk (from Figure 17)
HAV	3	1.77	2	1.26
HDIFF	4	3.08	2	1.95
Product		5.45		2.46

Figure 17. Relative risk versus AADT, HAV, HDIFF and GAV.



Thus the realignment would reduce the risk by a factor of  $5.45/2.46 = 2.2$ . However, care should be exercised when applying the Poisson model as in this illustrative example because:

- (a) all the numbers involved are subject to substantial statistical error;
- (b) the relative risk curves are unlikely to be of the exact form fitted;
- (c) the road geometry is typically far more complicated than is captured by the parameters utilised here; and

- (d) it has not been possible to align the crashes exactly with the road segments, resulting in some inevitable smudging of the information.

The risk (per  $10^9$  VKT) for a particular set of the key variables can be calculated as follows:

$$\text{Risk} = 54.92 (\text{DIR}) \exp \{ -0.0180 \text{HAV} + 0.0695 \text{HAV}^2 + 0.388 \text{HDIFF} - 0.0262 \text{HDIFF}^2 - 0.0252 \text{GAV} + 0.00613 \text{GAV}^2 - 0.189 \log_{10}(\text{AADT}) \} \quad (4)$$

where  $\text{DIR} = 1$  if the direction effect is ignored, or  $\text{DIR}$  can range from 0.74 to 1.44 as tabulated in Appendix 2 for specific directions.

For example, at a segment with  $\text{HAV} = 3$ ,  $\text{HDIFF} = 4$ ,  $\text{GAV} = 0$  and  $\text{AADT} = 10\,000$ , then (ignoring the direction effect) the risk of a crash is calculated to be  $142 \times 10^{-9}/\text{VKT}$ . Since yearly travel is 365 000 vehicle-kms (assuming 5000 vehicles per day in each direction over the 0.2 km segment), this risk converts to about one crash every 19 years. Note that this is one reported geometry related crash on a segment of this type on the rural state highway network, every 19 years, and could be considerably lower than the total crash rate from all factors relevant to this segment.

### 5.3 Additional Analyses

Particular extensions to the Poisson generalised linear model were constructed to study specific aspects of the data. In all cases, a comparison was made of two possible contrasting conditions as follows:

- State Highways 1 and 2 compared with the rest.
- "Coarse" compared with "smooth" surfaces.
- "Newer" compared with "older" surfaces.
- Wet road compared with dry road.
- Alcohol and drug factors present compared with these factors absent.
- Overtaking and head-on crashes compared with single vehicle crashes.

Details of these analyses are given in Appendix 2.

Crash rate on State Highways 1 and 2 is found to be 15% higher than that for the rest of the highways. This may just reflect more intensive patrolling and therefore more complete reporting.

Coarse surfaces appear to be more risky on straighter sections of highway, but less risky on windy sections. However, this effect is small and only just statistically significant.

Newer surfaces were found to have a reduced crash rate, being about 83% of the rate for older surfaces.

The effect of wet or dry road on the geometry variables was small and probably cannot be considered reliable. For instance, it was necessary to assume that there was no relationship between the geometry variables and the fraction of time a road is wet or dry, yet it is probable that windy roads are associated with hill country and therefore with more rain. This

may account for the small effect found that windy roads have a higher crash rate when wet rather than dry, and relatively straight roads have a higher rate when dry rather than wet.

In the comparison of geometry related crashes in which alcohol or drugs were implicated and were not implicated, no significant effects were found.

When overtaking and head-on crashes were compared to single vehicle crashes, significant effects related to traffic volume and curve severity were found. Single vehicle crashes were found to be less likely the greater the traffic volume, but the converse effect was not significant, i.e. the expected increase in risk of overtaking or head-on crashes with increasing traffic volume, although evident as a trend in the data, was not significant. With respect to curve severity, the risk of an overtaking or head-on crash was increased for left turning curves (negative HAV values) compared to right turning curves. Conversely, the risk of single vehicle crashes was increased for right turning curves (positive HAV values) compared to left turning curves.

## **6. DISCUSSION OF RESULTS**

### **6.1 Comparison with a Previous New Zealand Study of Crash Curve Geometry Relationships**

Matthews and Barnes (1988) constructed a database incorporating all curves on the 2000 km long state highway (State Highway 1) running the length of New Zealand. Also the route positions, angles of turn, direction of turn, lengths of adjacent tangents, traffic volumes and gradients were entered into the database in addition to the total amount of curvature in the 2 km of roadway preceding each curve. Details of crashes were derived from the TAR system over a five year period (1982-1986). The total number of crashes analysed to determine the effect of road and curve geometric elements on curve crashes were 1082 compared with 2365 total and 1053 in subset I in the present study. However, it should be noted that Matthews and Barnes in their analysis excluded curves on State Highway 1 with angles less than  $10^\circ$  (for a tangent length of 100 m this corresponds to a radius of 573 m), in restricted speed limit zones, or on sections of four lane highway, whereas the present study was confined to all curved on normal (i.e. not divided) two lane rural state highways.

Matthews and Barnes showed that the amount of prior curvature had the largest effect followed, in descending order, by gradient, radius, tangent length and direction of turn. Evaluation of the effects of combinations of elements showed that crash risk was particularly high on short radius curves located at the end of long tangents, on steep down gradients, or on relatively straight sections of highway. These findings are consistent with the present study which additionally considered straight road crashes, lane width, super-elevation, surface type and surface age, and gives confidence in the derived Poisson generalised linear model considering the independence of the studies.

## 6.2 Effects of Prior Highway Geometry

Matthews and Barnes included previous 2 km curvature (defined as the sum of the curve angles) and previous tangent length, and found both to be significant. In the present study we have used advisory speed minimums and averages over the previous 400 m and 1 km to provide a measure of prior highway geometry. The most significant of these was the minimum advisory speed in the previous 400 m. This is compatible with Matthews and Barnes' findings since, although they used curvature from the previous 2 km and had tangent lengths up to 2 km or more, most crash rate variation was found for tangent lengths less than 200 m and for previous curvatures less than 50°. (This curvature would be mostly from a previous curve, no more than 150 m from the crash curve, that is always present in the prior roadway curvature factor defined by Matthews and Barnes.)

There is an interaction between the minimum advisory speed at the crash location and the minimum in the previous 400 m. The relationship is complex but indicates:

- (a) for crash locations on more or less straight road (minimum advisory speed<sup>(3)</sup> >110 km/h), crash risk increases the lower the minimum advisory speed in the preceding 400 m of road;
- (b) for crash locations at severe curves (minimum advisory speed <70 km/h), crash risk decreases the lower the minimum advisory speed in the preceding 400 m of road.

For the first effect the data of Table 6 shows that the risk on a road with a minimum advisory speed of 130 km/h increases by a factor of 2 if the previous 400 m minimum advisory speed decreases from 130 km/h to 70 km/h. For the second effect the risk is decreased by 30% at a curve with a minimum advisory speed of 70 km/h for the same decrease in the previous 400 m.

Note, however, that because curves are more risky than straights, the reduction in crash rate is greater for the second effect (79 crashes/10<sup>9</sup> VKT) than the first (37 crashes/10<sup>9</sup> VKT).

The first effect is unexpected but, if real, indicates straight road manoeuvres soon after a curve are more risky than further along the straight. Perhaps this is impatient overtaking after a windy road section.

The second effect is not unexpected and is interpreted as the prior highway geometry providing speed control or warning for the potential crash site. This effect was significant in the curve crash data presented by Matthews and Barnes.

## 6.3 Curve Severity

As expected, a road segment with higher curvature is found to have a significantly higher crash rate. This effect is large. For example, Table 3 shows crash rates on a segment with average horizontal curvature of 4 rad/km (average radius of 250 m) to be up to four times that

---

(3) Minimum Advisory Speed as defined in equation (1), Section 3.1.3.

on segments that are straight or have average horizontal curvatures no greater than 1 rad/km (average radius of 1000 m).

The minimum advisory speed of a road segment is determined primarily by the maximum horizontal curvature, and Table 2 shows again the size of the curve severity effect. Segments with a minimum advisory speed between 60 and 80 km/h have a crash rate six times that of nearly straight segments with minimum advisory speeds between 140 and 160 km/h.

The horizontal curvature data in Table 3 also shows an effect related to direction of turn with crash rates higher for negative curvatures (left turning). This effect was also reported by Matthews and Barnes, and is usually attributed to better apex visibility allowing better driver perception of the curve severity for right turning curves.

#### **6.4 Gradient**

Road gradient was found to be a significant factor, and if the grade is descending or ascending was also found to influence the crash rate. This is illustrated in Figure 17 where the relative risk, calculated from the Poisson generalised linear model for subset I data, is shown as a function of the average gradient of the road segment. The crash rate is shown to be about 2.5 times the zero grade rate for a -10% grade (i.e. descending) but only about 1.5 times for a +10% grade. These effects are similar to those found in the curve crashes study of Matthews and Barnes. Their data also showed the minimum crash rate as a function of gradient occurred for ascending grades between 3 and 5%. Such a minimum is evident here in the data presented in Figure 17. Change in vehicle stability is probably the underlying cause of higher risk on descending grades. For straight or nearly straight road segments, unsafe speeds are more likely, and for curves, reduction of road/tyre friction is more likely when descending.

#### **6.5 Direction of Travel**

Unexpectedly, the direction of travel on a road segment was found to be a significant factor. Northerly/southerly travel was found to give a higher crash rate than easterly/westerly travel. The effect was substantial, with the worst direction (SE) showing a crash rate nearly twice that of the best direction (W), as detailed in the Poisson model analyses for data subsets I and II in Appendix 2.

No explanation of this effect has been found. It is tempting to attribute the effect to New Zealand's north/south orientation and alignment of major population centres and/or New Zealand's dominant topography of northeasterly/southwesterly mountain ranges. Thus it could be argued that roads linking major population centres would be more busy and therefore more risky, and roads directed normal to the mountain ranges (i.e. NW/SE) would be more windy and therefore more risky. However, exposure factors such as these should already be accounted for in the model by the normalisation with respect to AADT and total travel.

#### **6.6 AADT**

Traffic volume was found to have a minor effect on crash rate in addition to the direct proportionality assumed in the normalisation of the Poisson model. The effect was not quite

significant at the 95% level for the subset I data, as evident in the relative risk plot of Figure 17 where a horizontal line can be drawn within the 95% confidence limits. The effect for subset II data is significant and shows a peak in the relative risk at an AADT just greater than 2000 (Appendix 2, Figure 21). Table 1 also shows the same effect, although in this case the peak appears at an AADT just less than 1000, due presumably to interaction from other factors. The lower than expected crash rate at lower AADT values is possibly a result of under-reporting, but it is not clear why the higher AADT values should also show a lower than expected crash rate. The AADT effect beyond proportionality is small compared to the primary variables of curvature and grade, and is possibly a result of a correlation residual that the model cannot unravel. Thus the higher AADT roads tend to be those with lower values of average grade and average horizontal curvature, and this may still be influencing the model parameters.

### **6.7 Sealed Carriageway Width**

Sealed carriageway width was found to be a significant factor for the subset II data and, as with AADT, shows a peak in the relative risk (Appendix 2, Figure 25). The peak risk occurs at a width of about 10.5 m and the decrease in risk for greater widths is probably to be expected. It is surprising, however, that risk should decrease for more narrow roads, and the reasons for this are not clear. Again, it could be under-reporting but the effect seems too large given that the risk at a width of 6 m is almost half the peak risk. Perhaps it is due to a substantial behavioural effect in that drivers take a lot more care when roads are narrow, and/or there are severe roadside hazards present such as cliffs.

## **7. EFFECT OF SHAPE CORRECTION ON CRASH RISK**

The significant role of small radius curves in road crashes is well known and the problem is most noticeable on rural roads. Severe crashes and single vehicle crashes are disproportionately associated with curves with a radius of 600 m or less (Johnston 1982). A critical design parameter for such curves is superelevation, defined as the gradient from the centreline to the edge of the road width and taken to be positive if the pavement falls towards the centre of the curve. For a given curve radius and speed, a set force is required to maintain a vehicle in its path as it traverses the curve and, in road design, this is provided by side friction developed between tyre and pavement and by superelevation. Therefore the superelevation adopted is primarily on the basis of safety. Use of maximum superelevation occurs where the radius of curvature approaches the minimum for the speed environment. Normally, this will occur in steep terrain where there are often constraints on increasing the radius of a curve.

Because a road surface may be periodically shape corrected to improve its smoothness, a critical issue requiring investigation is whether current practices produce significant departures from the design superelevation, either by decreasing the rate of superelevation or by introducing abrupt changes in superelevation through resulting changes in road surface levels. Such poor shape correction practices, if left unrectified, in some situations may cause a sharp increase in the friction demand by a vehicle travelling at the design speed as it enters the

curve in question. While it can be shown that the friction value may be within the normal range drivers use, a sudden change in friction demand will lead to a sudden change in steering attitude of a vehicle negotiating the road and hence increased risk to run-off-road and head-on crashes. Therefore, although recent research efforts have provided considerable insights into the relationship between curve geometry and crashes, leading to various safety improvements on horizontal curves, an area that requires attention is whether crash rates on curves increase after shape correction. From the preceding discussion, an increase in crash rate could result from an increase in friction demand caused by superelevation deficiency (defined to be the difference between the design superelevation and the actual superelevation after shape correction) or from too great a rate of rotation of the pavement defined by the relation below:

$$\text{rate of rotation (radians/sec)} = (e_2 - e_1)V_d / 3.6L \quad (5)$$

where L = road section length of interest (m)  
 $e_1, e_2$  = superelevation at ends of road section length (m/m)  
 $V_d$  = design speed (km/h)

The rate of rotation of the pavement should not generally exceed 0.025 radians per second of travel time at the design speed with a maximum rate of 0.035 radians per second (AUSTROADS 1989). A rate of angular rotation of 0.025 radians per second is equivalent to a rate of change of superelevation of 2.5% per second. These rate of rotation criteria are based on vehicle occupant comfort considerations and so should be regarded as being reasonable but not inherently correct.

## 7.1 Statistical Study of Crash Sites

A subset of crashes relevant to this investigation is available from the RGDAS/RAMM/TAR database, and covers the period July 1987 to June 1992. Whilst it was originally suggested that only crashes in the lower half of the North Island be included in this study so that it would be feasible to visit them, this restriction was found to reduce the data set to such a small size that it threw doubt on whether any useful conclusions could be drawn. It was therefore decided to retain the crash data for the whole country.

Sites which had not had resurfacing, realignment or reshaping work carried out in the study period, or for which dates of modification were uncertain, were discarded from the data set, leaving some 320 records. Distinguishing between reshaped sites (to be included in this study) and realigned or resurfaced sites (which must be discarded) proved to be difficult, as the RAMM data provides only dates of modification, and not a full description of what modification was carried out. It was therefore necessary to contact each regional Transit New Zealand office in order to establish what had been done at each site.

One hundred and sixty four crash records were left once only shape correction modifications were included in the data set. Within this set only 28 sites had more than a single crash and only two sites had more than four crashes over the sample period. Because of this, the statistical analysis clearly could not focus on individual highway segments and so all 164 records were used to correlate the crash likelihood before and after shape correction modifications were made.

### 7.1.1 Statistical Analysis

The statistical analysis compared the expected outcome of having a crash before the modification date with the observed outcome. The null hypothesis used to compare with the observed data was that shape correction had no effect on the crash rate. For the null hypothesis each crash was treated as a binomial event with a probability of happening before the modification,  $p_i$ , given below:

$$p_i = A_i / T_i \quad (6)$$

where  $i$  = observation number (1... n)  
 $n$  = number of observations  
 $A_i$  = observation time before crash  
 $T_i$  = total observation time

Let  $X$  be the number of crashes occurring before modification. Then the expected value of  $X$  under the null hypothesis is  $\sum p_i$ . This expected outcome was compared with the actual number of crashes that occurred before shape correction. The standard deviation for a binomial sample is calculated as:

$$\sigma = \sqrt{\sum p_i (1 - p_i)} \quad (7)$$

The results were considered significant if the difference between the expected and observed outcomes was greater than two standard deviations.

With this analysis the road modification date should be independent of crash occurrences. Thus modifications made to highway segments in response to a crash or crashes need to be eliminated from the study. Unfortunately the decision to modify a road is rarely based solely on safety or the crash history of a road, although the decision will often include safety considerations as part of the justification. Responses from Dunedin, Hamilton, Napier and Wellington Transit New Zealand offices indicated that none of the shape corrected sites were modified primarily on safety grounds. These four regions were taken as being representative of all the sites, and so none of the highway segments were eliminated.

### 7.1.2 Results

Number of crashes on shape corrected sites ( $n$ ) = 164.

Number of crashes that occurred before shape correction ( $X$ ) = 81.

Expected number of crashes before shape correction ( $\sum p_i$ ) = 71.9.

$\sigma$  = 5.58.

Difference between the expected and observed outcome =  $-1.63\sigma$ .

### 7.1.3 Discussion

The outcome suggests that shape correction reduces the number of crashes, however the following points need to be considered.



The size of the data set is too small to be conclusive. This is apparent from the observed number of crashes before modification being only 1.63 standard deviations from that of the correction having no effect.

The data is biased due to the fact the likelihood of having a crash may be decreased after a crash occurs. This comes about because after a serious crash action is taken to make the piece of road safer. This may involve road modifications or other improvements such as painted lines and signs which will reduce the likelihood of a crash. These additional influences could not easily be quantified and so were not considered in the study.

Differences in the quality of the shape correction work tend to pull the actual outcome toward the null outcome. This means that the effect of poorly modified sites will be cancelled out to some extent by sites that have been properly shape corrected. This appears to be unavoidable as there are no single sites that have a sufficient number of crashes to give statistically significant results. Thus a multiple site analysis must be used.

Changes in traffic volume will affect the number of crashes occurring.

For the reasons stated above the statistical study is inconclusive in finding a link between shape correction modifications and crash likelihood. It is very difficult to design a study that will produce significant results given the available data. A more useful approach to this problem may be to split the study into two parts. The first part would be to investigate the road geometry before and after shape correction modifications, thereby physically establishing the quality of the work. The second part would be to use the risk models developed in this project to establish the influence of those road features affected during shape correction work (e.g. superelevation, etc) on the crash likelihood. This approach has the advantage of increasing the amount of data available to both studies thereby improving the quality of the results. The external influences and bias in the data are better isolated or eliminated and other studies can also be used to help verify the data giving improved confidence in the results.

## 7.2 Road Curvature and Superelevation

State Highway 58 was studied in a qualitative manner, without any statistical analysis, to see if there were commonly occurring geometric features of the roads at crash sites. This highway segment was chosen because its proximity allowed site investigation if necessary and the crash likelihood is high. The horizontal curvature, superelevation and their rates of rotation were studied using RGDAS data which was collected from March through June in 1992. The yaw rate of rotation and the roll rate of rotation were calculated as shown below.

$$\text{Yaw rate of rotation, } dH/dL = H_{i+1} - H_{i-1} / 2\delta L \quad (8)$$

$$\text{Roll rate of rotation, } dX/dL = X_{i+1} - X_{i-1} / 2\delta L \quad (9)$$

where H = horizontal curvature (radians)  
X = superelevation (%)  
 $\delta L$  = distance between adjacent points (km)

AUSTROADS recommended rotation rate for roll is 0.035 rads/s which equates to 126%/km at 100 km/h travelling speed, 158%/km at 80 km/h and 252%/km at 50 km/h.

Crash records for State Highway 58 over the period 1990 to 1994 were extracted from the TAR database and were used to identify crash prone parts of the highway. Crashes occurring at intersections and on straight pieces of State Highway 58 were eliminated from the data set. The stretch of highway from RP8 to RP10 was realigned during the study period, and crashes that occurred on this section after modification were eliminated from the investigation. The remaining crashes were associated with the increasing (Haywards to Paremata) or decreasing (Paremata to Haywards) RGDAS State Highway 58 data using the direction vehicle 1 was travelling in, as given in the TAR database. The crash positions were plotted using RP numbers given in the TAR database. While adjustments were made to the RP values to transform them to the RGDAS measured distance, there will still be some error in the crash positions given the errors in the RGDAS distances and the reported crash positions.

### 7.2.1 State Highway 58

Curves referred to in the discussion below are related to the RGDAS plots in Figures 18 to 22. The subscripts i or d refer to the increasing or decreasing data sets, and a curve or road segment is identified by the same letter in both the increasing and the decreasing data plots.

The curves  $A_i$ ,  $A_d$ ,  $B_d$ ,  $C_d$ ,  $D_i$ ,  $D_d$ ,  $F_i$ ,  $H_d$ ,  $I_i$ ,  $J_i$ ,  $K_i$ ,  $K_d$ ,  $N_i$ ,  $R_d$ ,  $S_i$ ,  $U_i$ ,  $W_i$ ,  $Y_i$  and  $Z_d$  on State Highway 58 have more than one crash on them. Commonly occurring features of these curves are some degree of mismatch between the horizontal curvature and the superelevation and a roll rate of rotation greater than the limit specified in AUSTROADS. Other features present to a lesser degree are large yaw rate of rotation (curves which 'tighten up'/straighten out quickly) and 'dips' in the curvature plots indicating curves with a non-uniform increase/decrease in curvature, effectively producing two apexes through the corner. Such curves are termed "broken back" curves and may have a safety impact when a driver "sets their line" on one course only to have the curve "tighten" up as they pass through it.

The final section of State Highway 58 (RP11 to RP15) has many curves with high roll and yaw rates of rotation. Whilst the speed is restricted over most of this section, the roll rates of rotation are still too high even when a 50 km/h design speed is used to calculate the limit. Examples of such curves are curves  $K_i$ ,  $P_d$ ,  $Q_i$ ,  $V_i$ ,  $W_d$ ,  $X_d$ ,  $Y_i$  and  $Z_d$ . While a large number of these curves are crash sites, many are not. Although no definite conclusions can be drawn from the data, the high rates of rotation, especially roll rate, appear to contribute to crashes. Similarly superelevation and horizontal curvature mismatches, while not unique to crash sites, do appear to be a contributory factor to the crashes.

Although non-uniform changes in horizontal curvature do not feature significantly at multiple crash locations, there are enough isolated crashes where non-uniform changes in curvature are one of the geometric features for it to warrant mention. The varying rate of change of curvature through a curve is often associated with, or causes, a mismatch between the superelevation and horizontal curvature. Examples of such curves are  $A_d$ ,  $D_d$ ,  $E_i$ ,  $G_i$ ,  $H_i$ ,  $J_i$ ,  $L_d$ ,  $M_i$ ,  $R_d$ ,  $S_d$ ,  $T_i$ ,  $U_i$ ,  $Z_d$ .

Crashes where alcohol was tested for and exceeded the legal limit did not influence the results as there were only five such crashes.

Where a crash history is developing, the use of RGDAS data to identify contributory factors at a more detailed level is seen as worthwhile. Issues such as adverse superelevation, loss of superelevation within a curve, "broken back" curves and "sub-standard" curves may be identified without expensive surveys through RGDAS.

Given that much of the New Zealand state highway system has evolved rather than having been designed, further research into the accident rates on adequately designed highways, i.e. those conforming to the Austroads and Transit New Zealand guidelines and those that do not, is seen as worthwhile.

It is of interest to note that the typical accident rates used to assess the benefits of a geometric improvement consider all highway lengths within a given description regardless of whether or not they conform to good design practice.

Figure 18. State Highway 58 as RGDAS X-Y traces, both directions.

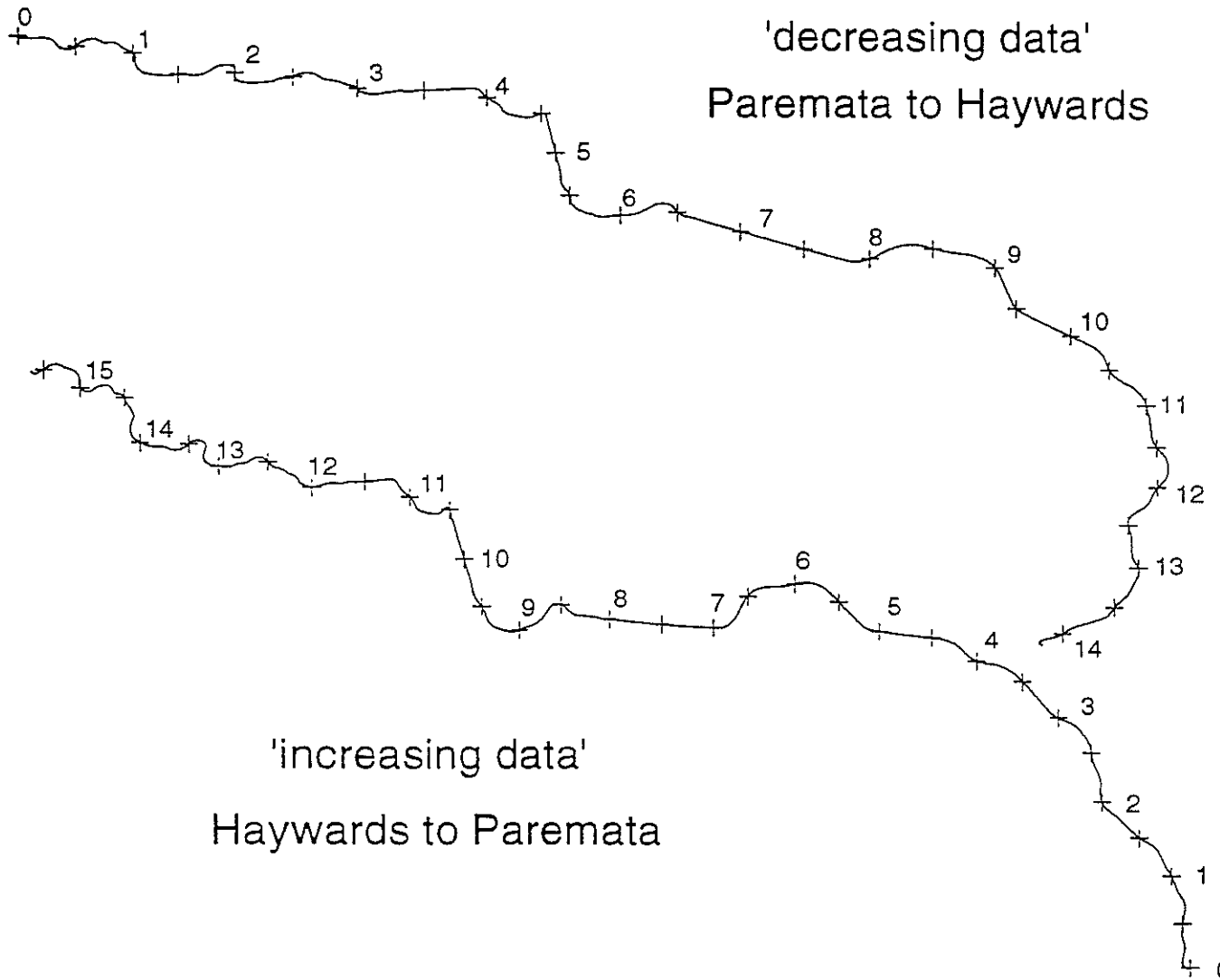
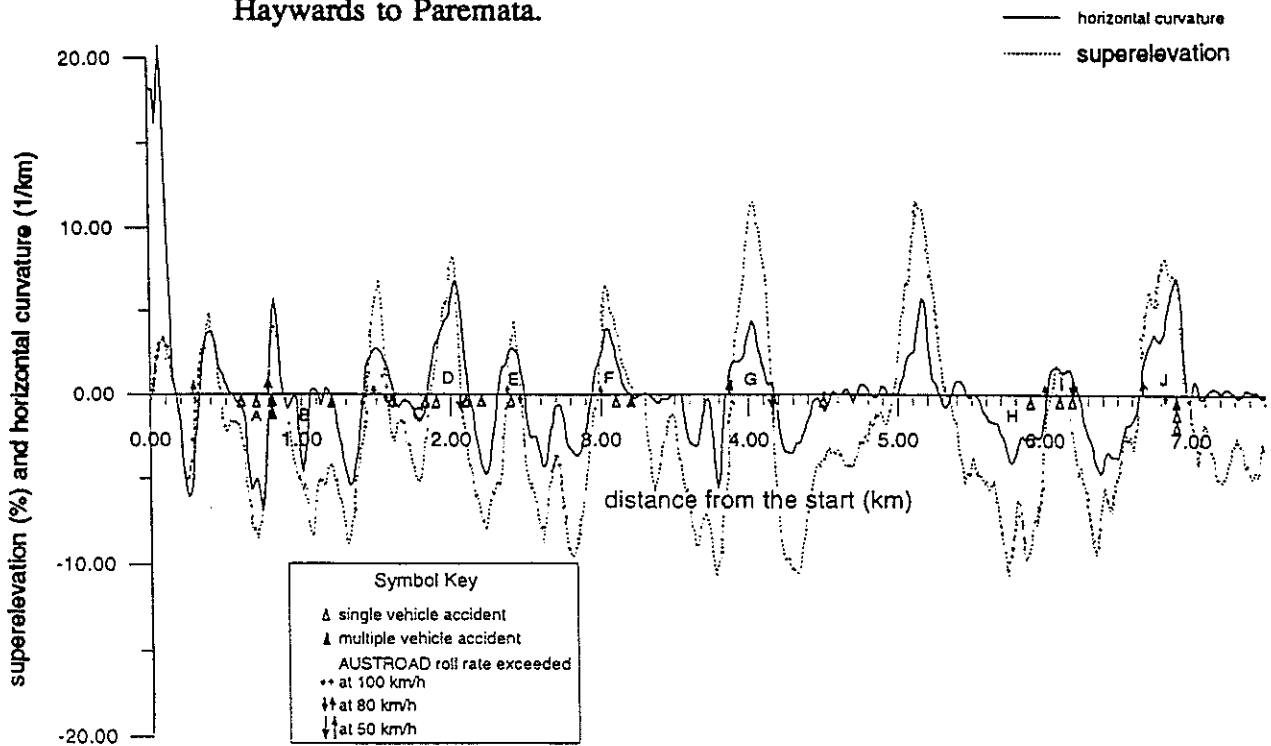


Figure 19. State Highway 58, superelevation and horizontal curvature. Haywards to Paremata.



SH58 - increasing

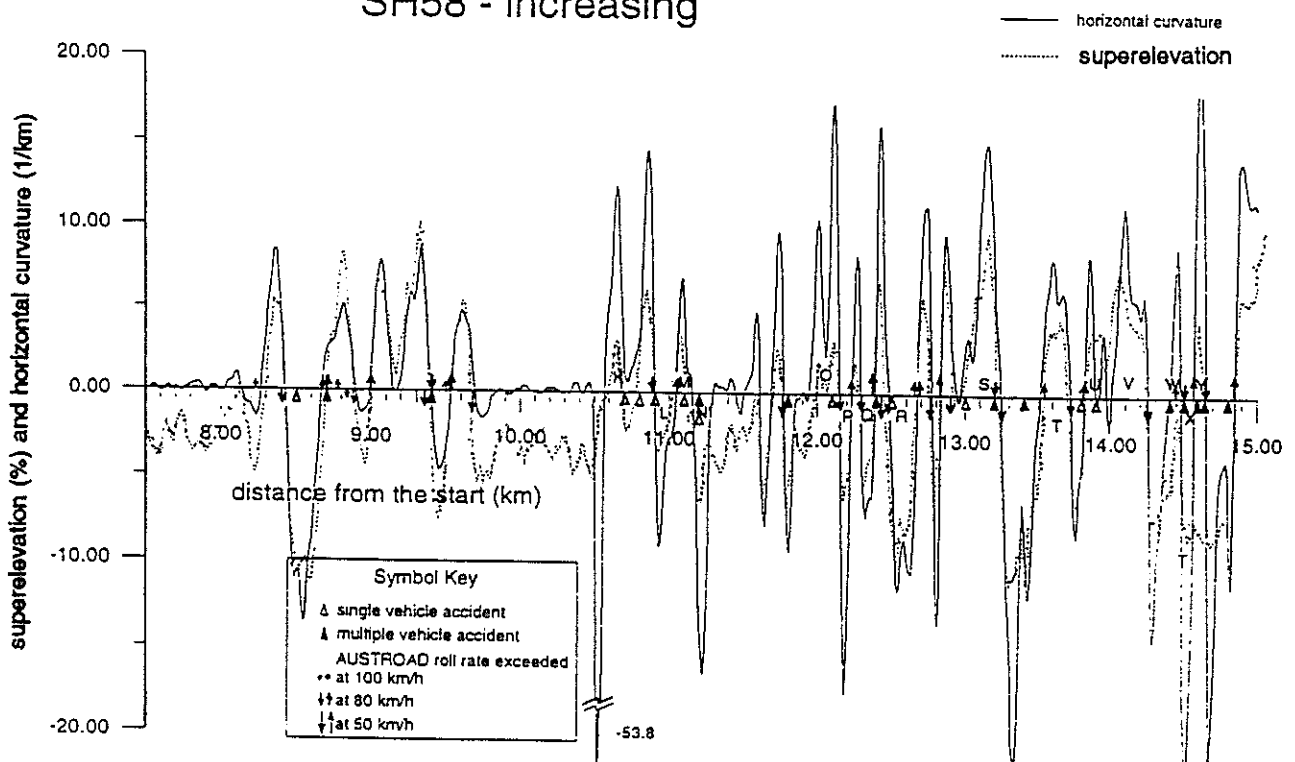


Figure 20. State Highway 58, yaw rotation rate and roll rotation rate. Haywards to Paremata.

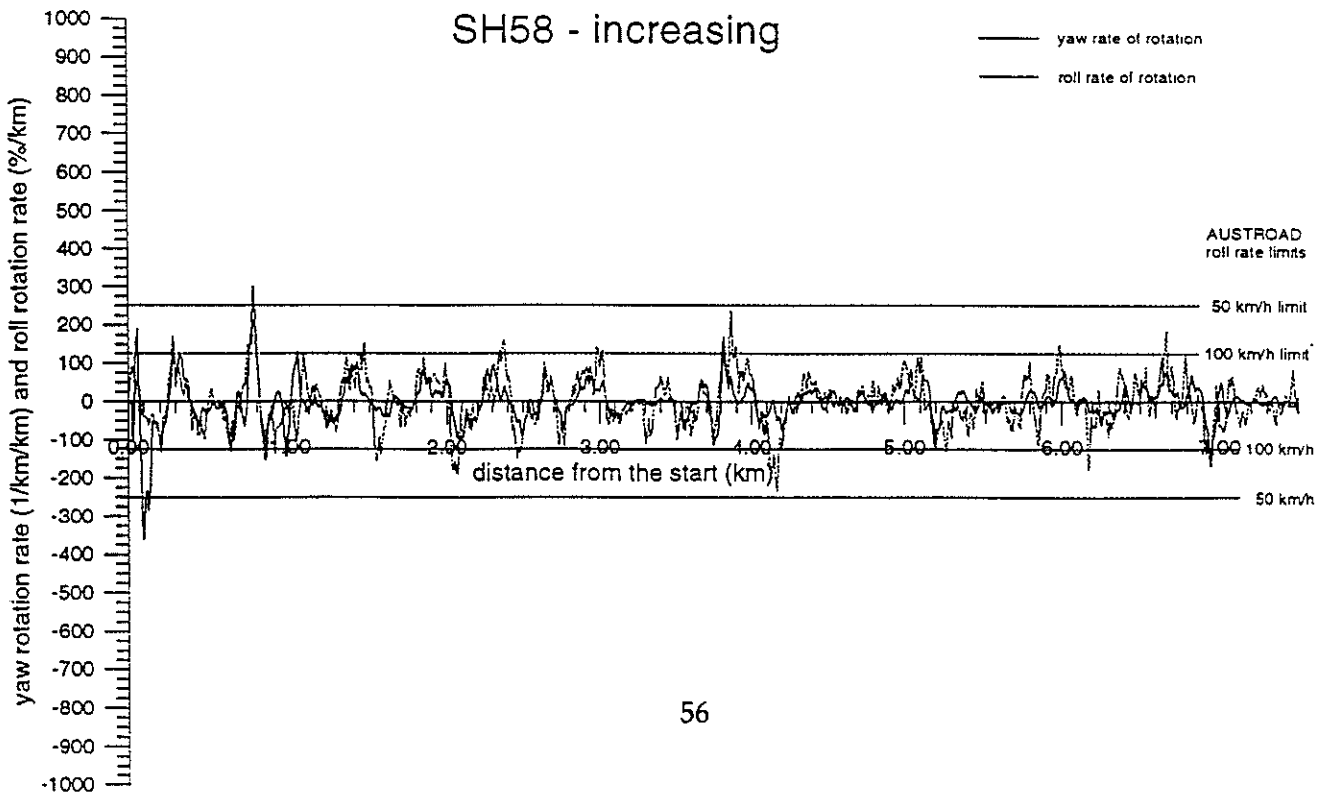
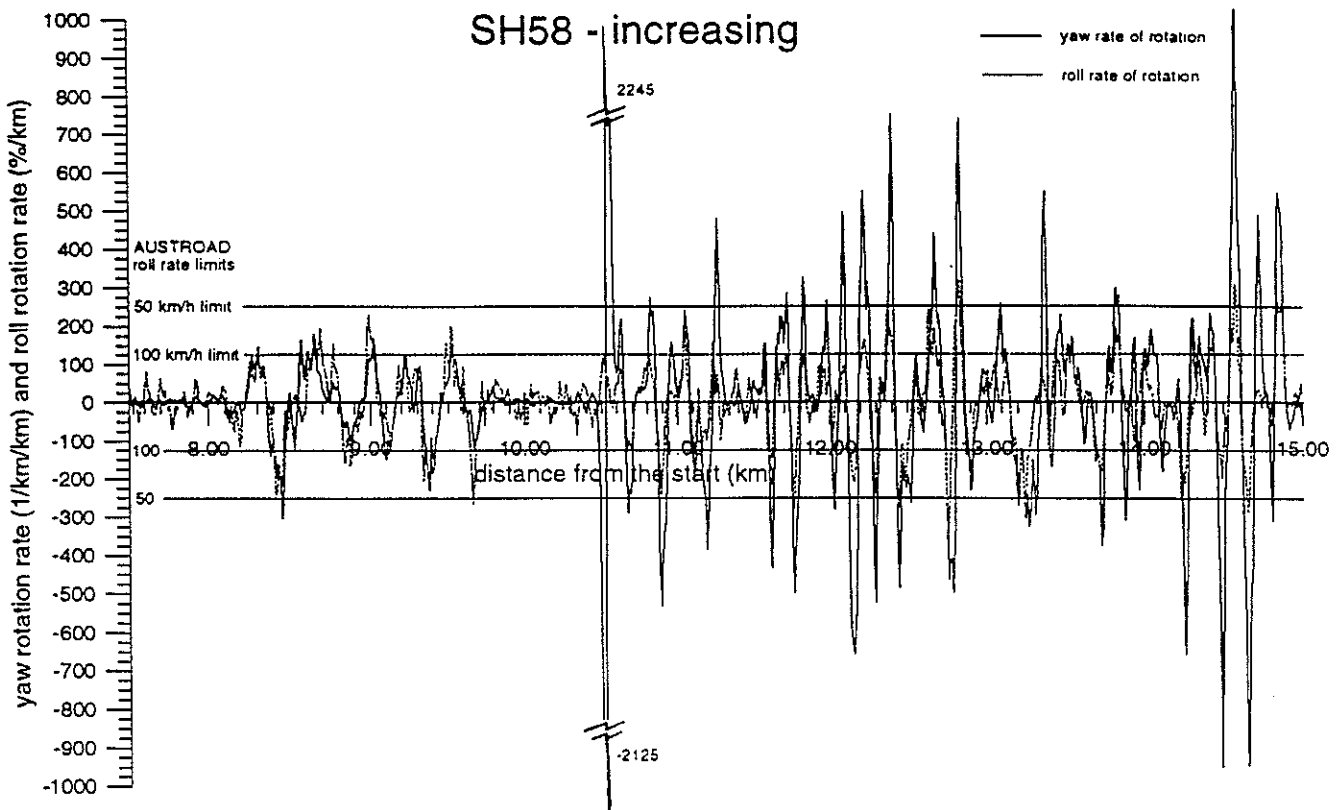


Figure 21. State Highway 58, superelevation and horizontal curvature. Paremata to Haywards.

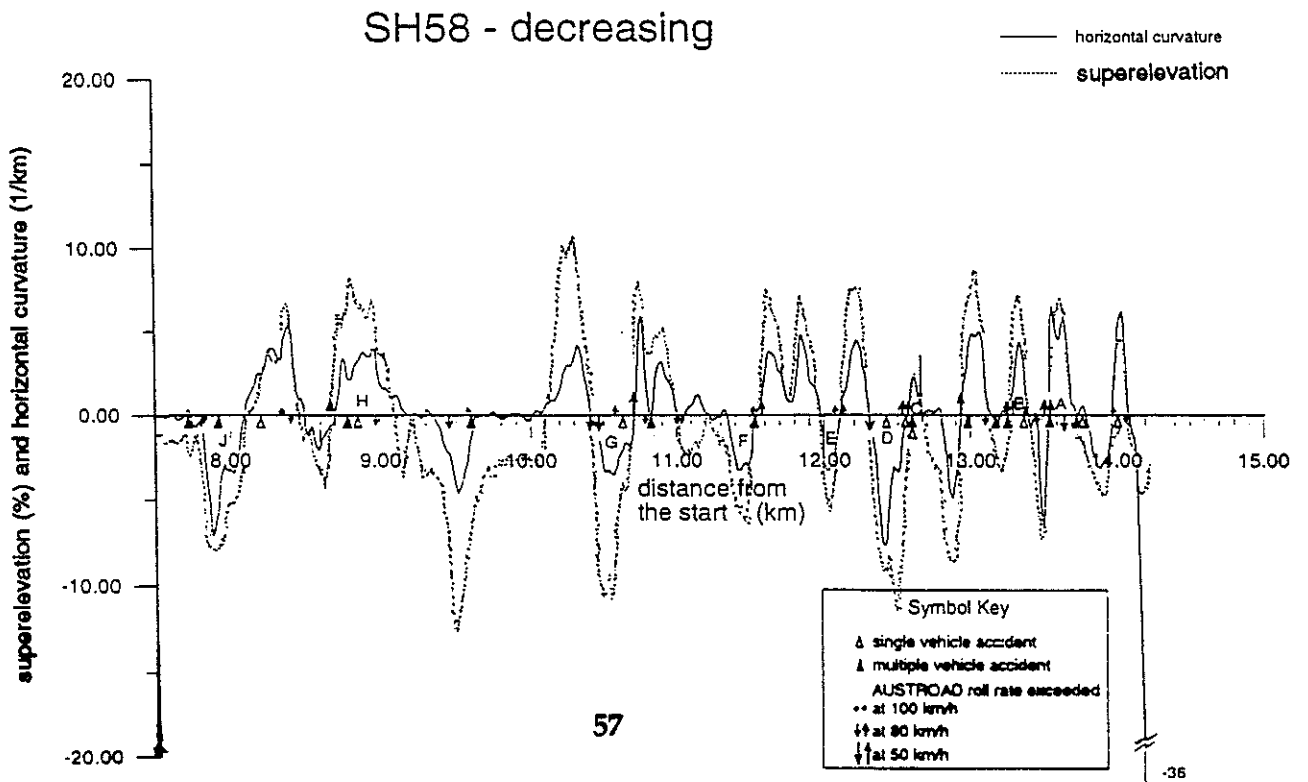
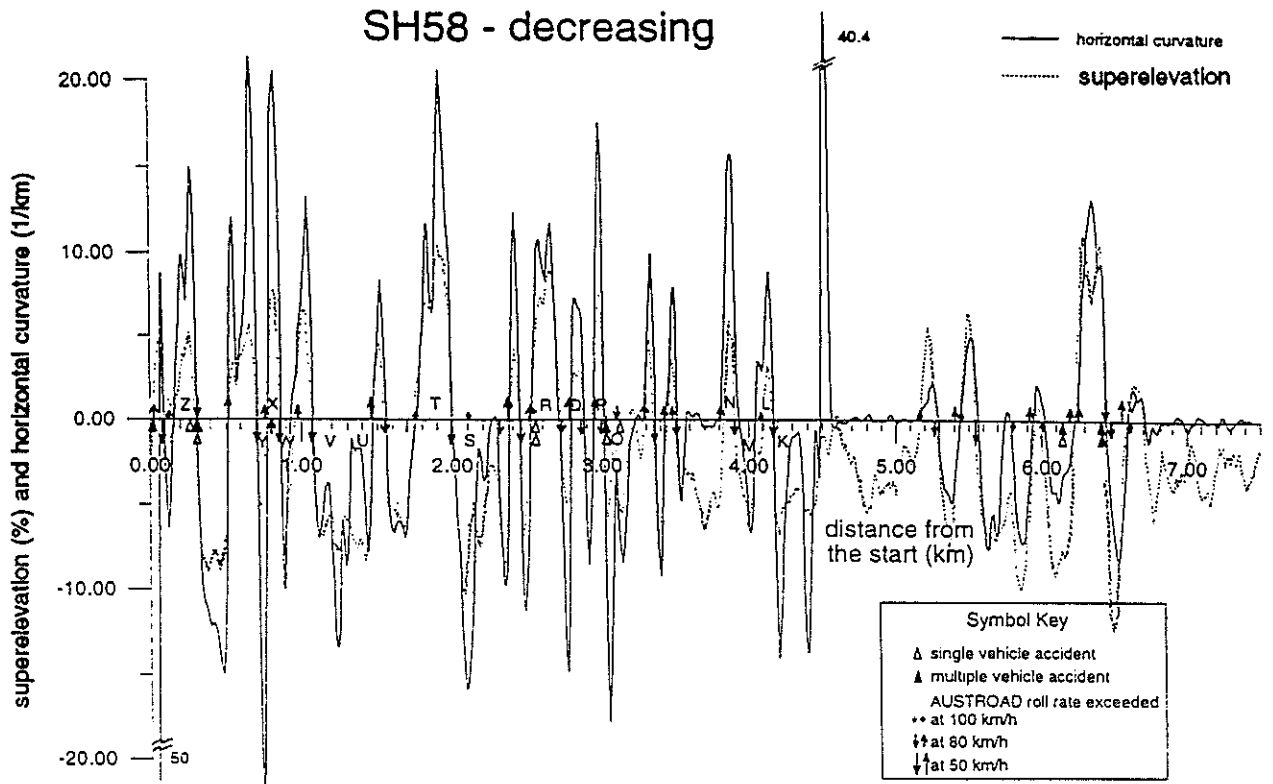
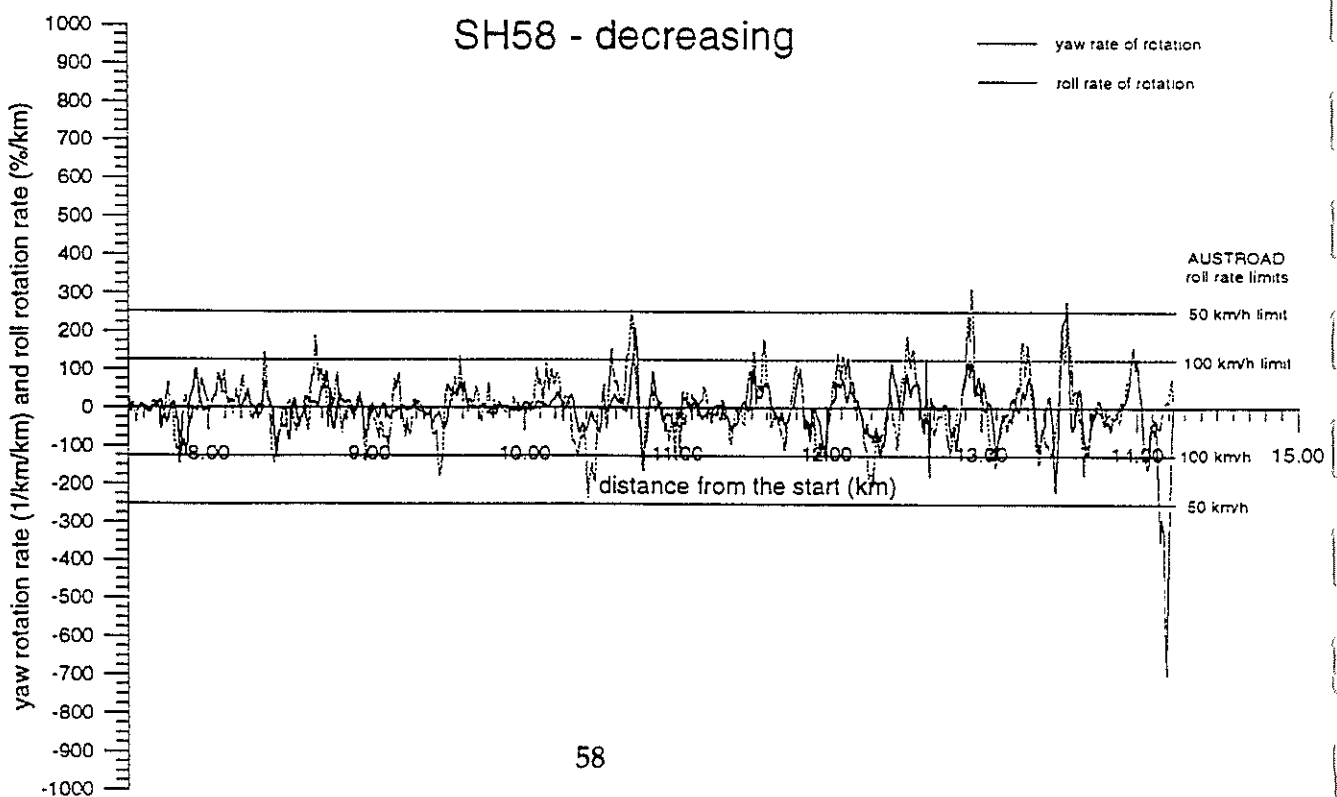
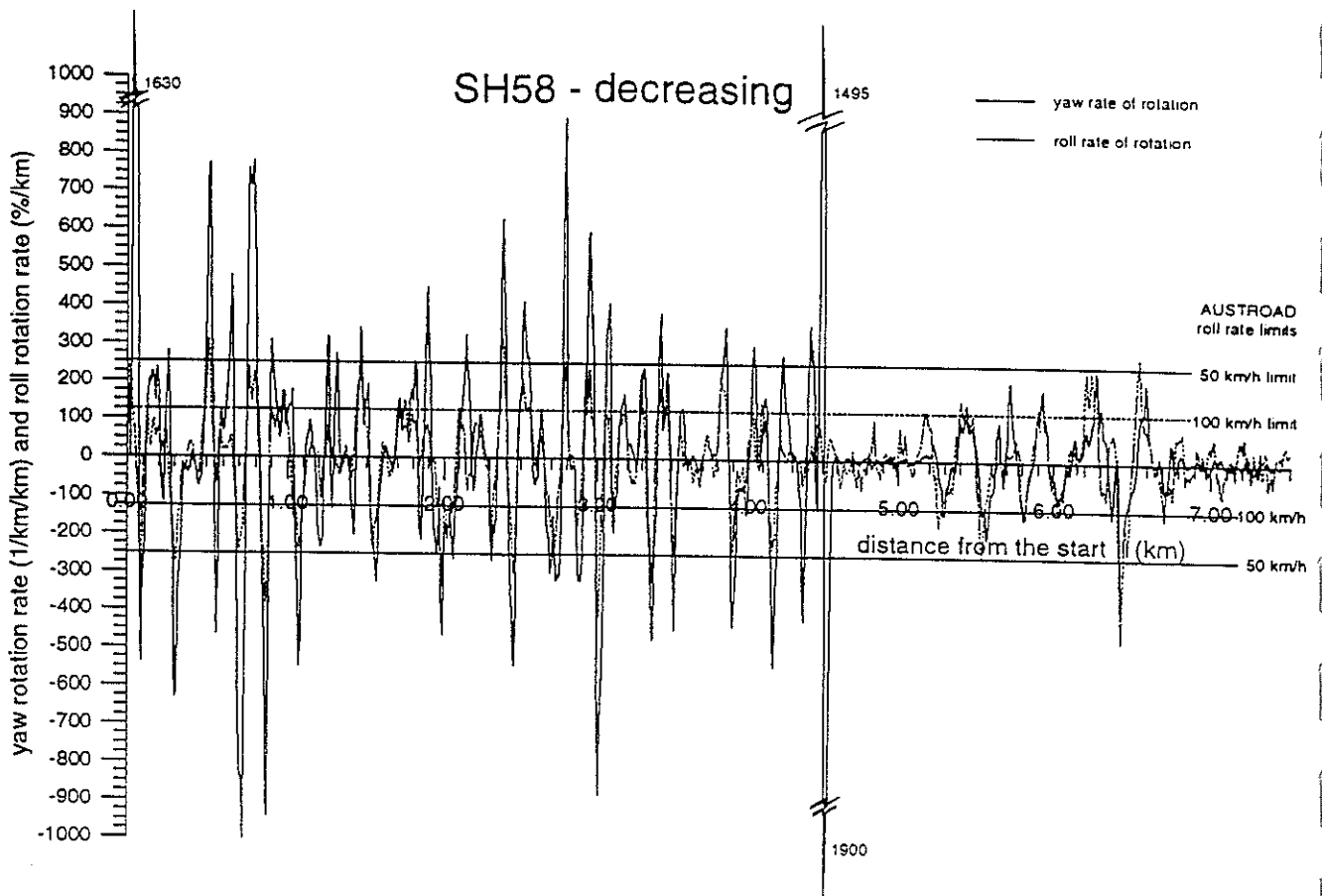


Figure 22. State Highway 58, yaw rotation rate and roll rotation rate. Paremata to Haywards.





## **8. CONCLUSIONS**

Within the scope of the research which has been undertaken, the following conclusions and associated recommendations have been derived.

### **8.1 Measurement of Highway Geometry**

In 1992 a road geometry survey of the New Zealand highway system was carried out using the Australian Road Research Board's Road Geometry Data Acquisition System (RGDAS). This survey covered virtually all sealed highways in New Zealand, some 22 000 km, and provided information on the vertical and horizontal curvature, superelevation and gradient. A combined database was constructed using this data together with information from the Transit New Zealand Road Asset Maintenance Management (RAMM) database and the Land Transport Safety Authority (LTSA) Traffic Accident Report (TAR) system, to enable investigation of the relationship between highway geometry and crash risk. A number of other uses for the RGDAS data have already been identified, such as theoretical derivation of advisory speeds for bends, adding value to this resource.

### **8.2 Accuracy of RGDAS Data**

The integrity and accuracy of the RGDAS data was investigated. The RGDAS road survey vehicle provides a useful measure of superelevation, gradient and radius of curvature. However, a moving average over 56 m that is applied to data compromises accuracy particularly for short arc length, small radius bends. Distance measurements by RGDAS often show errors of the order of hundreds of metres with respect to Transit New Zealand's reference stations. Hence in order to extract data for a particular feature (e.g. curve) a labour-intensive manual feature matching process must be used, as opposed to directly indexing the database by distance.

### **Recommendations**

The main limitation in the RGDAS data is the inaccuracy of the distance measurement, which makes extraction of data for a particular geographical point inefficient. Addition of differential GPS data to future surveys would remove the 'dead reckoning' component inherent in the coordinate data, providing an accurate mapping function and solving the problem of data location.

### **8.3 Poisson Generalised Linear Model**

Because road crashes are comparatively isolated events in New Zealand, a relatively new statistical technique called Poission regression analysis was applied to a specially constructed database comprising 200 m road segments of New Zealand's sealed state highway network classified as rural, two lane, not divided. This statistical technique enables the risk of a crash occurring to be related to explanatory variables. Emphasis was placed on crashes where road geometry factors were identified as the primary contributory cause as opposed to human and vehicle factors. Crashes that occurred at intersections or where alcohol or drugs were

suspected to be the primary causal factor were also excluded. As a result, the analysis was confined to a subset (approximately 15%) of all reported injury crashes on the state highway network.

The Poisson Generalised Linear Model developed and presented here goes some way toward providing a rational quantitative method for evaluating and hence reducing the crash risk associated with various geometric elements of highway design. The model allows formal significance tests to be carried out.

As in past studies, turn severity was found to be the major factor of road geometry affecting crash rates. More severe turns resulted in greater crash rates. A secondary effect was direction of turn, with left turns being riskier than right turns. Low values of calculated advisory speed (indicative of severe turns) in the 400 m prior to a severe turn was found to reduce the crash rate on such a turn. A reverse interaction was found, with severe turns prior to a straight increasing the risk of a crash on the straight section.

The gradient of the highway was found to be significant, with increasing absolute values giving an increase in crash rate. A secondary effect shows ascending grades to be safer than descending grades.

The consistency of the main effects found in the current work with those reported independently by Matthews and Barnes (1988) encourages confidence in the findings. There are, however, some peculiar effects seen in the data, such as the significance of direction of travel (northwest-southeast) to crash rate, that are not yet fully understood.

## **Recommendations**

Further validation and expansion to include other road features not yet investigated is suggested. Examples of such features which may yield useful results are the forward sight distance, clear formation width, and the roadside hazard rating.

### **8.4 Shape Correction and Crash Risk**

The quality of shape correction work cannot be gauged by crash rates as there are insufficient numbers of crashes for any degree of statistical significance. Whilst no definite conclusions can be reached, crash rates appear to be reduced after shape correction. However, as AADT and crash reporting systems change with time, and roadmarkings and signage may well change after shape correction, it is very hard to reach any definitive conclusions.

### **8.5 Prediction of Mid-Curve Speeds**

The relationship between road geometry and vehicle speed was investigated by comparing the RGDAS calculated advisory speed with the 85th percentile mid-curve vehicle speeds measured at a selection of curves. A clear linear relationship was found between the calculated and measured cornering speeds. This indicates that the RGDAS calculated advisory speed may provide a useful alternative or, in addition to, the traditional ball-bank indicator in selecting the signposted advisory speeds for curves. A further use may be to

search the database to find curves that have no advisory speed posted yet have low RGDAS calculated advisory speed.

## **8.6 Road Design Guide**

In New Zealand many roads pass over "difficult terrain". These roads have tended to "evolve" and consequently vary considerably in alignment standard. The Project Evaluation Manual (PEM) used in the past for roading improvements considers typical crash rates for roads classified into just three categories - flat, rolling and mountainous. The models developed in this study relating crash risk to a number of road geometry variables provide a vast improvement to the economic cost/benefit analysis of a proposed road modification. Crash risk and therefore economic cost can now be estimated for existing and proposed road designs, hence providing a valuable design tool for road design engineers.

### **Recommendations**

1. Consideration should be given to revising the way the PEM quantifies crash risk as the contribution to overall relative risk from each road environment variable such as bendiness (curvature), superelevation and so on can now be estimated. This represents a major improvement over the previously used three category classification system, which classified all rural highway environments simply as flat, rolling or mountainous.
2. More accurate recording of crash location (possibly using GPS) and an integrated database linking road geometry, surface characteristics, road condition, traffic data and the TAR database, would be of considerable help for future studies aimed at refining the statistical crash risk models and reducing traffic crashes.
3. The generalised description of terrain and the crash risk relationships developed in this research may be refined to allow the impact of adopting different design standards to be identified and an economically appropriate improvement strategy to be developed.

## 9. REFERENCES

AUSTROADS 1989. Rural road design : guide to the geometric design of rural roads. *7th edition, Austroads*, Sydney, Australia.

Cenek, P.D. and Shaw, P. 1989. Investigation of New Zealand tyre/road interactions. *Road Research Unit Bulletin 85*, Transit New Zealand, Wellington.

Johnston I.R. 1982. Modifying driver behaviour on rural road curves - a review of recent research. *Proc. 11th ARRB Conference*, 11(4): 115-124.

Matthews, L.R. and Barnes, J.W. 1988. Relation between road environment and curve accidents. *Proceedings 14th ARRB Conference*, Part 4, ARRB, Vermont South, Victoria, Australia: 105-120.

Rawlinson, W.R. 1983. The ARRB road geometry instrumented vehicle - general description. *ARRB Internal Report AIR 276-2*, ARRB, Vermont South, Victoria, Australia.

Wanty, D., McLarin, M.W., Davies, R.B. and Cenek, P.D. 1995. Application of the road geometry data acquisition system (RGDAS). *7th World Conference on Transport Research*, Sydney, Australia, 16-21 July.

**APPENDIX 1.      DATABASE FIELDS**

## **RGDAS(stats)**

SEG_ID	Segment identification number - key field for database linking
DIR_I	Codes NN/NE/EE/SE/SS/SW/WW/NW derived from the increasing average bearing
GAV_I	Average grade increasing
GMAX_I	Maximum grade increasing
GMIN_I	Minimum grade increasing
VAV_I	Average vertical curvature increasing
VMAX_I	Maximum vertical curvature increasing
VMIN_I	Minimum vertical curvature increasing
HAV_I	Average horizontal curvature increasing
HMAX_I	Maximum horizontal curvature increasing
HMIN_I	Minimum horizontal curvature increasing
XAV_I	Average cross slope increasing
XMAX_I	Maximum cross slope increasing
XMIN_I	Minimum cross slope increasing
ASAV_I	Average advisory speed increasing
ASMIN_I	Minimum advisory speed increasing
PASAV5_I	Average of previous 1 km (5 segments) advisory speeds increasing
PASMIN5_I	Minimum previous 1 km (5 segments) advisory speed increasing
PASAV2_I	Average of previous 400 m (2 segments) advisory speeds increasing
PASMIN2_I	Minimum previous 400 m (2 segments) advisory speed increasing

plus the 19 corresponding "\_D" fields for the data in the decreasing direction.

The database contains 57 710 records (13.91 Mb) with 2.8% missing data (1634 blank records) on unsealed sections of the state highway network.

## **RAMM**

SEG_ID	Segment identification number - key field for database linking
SH_NUM	State highway number
REF_STN	Last reference station number
REF_DIST	Distance of segment midpoint beyond last reference station
SCW	Total width of sealed road
AADT	Annual average daily traffic count

URBAN	Y, N, or blank if unknown
T_SURF	Type of surface
D_SURF	Date of surface
N_LANES	Number of lanes
M_WAY	Y/N logic field for motorways
CHANGE	Y/N logic field for changes (in any of the previous seven fields) within the segment
DIVIDED	Y/N logic field for division of highway (separation of opposite directions)

The database contains 57 710 records (3.35 Mb) with 11% missing data (6522 records with some blank entries) on unsealed and other apparently random sections of the state highway network.

#### TAR

SEG_ID	Segment identification number - key field for database linking
TAR_ID	Traffic crash record identification number to allow traceback
POSN	"-" or "0" or "+" depending on position in segment, i.e. "-" if in first 50 m , "0" if in middle 100m, "+" if in last 50 m.
SH_NUM	State highway number
REF_STATN	Last reference station number
MOVEMENT	Two letter code for traffic movement
TIME	Time of crash
DATE	Date of crash
DIR_KEY	Direction of key vehicle
FACTOR_1	First of three factors probably contributing to crash
FACTOR_2	Second of three factors probably contributing to crash
FACTOR_3	Third of three factors probably contributing to crash
CURVE	R/E/M/S for straight road / easy curve / moderate curve / severe curve
WET	Y/N logic field ("Y" if "W" in wetness column, otherwise "N")

The database contains 3589 records (0.18 Mb) with no missing data.

## Accident Exclusion Criteria

1. Intersections and driveways (I or D in DIR/INT column).
2. Key vehicle on side street (>1 in key vehicle direction. Probably equivalent to 1).
3. Movement codes unrelated to road geometry. (Exclude all codes **except** AB/AC/AD/AF/AO; BA/BB/BC/BD/BE/BO; CA/CB/CC/CO; DA/DB/DO).
4. Factors (in the first three) all unrelated to road geometry. (Exclude **unless** one of the first three is 111A/113A; 131A/132A/134A/139A; 151A/152A/153A/154A/157A).
5. Slippery road factors other than rain. (Exclude 802/803/804/805/806/807).
6. Urban data. (Exclude when speed limit is  $\leq 50$  km/h).
7. Snow and ice conditions. (Exclude when I in wetness column).



**APPENDIX 2. STATISTICAL CRASH RISK ANALYSIS**

## A2.1 INTRODUCTION

Robert Davies was commissioned to carry out the statistical analysis of crash risk. His report is reproduced here in its entirety for reference purposes.

The original numbering scheme remains unchanged. All figure, table and equation numbers apply to this report only.

# ROAD ACCIDENT RISK AND ROAD GEOMETRY

Prepared for Works Consultancy Services by

Robert B Davies\*

25 May 1995

## 1. INTRODUCTION

This paper investigates the relationship between accidents on rural roads in New Zealand's state highway system and the geometry of the roads.

Two methods of analysis are used. The first uses one and two way tables to give accident rates for the geometry variables viewed one or two at a time. The second uses a Poisson generalised linear model.

The analyses find significant effects due to the horizontal average curvature, difference between the maximum and minimum horizontal curvature, and the minimum advisory speed. Small effects were also found for the gradient, direction, sealed carriageway width and annual average daily travel. There are possibly effects associated with surface age, surface type, wet or dry surface, and accident type. There were no significant effects due to cross-section slope or vertical curvature.

## 2. THE DATA

The state highway system was divided into 200 m segments. For each segment and direction we have the following data:

- Horizontal curvature maximum, minimum and average (HMAX, HMIN, HAV)
- Cross-section slope maximum, minimum and average (XMAX, XMIN, XAV)
- Gradient maximum, minimum and average (GMAX, GMIN, GAV)
- Vertical curvature maximum, minimum and average (VMAX, VMIN, VAV)
- Advisory speed minimum and average (ASMIN, ASAV)
- Advisory speed over previous 400 m, minimum and average (PASMIN2, PASAV2)
- Advisory speed over previous kilometre, minimum and average (PASMIN5, PASAV5)
- Average compass direction (DIR).

\*Robert Davies, Consulting Statistician, 16 Gloucester Street, Wilton, Wellington. Phone (04) 475-3346, fax (04) 475-4206, cell phone (025) 444-935.

For each segment, but not by direction we have:

- an estimate of annual average daily travel (AADT). Throughout this report AADT means the two-way AADT;
- sealed carriage width (SCW);
- number of lanes, urban or rural, is it divided, is it a motorway, seal type and date of seal.

In addition we have an accident file which gives the segment identifier of each accident that occurred during the period of the study and some details of the accident. Accidents were limited to those for which road geometry may have been a factor. The severity of the accident was not taken into account.

In the data originally supplied to me the segments to which an accident was assigned frequently had been adjusted to a nearby one which seemed to match more closely to the description of the accident. Using this data seemed to produce seriously anomalous results. I use the unadjusted data in the analyses reported here. Undoubtedly some accidents have been assigned to wrong segments, so probably the effects we find in the present analysis are somewhat less than is really the case.

In the present study attention was restricted to road segments classified as:

- Rural
- Two lane
- Not divided
- Not motorway
- No missing values in the data (ASMIN, PASMIN5 > 0 to ensure geometry data present)

Four other sets of data were deleted from the analysis:

- Only road segments with  $5.5 \leq \text{SCW} \leq 14$  were included in the study.
- Some segments of highway 31 (connects Otorohanga and Kawhia) had unreasonably high AADTs. Segments with AADT > 1000 on highway 31 were omitted.
- A number of road segments have two highway numbers and appear in the geometry data twice. Where detected, the duplicates were omitted. The segments identified as being duplicated are listed in Section 2.1. One road segment had an extreme value for GMIN and was omitted.

This remaining dataset has 86 524 road segments (each direction counted separately) and 2356 accidents.

## 2.1 Overlapping Segments

The following segments were identified as having two highway numbers:

First highway number	segment range	Second highway number	segment range	direction
1N	01308339-01308387	3	03004411-03004459	same
1N	01305629-01305681	30	30001051-30001103	opposite
1N	01306003-01306051	5	05001253-05001301	same
2	02001565-02001589	29	29000091-29000115	opposite
5	05000557-05000563	30	30001423-30001431	?
6	06010851-06010871	94	94000617-94000637	opposite
72	72001767-72001809	79	79000091-79000133	same

This gives us an opportunity to compare the measurements from two runs. The segments will not exactly line up so we can expect some variation. Here are three examples, plotting HMAX and HMIN. While there is general agreement there are also places where the graphs do not agree and where the disagreement cannot be due to the segments not being exactly aligned.

## 3. INITIAL ANALYSIS

This section covers the preliminary inspection of the data and tables of accident rates classified by one and two variables.

### 3.1 Histograms

Figures 1 and 2 give histograms of the geometry data. The vertical scale gives an approximate indication of the total range of the data. Note the present of large outliers (extreme values), particularly in the horizontal and vertical curvature data. Possibly there is an as yet unlocated erroneous value in the horizontal curvature data.

Figure 3 gives histograms of the other variables.

### 3.2 Scatter-Plots

We look at the a selection of the geometry variables two at a time. Variables which are highly correlated will cause problems later in the analysis, so it is advisable to identify any strong relations at the beginning of the analysis. Figure 4 gives the pair-wise plots for the average values of four of the geometry variables,  $\log_{10}(\text{AADT})$  and SCW. These graphs try to overcome the problem of presenting a large number of points in a scatter diagram. The area of the graph has been divided into small rectangles and shaded according to the number of points falling into the rectangle. Each change in shading level corresponds to a change by a factor of 10 in the number of points falling into the rectangle. This shows correlation between HAV and XAV and an obvious relation between ASAV and HAV. This latter relationship is mirrored in the relation between ASAV and XAV. There is a strong

relationship between AADT and SCW. Higher values of GAV, VAV, HAV and lower values of ASAV tend to be associated with lower values of AADT and SCW. Otherwise there do not seem to be any strong correlations between the variables.

Figures 5 and 6 are scatter-plots for XAV and HAV. Both are on the same scale. Figure 5 is for road segments where  $HMAX-HMIN \leq 10$  and Figure 6 is for the rest. This shows the rather larger slope of the graph of XAV vs HAV for the segments with lower values of HMAX-HMIN. Figure 7 gives a scatter-plot of HMAX and HMIN with the region  $HMAX-HMIN \leq 10$  identified. Figure 8 gives just the points with  $HMAX-HMIN \leq 10$ . These graphs also use the shading technique. These show the very large variation in HMAX and HMIN. Some of these very large values may be due to erroneous measurements.

### 3.3 Cumulative Plots of AADT

This section investigates the range of values of AADT. Of particular interest is whether a relatively small percentage of road segments account for most of the travel.

Figure 9 was derived by sorting the road segments into order of AADT, numbering them and the graphing the AADT against the number. This shows that there are relatively few segments with large AADT. Figure 10 takes the cumulative sum of the AADT and graphs it against the segment number. This shows, however, that much of the travel takes place in the higher AADT segments; about 70% in the 20 000 segments with the highest AADT. Figure 11 looks at the relationship between the vertical axes of the previous two graphs. It shows, in particular, that if we limit attention to road segments with AADT between 500 and 20 000 we will capture most of the total AADT.

Figure 12 graphs the sum of the numbers of accidents against the sum of the AADT over the sorted road segments. The graph lies slightly above the diagonal which shows that lower AADT segments account for slightly more than their share of accidents, but the effect is not huge.

### 3.4 One-Way Classifications

Preliminary analysis using the  $\log_{10}$ -Poisson model identified an number of key variables. In this section, I have divided these key variables into ranges and then calculated the number of accidents per 1 000 000 000 vehicle-kilometres travelled (VKT).

Each table gives:

- the ranges of the classifying variable;
- the observed number of accidents in each of the ranges;
- the expected number of accidents in each of the ranges, assuming that the risk is proportional to the total AADT in that range;
- the total AADT in that range;

- the accident rate in accidents per 1 000 000 000 VKT.

One could carry out a chi-squared goodness of fit test using the observed and expected numbers to see whether there is a relationship between the accident rate and the classifying variable. In fact this is pointless in the following tables as the effects are very large. The reason for including the expected numbers to help understand whether a few anomalous points represent real effects or might arise from statistical fluctuation.

The accident rates may need some interpretation. They are calculated from:

$$\frac{\text{number of accidents} \times 10^9 \times 2}{\text{AADT} \times 0.2 \times 5 \times 365.25}$$

since the study was over five years and the road segments are 0.2 km long and AADT is the two-way AADT. However, an isolated curve in a road is essentially a point on a road and vehicle-kilometers-travelled over it is not a very meaningful concept. The meaningful concept would be simply total vehicles travelled. However, if we think of the risk item being a 200 m section of road including a bend then VKT does make sense. Multiply by  $0.2 \times 10^9$  to get the risk in travelling over that 200 m section.

Because we are looking at only one variable at a time we cannot say if any effect in accident rate is due to the variable in question or is due to some other variable which is correlated with the variable in question. As an example, lower AADT roads have higher accident rates. Probably the major reason for this is that lower AADT is associated with more difficult roads and it is the nature of the road that is causing the higher accident rates rather than the low AADT. In the next section I look at the classification variables two at a time in order to try to disentangle this effect.

### 3.4.1 Classification by AADT

AADT	<500	500-1k	1-2k	2-5k	5-10k	10-20k	>20k
Observed	81	254	432	980	447	161	1
Expected	71	211	390	913	541	204	27
AADT (000)	5271	15721	29091	68075	40328	15202	2008
Rate	84	88	81	79	61	58	3

This table probably under-estimates the accident rate for the low AADT roads because less serious accidents are less likely to be reported on these roads than on the higher AADT roads. Nevertheless the table shows a somewhat higher accident rate for the low AADT roads.

The rate for roads with AADT at least 20 000 is exceptionally low. This is not a statistical artifact as can be seen by comparing the observed and expected numbers. The roads segments with AADT are sections of highways 1 and 2 and a section of highway 30 in the tourist area of Rotorua. Most likely they should be thought of as essentially urban roads and should be excluded in the study.

### 3.4.2 Classification by ASMIN

ASMIN	<60	60-80	80-100	100-120	120-140	140-160	>160
Observed	350	586	612	303	376	124	5
Expected	112	241	470	448	732	332	22
AADT (000)	8321	17949	35062	33438	54569	24731	1627
Rate	230	179	96	50	38	27	17

Minimum advisory speed gives are better relationship with accident rates than average advisory speed so that is what is considered here. The rates for very low ASMIN are probably under-estimates due to reduced reporting rates.

The next table is from a re-analysis of the data after the alignment of the accident data with the road segment data.

ASMIN	<60	60-80	80-100	100-120	120-140	140-160	>160
Observed	249	719	784	117	282	201	19
Expected	112	240	469	452	742	334	22
AADT (000)	8406	18073	35324	34007	55866	25163	1677
Rate	162	218	122	19	28	44	62

The table shows a U shaped relationship between accident risk and ASMIN. There was no similar relationship with PASMIN2 and the results do not seem credible.

### 3.4.3 Classification by PASMIN2

PASMIN2	<60	60-80	80-100	100-120	120-140	140-160	>160
Observed	330	613	651	372	329	61	0
Expected	161	328	587	498	633	148	1
AADT (000)	12012	24490	43750	37117	47193	11034	101
Rate	150	137	81	55	38	30	0

PASMIN2 is the minimum advisory speed over the previous 400 m. This table is included because it was derived as part of the two-way classification considered in the next section.

### 3.4.4 Classification by HAV

HAV	<-5	-5 to -3	-3 to -1	-1 to +1	+1 to +3	+3 to +5	>+5
Observed	80	176	444	1081	387	124	64
Expected	22	61	282	1656	257	57	21
AADT (000)	1672	4547	21013	123464	19190	4249	1561
Rate	262	212	116	48	110	160	224



As expected, this shows a low accident rate for HAV (average horizontal curvature) near zeros, increasing as curvature increases either to the left or to the right.

### 3.4.5 Classification by HDIFF = HMAX-HMIN

HDIFF	<0.5	0.5 to 1	1 to 2	2 to 3	3 to 5	5 to 10	>10
Observed	276	241	255	251	408	468	457
Expected	691	417	363	251	286	204	144
AADT (000)	51562	31086	27092	18713	21301	15223	10719
Rate	29	42	52	73	105	168	233

HDIFF is the difference between maximum and minimum horizontal curvature and captures an aspect of the geometry not completely captured by the average curvature. Risk rises with increasing HDIFF.

### 3.4.6 Classification by Sealed Carriageway Width (SCW)

	SCW<7	7-8	8-9	9-10	10-11	11-12	>12
Observed	237	614	705	324	311	101	64
Expected	275	529	631	365	319	147	90
AADT (000)	20497	39437	47021	27225	23793	10976	6747
Rate	63	85	82	65	72	50	52

The effect of SCW is much weaker than for the other variables I have considered so far. It is included here because the effect found later is somewhat anomalous. This shows a lower accident rate for wide roads. There is also a suggestion of a lower rate for very narrow roads. This may, of course, be due to lower reporting rates.

### 3.4.7 Classification by Direction (DIR)

	N	NE	E	SE	S	SW	W	NW
Observed	343	307	215	344	333	332	188	294
Expected	335	333	251	262	327	356	240	253
AADT (000)	24945	24836	18744	19533	24371	26532	17905	18831
Rate	75	68	63	96	75	69	57	85

The effect is also weaker than for the other variables. It is included here because the effect is also unexpected. Apparently roads with directions NW and SE have higher accident rates and E or W have lower rates. At present I have no satisfactory explanation for this effect.

## 3.5 Two-Way Classifications

I look at accident risk when road segments are classified by two variables. The tables correspond to the lines in the previous section. The numbers of accidents in each cell are much smaller than in the previous section so the statistical fluctuation in the rates is rather

larger. I have put the rates in bold when the corresponding observed number of accidents is at least 25. There is not much information in the data when the number of accidents is less than 25.

With the two-way tables it is still possible for the variation in risks to be due to yet another factor which is correlated with the classifying variables. However, this is rather less likely than with the one-way classification.

### 3.5.1 Classification by ASMIN and AADT

#### Observed Numbers of Accidents

AADT	<500	500-1K	1-2K	2-5K	5-10K	10-20K	>20K
ASMIN<60	17	63	100	113	51	6	
60-80	24	77	114	278	68	25	0
80-100	17	57	105	238	133	62	0
100-120	6	21	41	124	79	31	1
120-140	13	24	57	169	82	31	0
140-160	4	12	14	54	34	6	0
>160	0	0	1	4	0	0	

#### Expected Numbers of Accidents

AADT	<500	500-1K	1-2K	2-5K	5-10K	10-20K	>20K
ASMIN<60	8	20	27	34	18	5	
60-80	13	35	57	81	40	14	0
80-100	17	46	89	167	104	44	3
100-120	11	34	68	172	105	53	6
120-140	14	48	99	305	186	67	13
140-160	7	26	47	144	83	19	4
>160	0	2	3	11	4	1	

#### AADT (000)

AADT	<500	500-1K	1-2K	2-5K	5-10K	10-20K	>20K
ASMIN<60	602	1499	2019	2510	1340	351	
60-80	950	2612	4287	6072	2964	1038	28
80-100	1243	3444	6602	12444	7769	3317	243
100-120	848	2501	5038	12796	7860	3974	422
120-140	1063	3554	7349	22717	13878	5004	1003
140-160	533	1975	3539	10709	6219	1445	312
>160	33	136	258	828	298	73	

Accidents per 1 000 000 000 VKT

AADT	<500	500-1K	1-2K	2-5K	5-10K	10-20K	>20K
ASMIN<60	155	230	271	247	208	94	
60-80	138	161	146	251	126	132	0
80-100	75	91	87	105	94	102	0
100-120	39	46	45	53	55	43	13
120-140	67	37	42	41	32	34	0
140-160	41	33	22	28	30	23	0
>160	0	0	21	26	0	0	

Very roughly the numbers in each row are around the same (although the figure for AADT in the range 2000-5000 and ASMIN in the range 60-80 is exceptionally large). This shows that for a given ASMIN the accident rate is not highly dependent on AADT (despite the observation in Section 3.4.1).

### 3.5.2 Classification by ASMIN and PASMIN2

Observed Numbers of Accidents

	PAS<60	60-80	80-100	100-120	120-140	140-160	>160
ASMIN<60	204	100	27	13	6	0	
60-80	79	276	135	56	37	3	
80-100	22	142	288	104	46	10	0
100-120	8	44	98	91	57	5	0
120-140	13	42	85	87	130	19	0
140-160	4	9	18	21	50	22	0
>160	0	0	0	0	3	2	0

Expected Numbers of Accidents

PASMIN2	<60	60-80	80-100	100-120	120-140	140-160	>160
ASMIN<60	76	22	7	3	3	0	
60-80	41	118	53	17	11	1	
80-100	18	89	231	80	47	6	0
100-120	11	42	130	159	95	12	0
120-140	13	46	126	177	320	50	0
140-160	3	11	38	59	147	73	1
>160	0	0	1	3	11	6	0

## AADT (000)

PASMIN2	<60	60-80	80-100	100-120	120-140	140-160	>160
ASMIN<60	5692	1671	510	210	224	14	
60-80	3038	8766	3985	1249	809	103	
80-100	1313	6650	17195	5979	3480	443	0
100-120	816	3104	9717	11854	7066	880	0
120-140	934	3419	9430	13196	23834	3727	29
140-160	206	857	2814	4416	10933	5445	60
>160	12	23	99	212	847	422	11

## Accidents per 1 000 000 000 VKT

PASMIN2	<60	60-80	80-100	100-120	120-140	140-160	>160
ASMIN<60	196	328	290	339	147	0	
60-80	142	172	186	245	251	160	
80-100	92	117	92	95	72	124	0
100-120	54	78	55	42	44	31	0
120-140	76	67	49	36	30	28	0
140-160	107	58	35	26	25	22	0
>160	0	0	0	0	19	26	0

There is some evidence of the risk rising towards the top right hand side of the table corresponding to a sudden transition from a high advisory speed to a low advisory speed. The higher numbers in the column corresponding to PASMIN2 in the range 60-80 are possibly due to accidents being assigned to incorrect segments, or possibly represent a real effect.

### 3.5.3 Classification by HAV and HDIFF

#### Observed Numbers of Accidents

HDIFF	<0.5	0.5 to 1	1 to 2	2 to 3	3 to 5	5 to 10	>10
HAV< -5		0	1	0	2	8	69
-5 to -3	0	0	10	11	25	55	75
-3 to -1	1	13	32	60	131	129	78
-1 to +1	271	212	183	125	91	96	103
+1 to +3	2	14	22	49	135	109	56
+3 to +5	2	2	7	6	22	55	30
> +5	0	0	0	2	16	46	

Expected Numbers of Accidents

HDIFF	<0.5	0.5 to 1	1 to 2	2 to 3	3 to 5	5 to 10	>10
HAV< -5		0	0	0	1	5	16
-5 to -3	1	2	6	5	12	21	16
-3 to -1	5	17	35	57	89	55	23
-1 to +1	681	383	285	135	88	50	33
+1 to +3	4	14	32	50	84	50	25
+3 to +5	0	1	5	4	10	21	15
> +5		0	0	0	1	3	16

AADT (000)

HDIFF	<0.5	0.5 to 1	1 to 2	2 to 3	3 to 5	5 to 10	>10
HAV<-5		14	26	26	86	344	1176
-5 to -3	41	122	422	339	877	1582	1165
-3 to -1	408	1284	2622	4215	6650	4084	1750
-1 to +1	50802	28536	21276	10094	6593	3706	2457
+1 to +3	300	1013	2352	3702	6268	3720	1836
+3 to +5	12	108	380	309	749	1538	1153
> +5		10	15	28	78	250	1181

Accidents per 1 000 000 000 VKT

HDIFF	<0.5	0.5 to 1	1 to 2	2 to 3	3 to 5	5 to 10	>10
H< -5		0	214	0	127	127	321
-5 to -3	0	0	130	178	156	190	352
-3 to -1	13	55	67	78	108	173	244
-1 to +1	29	41	47	68	76	142	230
+1 to +3	37	76	51	72	118	160	167
+3 to +5	910	101	101	106	161	196	142
> +5		0	0	0	140	351	213

This shows the rise in accident rate when HAV is away from zero or HDIFF is large.

### 3.5.4 Classification by ASMIN and SCW

#### Observed Numbers of Accidents

	SCW<7	7-8	8-9	9-10	10-11	11-12	>12
ASMIN<60	68	102	118	23	26	7	6
60-80	61	181	186	82	64	9	3
80-100	45	141	185	91	100	35	15
100-120	21	74	69	44	47	29	19
120-140	33	88	108	63	52	17	15
140-160	9	27	37	20	21	4	6
>160	0	1	2	1	1	0	0

#### Expected Numbers of Accidents

	SCW<7	7-8	8-9	9-10	10-11	11-12	>12
ASMIN<60	31	37	29	5	6	1	2
60-80	41	77	67	24	22	7	2
80-100	55	111	122	74	63	31	15
100-120	43	93	116	75	60	36	25
120-140	69	143	199	127	105	54	35
140-160	34	64	92	55	59	17	12
>160	2	4	6	5	4	1	1

#### AADT (000)

	SCW<7	7-8	8-9	9-10	10-11	11-12	>12
ASMIN<60	2342	2790	2141	396	478	59	114
60-80	3083	5745	5005	1797	1656	521	143
80-100	4102	8257	9115	5482	4697	2302	1107
100-120	3173	6962	8625	5614	4485	2720	1859
120-140	5132	10675	14831	9491	7804	4044	2592
140-160	2501	4736	6853	4095	4375	1284	887
>160	163	273	451	350	298	46	46

Accidents per 1 000 000 000 VKT

	SCW<7	7-8	8-9	9-10	10-11	11-12	>12
ASMIN<60	159	200	302	318	298	645	287
60-80	108	173	203	250	212	95	115
80-100	60	94	111	91	117	83	74
100-120	36	58	44	43	57	58	56
120-140	35	45	40	36	36	23	32
140-160	20	31	30	27	26	17	37
>160	0	20	24	16	18	0	0

As in Section 3.4.6 there seems to be a drop in accident rate in roads with low values of SCW, particularly when ASMIN is low.

#### 4. POISSON MODEL ANALYSIS

This section describes the fitting of the Poisson generalised linear model. The two-way tables in Section 3.5 could look at variables only two at a time. While it is possible to construct three-way tables, the number of points in each cell would tend to be too small to provide meaningful data and the overall tables would be too large to interpret. The generalised linear model described here provides an alternative way at looking at the effects of several variables at a time and for carrying out formal significance tests. The down side, however, is that one can look at only fairly simple relationships.

We suppose each road segment provides an observation (in each direction). We suppose the number of accidents on this road segment has a Poisson distribution with expected value depending on the AADT and road geometry. Most road segments do not have accidents so that in most cases the expected (average) number of accidents will be rather less than one.

Suppose  $Y_i$  denotes the number of accidents in the  $i$ -th road segment (where  $i$  runs from 1 to  $n$ ), and  $x_{i,1}, \dots, x_{i,m}$  denote  $m$  explanatory variables (e.g. the geometry variables). Then the generalised linear model for the Poisson distribution with  $\log_{10}$  link function supposes that the  $Y_i$  are independently distributed with Poisson distributions and

$$E(Y_i) = \lambda_i = \gamma_i \exp \left( \beta_0 + \sum_{j=1}^m x_{i,j} \beta_j \right) = \gamma_i e^{\beta_0} \prod_{j=1}^m \exp(x_{i,j} \beta_j) \quad (1)$$

where the  $\beta_j$  are the unknown regression coefficients which need to be estimated. I let  $\gamma$  be the AADT for the segment since we expect the number of accidents to be approximately proportional to the AADT. A  $\log_{10}(\text{AADT})$  term can be included as a  $\beta$  to detect a deviation from strict proportionality. The last expression in (1) can be interpreted as expressing the accident risk as a product of risk factors.

One can test for the statistical significance of each of the explanatory variables in much the same way as one does in an analysis of variance or regression analysis using a quantity known as the deviance:

$$\sum_{i=1}^n d_i \quad (2)$$

where  $d_i = 2\lambda_i$  if  $Y_i = 0$  and  $2 Y_i \log_{10} (Y_i/\lambda_i) - (Y_i - \lambda_i)$  otherwise\*\*.

There is no guarantee that the geometry variables enter in a purely linear manner. For example, HAV certainly will not since HAV=0 probably corresponds to a minimum risk. Therefore I consider polynomial functions of the variables. This proceeds in a step-wise manner trying different variables and trying different degrees of the polynomial until increasing the number of variables or degree of the polynomial until there is no statistically significant improvement in the fit.

However, I am reluctant to include two highly correlated variables in the same model because of the difficulty in interpreting the results. Hence I try two different models: one starting with horizontal curvature and cross-slope variables and the other with ASMIN or ASAV.

It will also be unreasonable to expect to be able to fit a model covering the wide range of geometry variables. Also I want to avoid the very low AADT roads which probably have unreliable measures of AADT and poor reporting of accidents. The analyses include two ranges of data.

I frequently use HDIFF = HMAX-HMIN as one of my variables as in Sections 3.4.5 and 3.5.3.

#### 4.1 Selecting Subsets of the Data for Analysis

We cannot expect the generalised linear model to be valid for the very wide range of geometry variables encountered. I would also like to avoid the very low AADT roads, both because the AADT data on these roads may be unreliable and the accident reporting rates low. Also I would like to reduce the number of road segments that we need to analyse. We also want to avoid the very high AADT roads since these seem to behave differently.

I selected two subsets of the data: a more restricted one which I call subset I and a less restricted one which I call subset II.

\*\*Note that we cannot use the residual deviance for assessing goodness of fit or testing for extra variation as is commonly done because of the tiny average number of accidents per segment.



#### **4.1.1 Subset I**

This is the more restricted subset of the data.

I restrict attention to road segments with AADT less than 20 000 and greater than or equal to 2000; HDIFF less than or equal to 10; ASMIN greater or equal to 80.

This gave a dataset with 24896 road segments and 1053 accidents.

Histograms of the geometry variables with this restricted dataset are given in Figures 13, 14 and 15. Naturally, the variables have a narrower range and some of the outlying values have been removed.

#### **4.1.2 Subset II**

This is the less restricted subset of the data. I restrict attention to segments with AADT less than 20 000 and greater than or equal to 500; ASMIN greater than or equal to 60; HDIFF less than or equal to 20.

This gave a dataset with 66711 road segments and 1944 accidents.

### **4.2 Analysis Using HAV and HDIFF and Subset I**

I tested a number of predictor variables (excluding the advisory speed and previous advisory speed variables) and found the following to be statistically significant (in most cases highly significant).

- HAV (polynomial, degree 2)
- HDIFF (polynomial, degree 2)
- DIR (direction)
- GAV (polynomial, degree 2)

I tried fitting a variable XAV.Adj being the residual when XAV is fitted to HAV, but did not get a significant result (at the 5% level). In an earlier analysis with a less restricted range of SCW, SCW also came out as significant, but this was not the case in the present analysis. In the earlier analysis I also tried XAV, XMAX, XMIN, VAV and a variety of interaction terms but did not get significant results.

I have also included  $\log_{10}(\text{AADT})$  in the analysis even though it is not significant. This is partly as a result of originally believing incorrectly that it was significant when I was developing the analysis. However, it is probably worth including to prevent any small AADT effects getting translated into effects of variables correlated with AADT.

Here is the step-wise analysis of deviance\*\*\* table.

\*\*\*This is analogous to the analysis of variance table in a standard multiple regression analysis.

	Df	Deviance	Resid. Df	Resid. Dev	Pr(Chi)
NULL			24895	6720.6	
log <sub>10</sub> (AADT)	1	1.3	24894	6719.3	0.2530
poly(HAV, 2)	2	118.4	24892	6600.9	0.0000
poly(HDIFF, 2)	2	150.8	24890	6450.0	0.0000
DIR	7	40.8	24883	6409.3	0.0000
poly(GAV, 2)	2	8.9	24881	6400.4	0.0119

The column labelled deviance gives the reduction in the residual deviance through adding in a variable. If the value in this column is rather more than the number of degrees of freedom in the previous column, then the effect tends to be significant. Pr(Chi) gives the significance probability. If this is less than 0.05 then the effect is significant at the 5% level. Since I am including only significant effects (except log<sub>10</sub>(AADT)) in this analysis, all values (except that of log<sub>10</sub>(AADT)) are less than 0.05.

The estimates of the effects when expressed as coefficients of the polynomial terms are difficult to interpret directly and so I have expressed them graphically. For completeness, and to show the list of variables actually fitted, here is the table of estimates:

	Value	Std Error	t value
(Intercept)	-11.0	0.5	-22.38
log <sub>10</sub> (AADT)	(0.2	0.1	-1.42
poly(HAV, 2) 1	-3.9	3.5	-1.10
poly(HAV, 2) 2	20.0	3.7	5.44
poly(HDIFF, 2) 1	55.1	4.7	11.73
poly(HDIFF, 2) 2	-10.6	3.8	-2.77
DIR 1	0.076	0.069	1.10
DIR 2	0.101	0.034	2.92
DIR 3	0.058	0.025	2.28
DIR 4	0.072	0.018	3.99
DIR 5	-0.025	0.016	-1.63
DIR 6	-0.009	0.013	-0.73
DIR 7	-0.043	0.015	-2.87
poly(GAV, 2) 1	-8.1	4.1	-1.95
poly(GAV, 2) 2	8.4	3.8	2.18

T values\*\*\*\* greater than 2 indicate statistically significant effects (at about the 5% level).

\*\*\*\*S-plus calls these t values. Probably one should call them z values since we are not estimating a variance in this analysis, and they should be close to being normally distributed.

Figure 16 shows the effect of  $\log_{10}(\text{AADT})$ . This gives relative risks (i.e. relative accident rates). Here, as elsewhere, the vertical scale is a logarithmic one. I have arbitrarily set the relative risk at 4 (AADT=10 000) to be equal to 1. Then the central dotted line gives the relative risk for other values of AADT. The lighter outside dotted lines give confidence intervals (two standard errors, so they are about 95% confidence intervals). Since  $\log_{10}(\text{AADT})$  is not significant, a horizontal straight line is contained within the confidence lines.

Here, and in the other graphs, the confidence intervals are based on the assumption that the fitted line is exactly of the correct form. In reality, this will not be true and one should think of the confidence intervals, particularly at the ends, as being somewhat wider.

Figure 17 shows the relative risk for HAV. Here I have taken  $\text{HAV} = 0$  as the point where I set the relative risk = 1. Risk is doubled for HAV around 3. Figure 18 shows the relative risk for HDIFF. Figure 19 shows the effect of GAV. The effect is rather poorly determined and the confidence intervals wide. The effect of DIR also requires translating. Here are the regression coefficients expressed as differences from the average value. The last column gives the risk multiplier effect.

	Coefficients	SEs	t values	multiplier
N	0.15	0.07	2.01	1.16
NE	-0.08	0.08	-0.94	0.93
E	-0.23	0.10	-2.30	0.79
SE	0.37	0.08	4.87	1.44
S	-0.07	0.08	-0.93	0.93
SW	-0.01	0.08	-0.16	0.99
W	-0.30	0.11	-2.87	0.74
NW	0.18	0.08	2.20	1.08

The results are similar to those found in Section 3.4.7. East and west have the lowest risks, north and south east have the highest risks. In order to illustrate the use of the graphs consider a road segment with average horizontal curvature (HAV) equal to 3 and difference between the maximum and minimum curvature (HDIFF) equal to 4. Now suppose the road is realigned so that HAV and HDIFF are both equal to 2. The change in relative risk is calculated in the following table:

	Before realignment		After realignment	
	value	relative risk (from graph)	value	relative risk (from graph)
HAV	3	1.77	2	1.26
HDIFF	4	3.08	2	1.95
Product		5.45		2.46

Thus the realignment would reduce the risk by a factor of  $5.45/2.46 = 2.2$ . But remember that all the numbers involved are subject to substantial statistical error, the curves are unlikely to be of the exact form fitted, road geometry is much more complicated than is captured by

the simple measurements used here. And finally, as it was not possible to align the accidents exactly with the road segments, some smudging of the information is inevitable. Probably the effects are under-estimated.

The risk can be calculated from the following table:

term	coefficient
$\log_{10}(\text{AADT})$	-0.189
HAV	-0.0180
HAV <sup>2</sup>	0.0695
HDIFF	0.388
HDIFF <sup>2</sup>	-0.0262
GAV	-0.0252
GAV <sup>2</sup>	0.00613

Take the value of each item on the left hand side of the table, multiply by the corresponding coefficient. Take exp of the sum, multiply by 54.92 and this gives risk per 109 VKT. If appropriate, multiply by the multiplier from the table of the effects of DIR. For example, if AADT (two-way) = 10 000, HAV = 3, HDIFF = 4, GAV = 0 then the risk of a (reported) accident is  $142 \times 10^{-9}$  per VKT.

### 4.3 Analysis Using ASMIN and Subset I

This follows the same approach as the previous section except that I include ASMIN and PASMIN2 and omit HAV and HDIFF. ASMIN fits better than ASAV and PASMIN2 fits better than any of PASMIN5, PASAV2, PASAV5.

Here is the analysis of deviance table:

	Df	Deviance	Resid. Df	Resid. Dev	Pr(Chi)
NULL		24895	6720.6		
$\log_{10}(\text{AADT})$	1	1.3	24894	6719.3	0.2530
poly(ASMIN, PASMIN2, 2)	5	294.1	24889	6425.2	0.0000
DIR	7	40.4	24882	6384.8	0.0000
poly(GAV, 2)	2	7.2	24880	6377.6	0.0277

I was able to detect an interaction between ASMIN and PASMIN2 and so have included both terms in a single second degree polynomial. As well as including the first and second degree terms of ASMIN and PASMIN2, it includes a single product term.

Here is the table of estimates:

	Value	Std Error	t value
(Intercept)	(10.96	0.49	-22.4
$\log_{10}(\text{AADT})$	(0.2	0.1	(1.5
poly(ASMIN, PASMIN2, 2)1.0	-58.6	5.7	-10.29
poly(ASMIN, PASMIN2, 2)2.0	26.5	5.4	4.90
poly(ASMIN, PASMIN2, 2)0.1	-25.8	5.9	-4.38
poly(ASMIN, PASMIN2, 2)0.2	0.2	4.8	0.04
poly(ASMIN, PASMIN2, 2)1.1	-2184	818	-2.67
DIR1	0.089	0.069	1.29
DIR2	0.099	0.034	2.87
DIR3	0.056	0.025	2.21
DIR4	0.071	0.018	3.92
DIR5	-0.025	0.016	-1.64
DIR6	-0.007	0.013	-0.57
DIR7	-0.044	0.015	-2.95
poly(GAV, 2)1	-7.4	4.1	-1.81
poly(GAV, 2)2	7.4	3.9	1.90

Again, these numbers are not very meaningful except to show that the interaction term between ASMIN and PASMIN2 is significant. The quadratic term in PASMIN2 could have been omitted.

The graphs of the effects of AADT and GAV are very similar to those given in the previous section and I have not repeated them.

I have printed out the effect of ASMIN and PASMIN2 as a contour plot in Figure 20. One needs to take the anti- $\log_{10}$  of the numbers on the contours to get the relative risk as in the following table.

Contour value	Risk
(0.4	0.40
(0.2	0.63
0	1
0.2	1.6
0.4	2.5

The dotted line shows the convex hull of the data points. Contours outside the dotted line or near its edge are probably not meaningful.

Probably the high point to the lower right of the graph is due to accidents placed in the wrong segment.

The table of the effects of DIR is similar to that in Section 4.2 and I have not repeated it.

#### 4.4 Analysis Using HAV and HDIFF and Subset II

I repeat the analysis of Section 4.2 on subset II, the less restricted set of data.

I found the following variables to be statistically significant:

- $\log_{10}(\text{AADT})$  (polynomial; degree 2)
- HAV (polynomial, degree 4)
- HDIFF (polynomial, degree 3)
- DIR (direction)
- GAV (polynomial, degree 2)
- SCW (polynomial, degree 2)

These are as before, except that the SCW and  $\log_{10}(\text{AADT})$  terms are significant and the degrees of HAV and HDIFF have been increased.

Here is the step-wise analysis of deviance table.

	Df	Deviance	Resid. Df	Resid. Dev	Pr(Chi)
NULL		66710	13274.0		
poly( $\log_{10}(\text{AADT})$ , 2)	2	16.4	66708	13257.6	0.0003
poly(HAV, 4)	4	415.8	66704	12841.8	0.0000
poly(HDIFF, 3)	3	440.4	66701	12401.4	0.0000
DIR	7	56.7	66694	12344.7	0.0000
poly(GAV, 2)	2	27.6	66692	12317.2	0.0000
poly(SCW, 2)	2	27.7	66690	12289.5	0.0000

and the table of estimates

	Value	Std Error	t value
(Intercept)	-1154	0.03	-332.86
poly( $\log_{10}(\text{AADT})$ , 2)1	2.0	9.2	0.22
poly( $\log_{10}(\text{AADT})$ , 2)2	-16.3	5.5	-2.96
poly(HAV, 4)1	-3.3	4.3	-0.76
poly(HAV, 4)2	28.6	5.0	5.77
poly(HAV, 4)3	6.6	4.5	1.46
poly(HAV, 4)4	-11.4	5.3	-2.17
poly(HDIFF, 3)1	133.7	6.3	21.28
poly(HDIFF, 3)2	-46.0	5.1	-8.97
poly(HDIFF, 3)3	13.7	4.5	3.04
DIR1	0.109	0.050	2.17
DIR2	0.069	0.026	2.65
DIR3	0.055	0.018	2.98
DIR4	0.056	0.013	4.14
DIR5	-0.004	0.011	-0.32

DIR6	-0.001	0.009	-0.14
DIR7	-0.049	0.010	-4.56
poly(GAV, 2)1	-24.2	5.4	-4.52
poly(GAV, 2)2	11.3	5.4	2.08
poly(SCW, 2)1	37.8	7.7	4.93
poly(SCW, 2)2	-21.2	5.9	-3.63

The graphs of the relative risks are given in Figure 21 (AADT), Figure 22 (HAV), Figure 23 (HDIFF), Figure 24 (GAV) and Figure 25 (SCW). The lowering of the estimated risk for extreme values of HAV in Figure 22 is most likely a consequence of fitting a polynomial rather than a real effect. Figure 21 is unexpected. Both very high and very AADT roads show lower risk. Possibly the effect for high AADT roads has the same cause as the very low accident rates observed for the AADT>20000 roads. For low AADT roads the effect may be due directly to the lower traffic plus reduced reporting.

Figure 25 is also strange. It shows that risk decreases for wide roads, which is expected, but also decreases for narrow roads, which is unexpected. The effect was also noted in Section 3.5.4. Possibly it is a reporting rate effect or perhaps people take more care when winding roads are narrow.

Here is the table of the effect of direction:

Coefficients	SEs	t values	multiplier	
N	0.08	0.06	1.44	1.08
NE	-0.02	0.06	-0.27	.98
E	-0.23	0.07	-3.27	.79
SE	0.28	0.06	4.95	1.32
S	0.03	0.06	0.57	1.03
SW	0.04	0.06	0.73	1.04
W	-0.35	0.08	-4.56	.71
NW	0.16	0.06	2.77	1.18

The results are similar to those found previously.

#### 4.5 Analysis Using ASMIN and Subset II

I repeat the analysis of Section 4.3 on the less restricted subset II data. As in Section 4.4, SCW is included in the model; otherwise the results are similar to those of Section 4.3. Here is the step-wise analysis of deviance table:

	Df	Deviance	Resid. Df	Resid. Dev	Pr(Chi)
NULL			66710	13274.0	
poly(log <sub>10</sub> (AADT), 2)	2	16.4	66708	13257.6	0.0003
poly(ASMIN, PASMIN2, 2)				5	892.5
66703 12365.1 0.0000					
DIR	7	57.9	66696	12307.2	0.0000
poly(GAV, 2)	2	28.3	66694	12278.9	0.0000
poly(SCW, 2)	2	28.3	66692	12250.6	0.0000

and the table of estimates

	Value	Std Error	t value
(Intercept)	-11.45	0.04	-308.33
poly(log <sub>10</sub> (AADT), 2)1	1.3	9.2	0.14
poly(log <sub>10</sub> (AADT), 2)2	-16	5	-2.97
poly(ASMIN, PASMIN2, 2)1.0	-145	7	-19.41
poly(ASMIN, PASMIN2, 2)2.0	58	7	8.40
poly(ASMIN, PASMIN2, 2)0.1	-41	8	-5.19
poly(ASMIN, PASMIN2, 2)0.2	-3	7	-0.50
poly(ASMIN, PASMIN2, 2)1.1	-12570	1857	-6.78
DIR1	0.122	0.050	2.43
DIR2	0.069	0.026	2.68
DIR3	0.052	0.018	2.80
DIR4	0.056	0.013	4.16
DIR5	-0.004	0.011	-0.33
DIR6	0.001	0.009	0.07
DIR7	-0.050	0.011	-4.63
poly(GAV, 2)1	-23.8	5.4	-4.43
poly(GAV, 2)2	12.6	5.4	2.32
poly(SCW, 2)1	37.9	7.7	4.94
poly(SCW, 2)2	-22.0	5.8	-3.77

The graphs of the risk functions for AADT, GAV and SCW are similar to those given in the previous section and I have not repeated them. The contour plot for risk versus ASMIN and PASMIN2 is given in Figure 26. The table for translating the contour levels to risk follows:

Contour value	Risk
(1	0.10
(0.5	0.32
0	1
0.5	3.1
1	10.0

The table of the effects of direction is close to that in Section 4.4 and is omitted.



## 5. ADDITIONAL ANALYSES

This section looks at additional variables. The analyses are extensions of the  $\log_{10}$ -Poisson regressions of Section 4. Except where noted the analyses are restricted to subset I.

### 5.1 Highways 1 and 2

Are the accident rates for highways 1 and 2 the same as for the rest of the state highway system? A new explanatory variable, HW1&2, was introduced, taking the value 1 if a road segment belonged to highway 1 or 2 and zero otherwise. About half the AADT and accidents were on highways 1 and 2 with their overall accident rate being about the same as the overall value.

Here are two-way tables for accidents rates classified by HW1&2 and ASMIN and by HW1&2 and DIR.

#### 5.1.1 Classification by HW1&2 and ASMIN

Observed Numbers of Accidents

ASMIN	<60	60-80	80-100	100-120	120-140	140-160	>160
other	214	346	305	137	190	58	4
HW1&2	136	240	307	166	186	66	1

Expected Numbers of Accidents

ASMIN	<60	60-80	80-100	100-120	120-140	140-160	>160
other	81	156	253	215	355	159	11
HW1&2	30	85	217	233	377	172	10

AADT (000)

ASMIN	<60	60-80	80-100	100-120	120-140	140-160	>160
other	6069	11638	18894	16038	26450	11871	857
HW1&2	2252	6312	16168	17400	28118	12860	770

Accidents per 1 000 000 000 VKT

ASMIN	<60	60-80	80-100	100-120	120-140	140-160	>160
other	<b>193</b>	<b>163</b>	<b>88</b>	<b>47</b>	<b>39</b>	<b>27</b>	<b>26</b>
HW1&2	<b>331</b>	<b>208</b>	<b>104</b>	<b>52</b>	<b>36</b>	<b>28</b>	<b>7</b>

The accidents rates are similar for ASMIN greater than 80; otherwise they are higher on highways 1 and 2. This may well be due to reporting rate differences.

### 5.1.2 Classification by HW1&2 and Direction

#### Observed Numbers of Accidents

	N	NE	E	SE	S	SW	W	NW
other	168	143	143	190	155	166	113	176
HW1&2	175	164	72	154	178	166	75	118

#### Expected Numbers of Accidents

	N	NE	E	SE	S	SW	W	NW
other	162	146	154	158	156	158	141	157
HW1&2	172	188	97	104	171	198	99	95

#### AADT (000)

	N	NE	E	SE	S	SW	W	NW
other	12084	10851	11518	11773	11606	11778	10491	11716
HW1&2	12862	13985	7225	7759	12764	14754	7413	7116

#### Accidents per 1 000 000 000 VKT

	N	NE	E	SE	S	SW	W	NW
other	<b>76</b>	<b>72</b>	<b>68</b>	<b>88</b>	<b>73</b>	<b>77</b>	<b>59</b>	<b>82</b>
HW1&2	<b>75</b>	<b>64</b>	<b>55</b>	<b>109</b>	<b>76</b>	<b>62</b>	<b>55</b>	<b>91</b>

The directional influence on the accident rate seems to be stronger on highways 1 and 2 (although I do not find the difference statistically significant in the generalised linear model analysis). However, the direction for the increased accident rate seems unrelated with the dominant direction of flow of highways 1 and 2 so the alignment of highways 1 and 2 do not seem to provide an explanation for the effect. Nevertheless, it would be a good idea to carry out some further analysis here.

### 5.1.3 Poisson Model Analysis

The method is to include the variable HW1&2 in the Poisson model, but also to include its interactions with the other variables. Including the interactions checks whether the other variables have the same effects on highways 1 and 2 as they do on the other highways. I carried out the analysis on both the subsets of the data with ASMIN and PASMIN2 as the main geometry variables. For subset I here is the analysis of variance table:

	Df	Deviance	Resid. Df	Resid. Dev	Pr(Chi)
NULL		24895	6720.6		
log <sub>10</sub> (AADT)	1	1.3	24894	6719.3	0.2530
poly(ASMIN,PASMIN2, 2)	5	294.1	24889	6425.2	0.0000
DIR1	7	40.4	24882	6384.8	0.0000
poly(GAV, 2)	2	7.2	24880	6377.6	0.0277
HW1&2	1	4.2	24879	6373.4	0.0402
HW1&2:ASMIN	1	3.2	24878	6370.2	0.0753
HW1&2:DIR	7	6.3	24871	6364.0	0.5107
HW1&2:log <sub>10</sub> (AADT)	1	0.0	24870	6363.9	0.9214

Only HW1&2 is significant. In particular, there is no evidence of a stronger directional effect on highways 1 and 2. Re-running the analysis, with the interactions omitted we get an estimate of the HW1&2 effect:

	Value	Std Error	t value
HW1&2	0.14	0.07	2.05

This corresponds to the reported accident rate being 15% higher on highways 1 and 2.

Going to subset II, we do find an interaction with ASMIN showing a slightly different relationship with ASMIN on highways 1 and 2. Here is the analysis of deviance table:

	Df	Deviance	Resid. Df	Resid. Dev	Pr(Chi)
NULL		66710	13274.0		
log <sub>10</sub> (AADT)	1	11.0	66709	13263.0	0.0009
poly(ASMIN, PASMIN2, 2)	5	880.0	66704	12383.0	0.0000
DIR1	7	57.5	66697	12325.5	0.0000
poly(GAV, 2)	2	28.0	66695	12297.5	0.0000
poly(SCW, 2)	2	37.8	66693	12259.7	0.0000
HW1&2	1	6.0	66692	12253.7	0.0146
HW1&2:poly(ASMIN, 2)	2	8.0	66690	12245.7	0.0181

As the effect is small and a graphical representation would be awkward, I have not made a plot of it. If we leave out the interaction term we get an estimate of the effect of HW1&2.

	Value	Std Error	t value
HW1&2	0.12	0.05	2.44

which is similar to the figure we found with the more restricted subset.

## 5.2 Surface Type

Road surface types were divided into two categories. The following surface types were classified as coarse:

Surface	Group
COAT1/ 1	Chip1
COAT1/ 2	Chip2
COAT1/ 3	Chip3
COAT2/ 1	Chip1
COAT2/ 2	Chip2
COAT2/ 3	Chip3
COAT2/23	Chip2
COAT2/25	Chip2
RSEAL/ 1	Chip1
RSEAL/ 2	Chip2
RSEAL/ 3	Chip3
T2	Chip2
T3	Chip3
TEXT / 3	Chip3
VFILL/ 3	Chip3

The others were classified as smooth.

The analysis then proceeded as in Section 5.1. A variable Coarse was defined which took the value 1 if the surface of a segment was coarse and 0 otherwise. I included the interaction with ASMIN in the analysis. In each of the analyses with the more restricted and less restricted subsets the Coarse effect by itself was not significant but the interaction with ASMIN was just significant. Here are the analysis of deviance tables and estimates.

### Subset I

	Df	Deviance	Resid. Df	Resid. Dev	Pr(Chi)
NULL		24895	6720.6		
$\log_{10}(\text{AADT})$	1	1.3	24894	6719.3	0.2530
poly(ASMIN,PASMIN2, 2)	5	294.1	24889	6425.2	0.0000
DIR	7	40.4	24882	6384.8	0.0000
poly(GAV, 2)	2	7.2	24880	6377.6	0.0276
Coarse	1	3.6	24879	6374.0	0.0568
Coarse:ASMIN	1	4.1	24878	6369.9	0.0436
	Value	Std Error	t value		
Coarse	(0.60	0.37	(1.63		
Coarse:ASMIN	0.0065	0.0032	2.02		

## Subset II

	Df	Deviance	Resid. Df	Resid. Dev	Pr(Chi)
NULL		66710	13274.0		
poly(log <sub>10</sub> (AADT), 2)	2	16.4	66708	13257.6	0.0003
poly(ASMIN,PASMIN2, 2)	5	892.5	66703	12365.1	0.0000
DIR	7	57.9	66696	12307.2	0.0000
poly(GAV, 2)	2	28.3	66694	12278.9	0.0000
poly(SCW, 2)	2	28.3	66692	12250.6	0.0000
Coarse	1	2.1	66691	12248.6	0.1484
Coarse:ASMIN	1	4.8	66690	12243.7	0.0283

	Value	Std Error	t value
Coarse	(0.35	0.20	(1.76
Coarse:ASMIN	0.0043	0.0019	2.19

In each case this corresponds to an increase of risk associated with a coarse surface on high ASMIN roads and a decrease on low ASMIN roads. But remember that the effects are only just statistically significant and subject to substantial error. Also surfacing with coarse material may be associated with known danger spots.

### 5.3 Surface Age

The date of the most recent resealing of each road segment is known. In this analysis we suppose that a road surface was new for two years after resealing and then old. It was unknown before the date of resealing. We want to know the effect of surface age on accident risk.

I suppose each road segment provides up to two observations (in each direction). The first corresponds to the period when the surface was new and the second when it was old. The period when the surface age was unknown was not used in this analysis. The geometry variables are the same for both of the observations but one of the Y values corresponds to the number of accidents on the old surface and the other to the number on the new surface. A new explanatory variable age is introduced, which takes the value 1 for the observations on the new surface and 0 for the observations on the old surface.

The value of  $\gamma_i$  in equation (1) needs to be modified. For the  $Y_i$  corresponding to the new surface, it needs to be set to AADT times the fraction of time the surface was new during the five years of observations and for the  $Y_i$  corresponding to the old surface, it needs to be set to AADT times the fraction of time the surface was old.

I considered it feasible to carry out the analysis only for the more restricted subset of data. I included coarse in the analysis as I could check for an interaction between age and coarse. In fact, I was unable to detect any interaction but coarse was significant by itself with this

set of data so I left it in the analysis. Leaving it out makes little difference to the rest of the analysis.

Here is some initial data.

	Restricted subset	New surface	Old Surface
Number of segments	24896	17819	21067
Number of accidents	1053	204	566
Adjusted AADT	109.9(106	25.9(106	58.7(106
Accident rate	52.5(10(9	43.1(10(9	52.8(10(9

The new surface seems to have a lower accident rate than the old surface.

Here is the analysis of deviance table:

	Df	Deviance	Resid. Df	Resid. Dev	Pr(Chi)
NULL		38885	5760.1		
log <sub>10</sub> (AADT)	1	3.4	38884	5756.7	0.0660
poly(ASMIN, PASMIN2, 2)	5	196.5	38879	5560.2	0.0000
DIR	7	32.2	38872	5528.0	0.0000
poly(GAV, 2)	2	6.7	38870	5521.3	0.0354
Coarse	1	9.7	38869	5511.6	0.0018
Age	1	5.2	38868	5506.4	0.0221

and table of estimates:

	Value	Std Error	t value
Coarse	0..24	0.09	2.70
Age	(0.19	0.08	(2.26

Coarse appears to increase the accident rate. However, new surfaces seem to have a reduced accident rate; about 83% of old surfaces.

Because old surfaces will be present later in the observation period than new surfaces it is possible for time trends to influence the result. The following table gives the numbers of accidents each year (July to June the following year) in the subset of the TAR database that I was provided with.

Year	Number of accidents
87-88	554
88-89	561
89-90	504
90-91	570
91-92	600

Any linear time trends present seem to be small.

The situation represented here, where the statistician has no control on how the treatments are applied, is notoriously difficult to analyse. Before accepting that a cause and effect relationship exists one has to think through all other ways that a relationship could be generated (e.g. through a time trend), and attempt to allow for these in the analysis.

In the present case, the effect is small and should be taken only as an indication of an effect.

#### 5.4 Wet Road

The TAR database indicates whether the road was wet at the time of an accident. We want to know whether the effect of geometry variables is different on wet roads as opposed to dry roads.

I would like to proceed as in Section 5.3. However, this requires a knowledge of the AADT values for the times each road segment is wet and for the times it is dry. This information is not available<sup>†</sup>. So I suppose there is no relationship between the geometry variables and the fraction of time a road is wet and let  $\gamma_i = \text{AADT}$  in (1). We will not be able to get any information on the absolute risk of wet roads as compared with dry roads, but there may be useful information on the differences in the effects of the geometry variables. Suppose we define a variable wet which is equal to 1 on the lines corresponding to wet accidents and 0 on the lines corresponding to dry accidents. Then interactions between wet and the other variables will correspond to those variables having different effects on wet and dry roads. The number of accidents on wet roads was 403 and the number on dry roads was 650. Here is the analysis of deviance table:

	Df	Deviance	Resid. Df	Resid. Dev	Pr(Chi)
NULL			49791	8066.6	
$\log_{10}(\text{AADT})$	1	1.3	49790	8065.3	0.2510
poly(ASMIN, PASMIN2, 2)	5	294.1	49785	7771.2	0.0000
DIR	7	40.4	49778	7730.8	0.0000
poly(GAV, 2)	2	7.2	49776	7723.6	0.0277
Wet	1	58.5	49775	7665.1	0.0000
$\log_{10}(\text{AADT})$ :Wet	1	1.6	49774	7663.5	0.2057
poly(ASMIN, PASMIN2, 2):Wet	5	37.7	49769	7625.8	0.0000
DIR:Wet	7	1.0	49762	7624.8	0.9941
poly(GAV, 2):Wet	2	1.8	49760	7622.9	0.4012

<sup>†</sup>But it might be possible to get an approximation to it from climate data.

The only significant interaction is with the polynomial function of ASMIN and PASMIN2. I also ran the analysis with HAV and HDIFF rather than ASMIN and PASMIN2, but the effect although still present was much smaller. To try to understand the meaning of the difference I re-ran the analysis of Section 4.3 but first with the accidents limited to those that occurred on wet roads and second with those that occurred on dry roads and then drew contour plots of risk as a function of ASMIN and PASMIN2. The results are in Figures 27 and 28. Although the graphs at first site look quite different, in fact they are similar for high ASMIN. But for low to moderate ASMIN roads with low PASMIN2 are relatively more dangerous when wet, but the opposite is true for dry roads.

But this needs to be analysed again when the problem of misplaced accidents is investigated further.

### 5.5 Alcohol and Drug Related Accidents

This is handled in the same way as the effect of wet road. Again we cannot calculate absolute risk, since we do not know the fraction of drivers affected by alcohol or drugs. I define a variable alcohol which is 1 if the TAR database includes any of the following factors as being associated with an accident:

- 101 Alcohol suspected
- 103 Alcohol test above limit or alcohol suspected
- 108 Drugs suspected
- 109 Drugs proven

and 0 otherwise. Alcohol or drugs were implicated in 274 accidents and were not implicated in 779.

In fact I found no significant results. Here is the analysis of deviance table:

	Df	Deviance	Resid. Df	Resid. Dev	Pr(Chi)
NULL			49791	8080.2	
log <sub>10</sub> (AADT)	1	1.3	49790	8078.8	0.2511
poly(ASMIN, PASMIN2, 2)	5	294.1	49785	7784.8	0.0000
DIR	7	40.4	49778	7744.3	0.0000
poly(GAV, 2)	2	7.2	49776	7737.2	0.0277
Alcohol	1	252.4	49775	7484.7	0.0000
log <sub>10</sub> (AADT):Alcohol	1	0.7	49774	7484.1	0.4121
poly(ASMIN, PASMIN2, 2):Alcohol	5	9.9	49769	7474.2	0.0789
DIR:Alcohol	7	9.8	49762	7464.4	0.2041
poly(GAV, 2):Alcohol	2	2.0	49760	7462.4	0.3659



## 5.6 Overtaking and Head-On Accidents

We want to see how the analyses compared for accidents that involve isolated vehicles as opposed to those in which traffic density would be a factor. The analysis is similar in layout to those in Sections 5.4 and 5.5. Here, I classify the accident according to the main code on the vehicle movement coding sheet. A indicates a overtaking or lane change accident and B a head-on accident. So I define a variable AB which takes the value 1 when the accident is of type A or B and 0 when it is of type C or D. (Only A, B, C and D occur in the data used here.)

The interpretation of the analysis here is different from that in Sections 5.3, 5.4 and 5.5. In those sections the extra variable was an explanatory variable describing the condition of the road or driver. In this section the extra variable is describing part of the outcome so is part of the dependent variable. Nevertheless the same type of analysis is still effective and any interaction between AB and the geometry variables will indicate that the geometry variables have different effects on the different types of accidents.

578 accidents were of type A or B and 475 of type C or D. The analysis using HAV and HDIFF was similar to that using ASMIN and PASMIN2 so I use the HAV and HDIFF one. Here is the analysis of deviance table:

	Df	Deviance	Resid. Df	Resid. Dev	Pr(Chi)
NULL			49791	8079.1	
$\log_{10}(\text{AADT})$	1	1.3	49790	8077.8	0.2511
poly(HAV, 2)	2	118.4	49788	7959.4	0.0000
poly(HDIFF, 2)	2	150.8	49786	7808.6	0.0000
DIR	7	40.8	49779	7767.8	0.0000
poly(GAV, 2)	2	8.9	49777	7758.9	0.0119
AB	1	10.1	49776	7748.9	0.0015
$\log_{10}(\text{AADT}):AB$	1	14.9	49775	7733.9	0.0001
poly(HAV, 2):AB	2	8.3	49773	7725.7	0.0159
poly(HDIFF, 2):AB	2	2.1	49771	7723.6	0.3493
DIR:AB	7	3.9	49764	7719.6	0.7888
poly(GAV, 2):AB	2	3.0	49762	7716.6	0.2209

The interactions with AADT and HAV are significant, so I re-ran the analysis of Section 4.2, first with just the AB data and then with the CD data. Graphs of the risk versus  $\log_{10}(\text{AADT})$  are given in Figures 29 and 30. The AB accidents show an increasing, but not statistically significant increase in risk with increasing AADT; the CD accidents show a decrease in risk with increasing AADT. Graphs of the risk versus HAV are given in Figures 31 and 32. The graphs are skewed in opposite direction but the relative risks are of the same general size.

## 6. FURTHER WORK

Further work that should be carried out on the present set of data under a new contract. This work is not included under the present contract.

- Recalculation of geometry data using outlier resistant methods. The geometry data appears to be subject to occasional erroneous measurements. It should be possible to eliminate the effects of at least some of these by using an improved method of deriving the 200 m data. If the errors arise from isolated outliers in the 10 m data then it may be sufficient to apply a simple robust smoother<sup>‡</sup> to the 10 m data. I do not expect this will have a big effect on the present analysis. Nevertheless, this recalculation needs to be done before any further analysis is carried out using the geometry data.
- Improving the model (1) to allow for misplaced accidents. For example, as a simple improvement, let  $\lambda_i$  be as in (1) but suppose  $E(Y_j) = \frac{1}{2}\alpha\lambda_{i-1} + (1 - \alpha)\lambda_i + \frac{1}{2}\alpha\lambda_{i+1}$ . Here,  $\alpha$  is between 0 and 1 and shows the probability of an accident being displaced to an adjacent segment. Then we have a model which it would be feasible to fit and which would allow for displacement of accidents by one segment. It would probably be better to use a standard programming language<sup>\*\*</sup> rather than S-plus for doing this fit.
- Carry out goodness of fit tests. One way of doing this is to reconstruct the one and two way tables from the Poisson model and see how well they agree with the actual tables.
- Investigation of reporting rates and seriousness of accidents. By repeating the analysis on only moderately serious accidents, it should be possible to get some indication on how variable reporting rates are affecting the results.
- Another look at the effect of surface age; this time looking at risk in the year preceding resealing versus the year following resealing.
- Investigate to what extent the model predicts known black-spots.
- Look at effects of surface type, surface age and wet road together.
- Further investigation of the unexpected effects of SCW and DIR.

<sup>‡</sup>See Chapter 6 of "Applications, Basics and Computing of Exploratory Data Analysis" by P.F. Velleman and D.C. Hoaglin, published by Duxbury Press, Boston in 1981.

<sup>\*\*</sup>My C++ matrix library has the basis of the appropriate routines for doing this analysis.

## 7. THE FIGURES

Here is the list of figures.

- Figure 1: histograms of geometry data
- Figure 2: histograms of geometry data
- Figure 3: histograms of other data
- Figure 4: pair-wise plots of geometry data
- Figure 5: XAV vs HAV: HMAX-HMIN<10
- Figure 6: XAV vs HAV: HMAX-HMIN>10
- Figure 7: HMAX vs HMIN
- Figure 8: HMAX vs HMIN: HMAX-HMIN<10
- Figure 9: sorted AADT
- Figure 10: cumulative sum of sorted AADT
- Figure 11: cumulative sum of AADT vs AADT
- Figure 12: sum of accidents vs sum of AADT
- Figure 13: subset I - histograms of geometry data
- Figure 14: subset I - histograms of geometry data
- Figure 15: subset I - histograms of other data
- Figure 16: subset I - risk vs AADT
- Figure 17: subset I - risk vs HAV
- Figure 18: subset I - risk vs HDIFF
- Figure 19: subset I - risk vs GAV
- Figure 20: subset I - risk vs ASMIN and PASMIN2
- Figure 21: subset II - risk vs AADT
- Figure 22: subset II - risk vs HAV
- Figure 23: subset II - risk vs HDIFF
- Figure 24: subset II - risk vs GAV
- Figure 25: subset II - risk vs SCW
- Figure 26: subset II - risk vs ASMIN and PASMIN2
- Figure 27: dry roads - risk vs ASMIN and PASMIN2
- Figure 28: wet roads - risk vs ASMIN and PASMIN2
- Figure 29: AB accidents - risk vs AADT
- Figure 30: CD accidents - risk vs AADT
- Figure 31: AB accidents - risk vs HAV
- Figure 32: CD accidents - risk vs HAV

Figure 1: histograms of geometry data

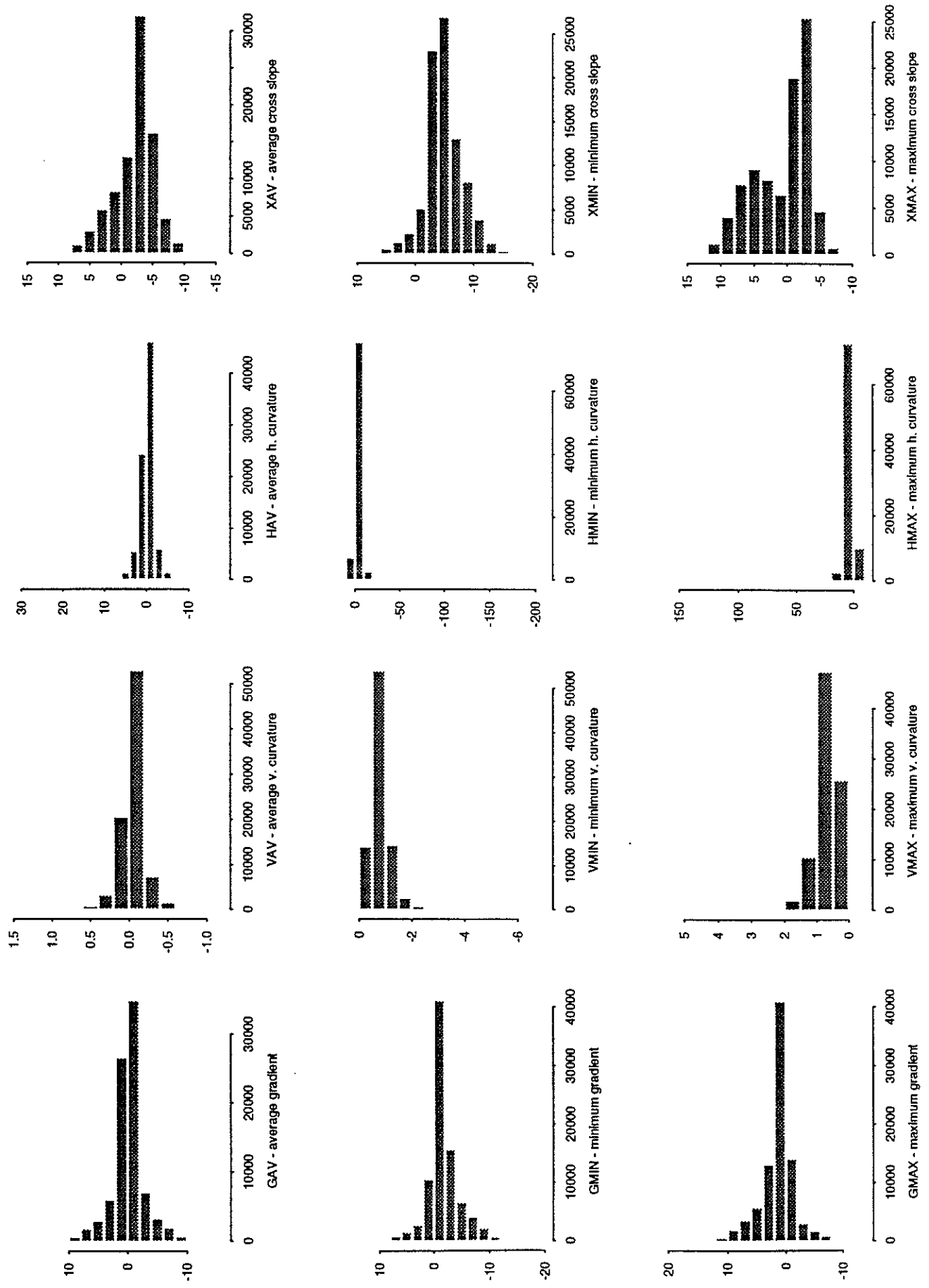


Figure 2: histograms of geometry data

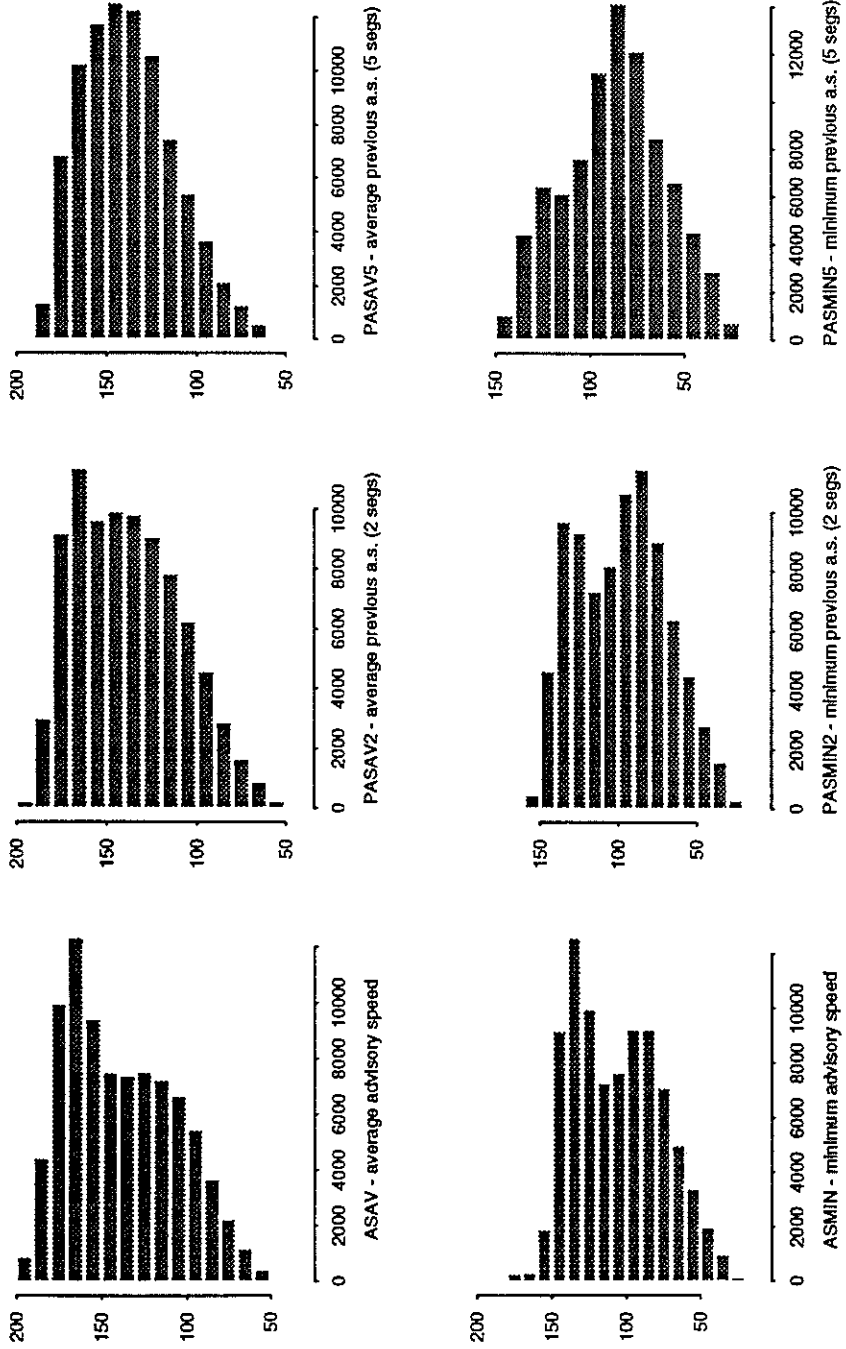


Figure 3: histograms of other data

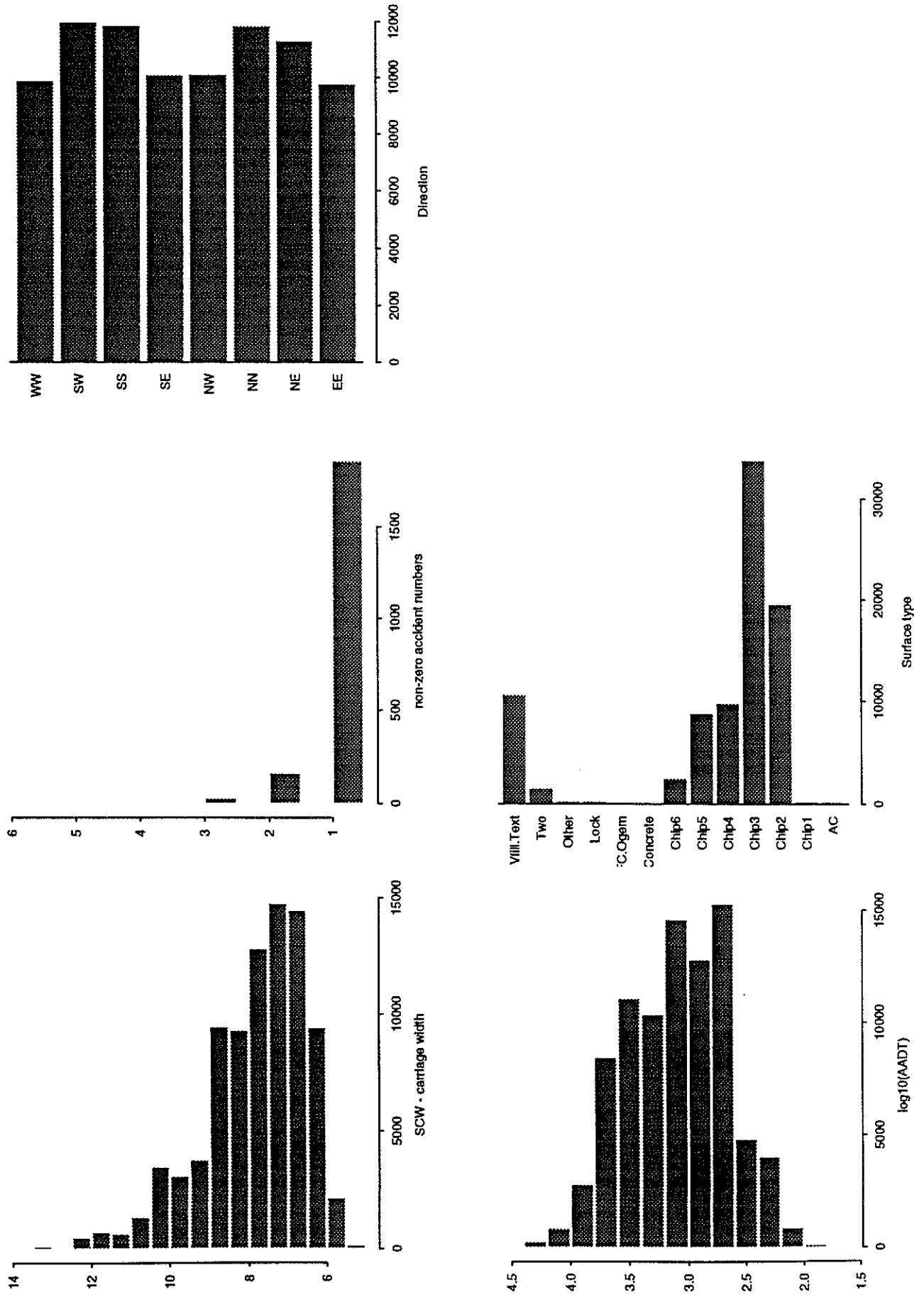


Figure 4: pairwise plots of geometry data

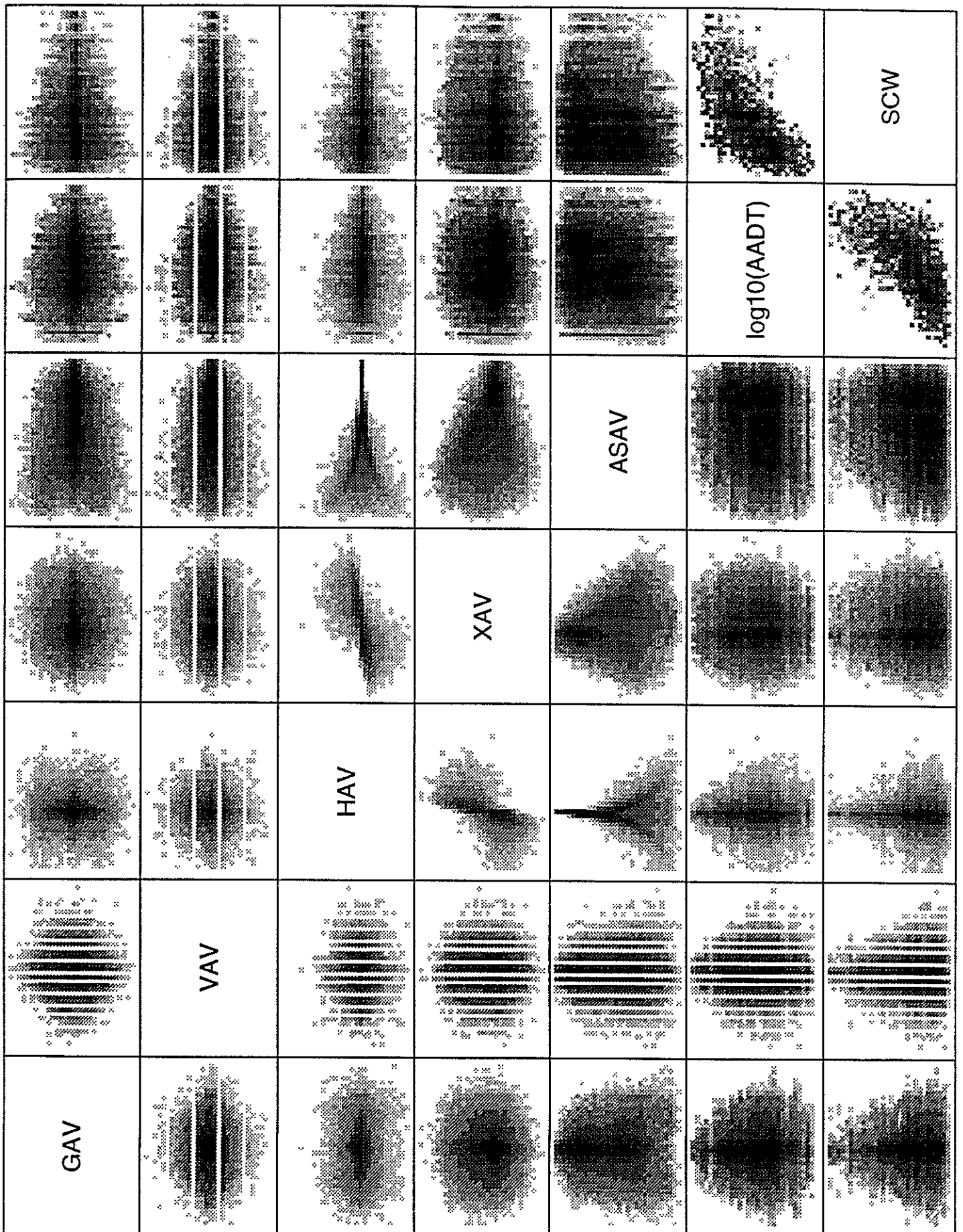


Figure 5: XAV vs HAV: HMAX-HMIN < 10

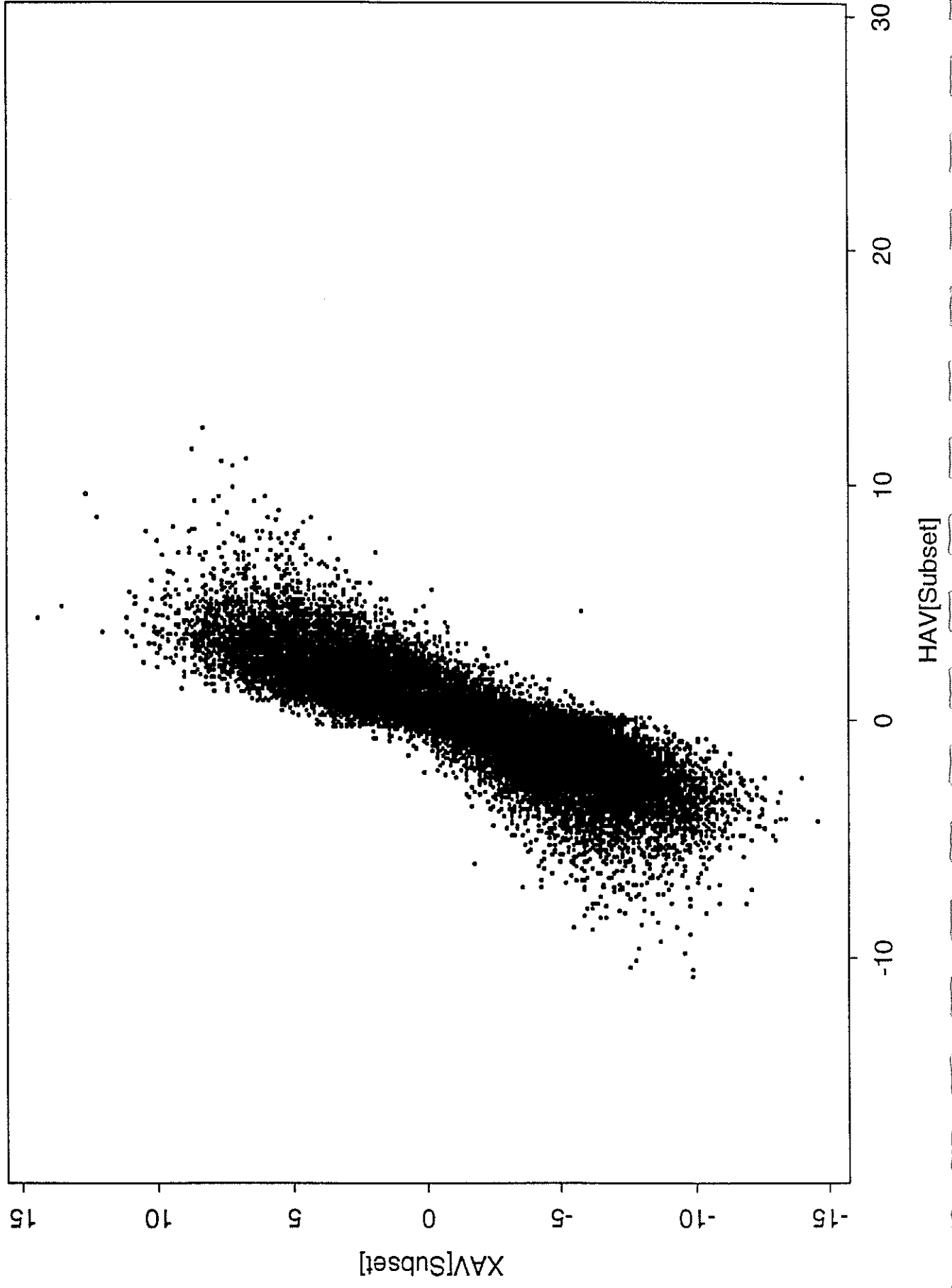




Figure 6: XAV vs HAV: HMAX-MIN > 10

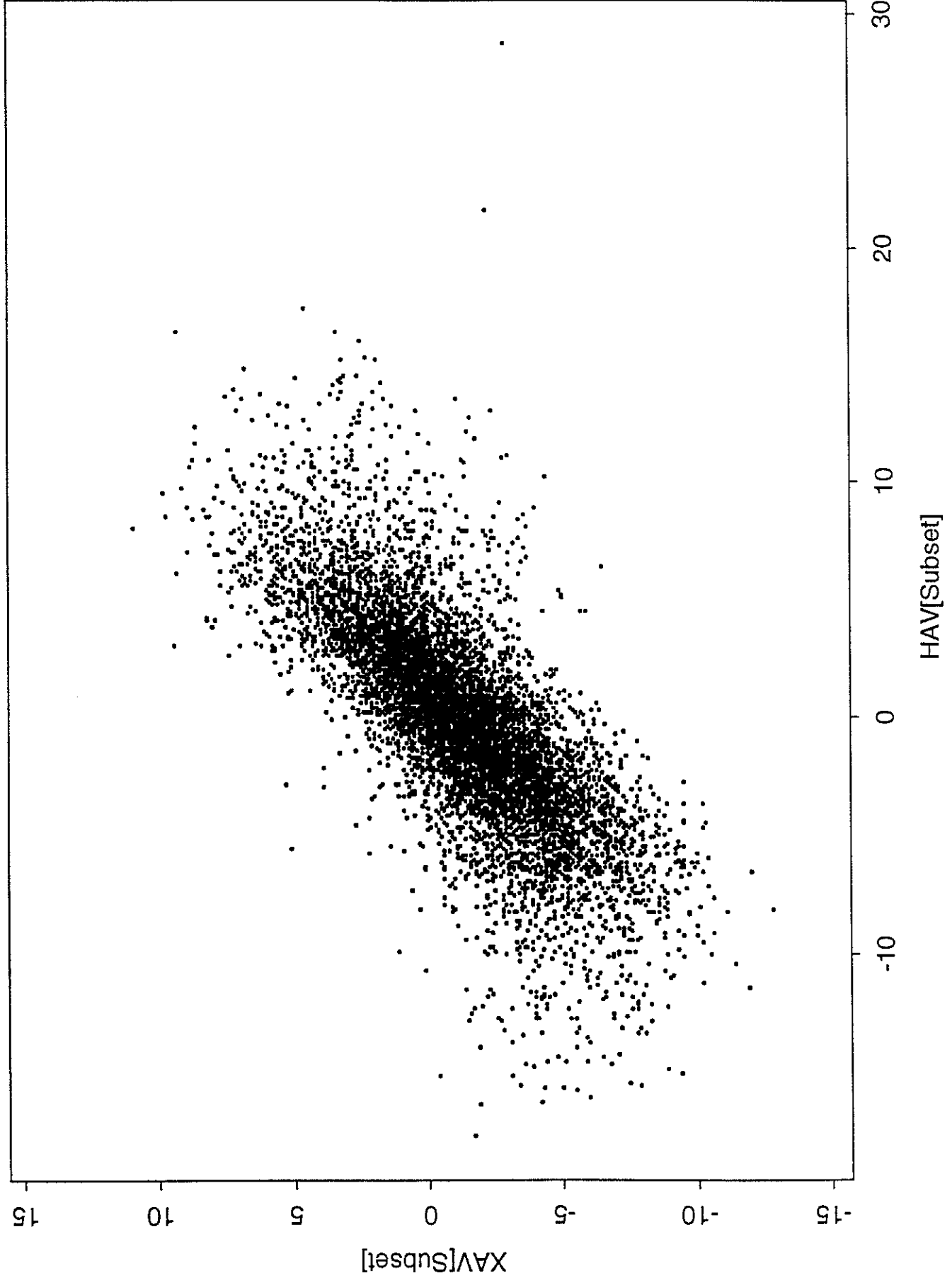


Figure 7: HMAX vs HMIN

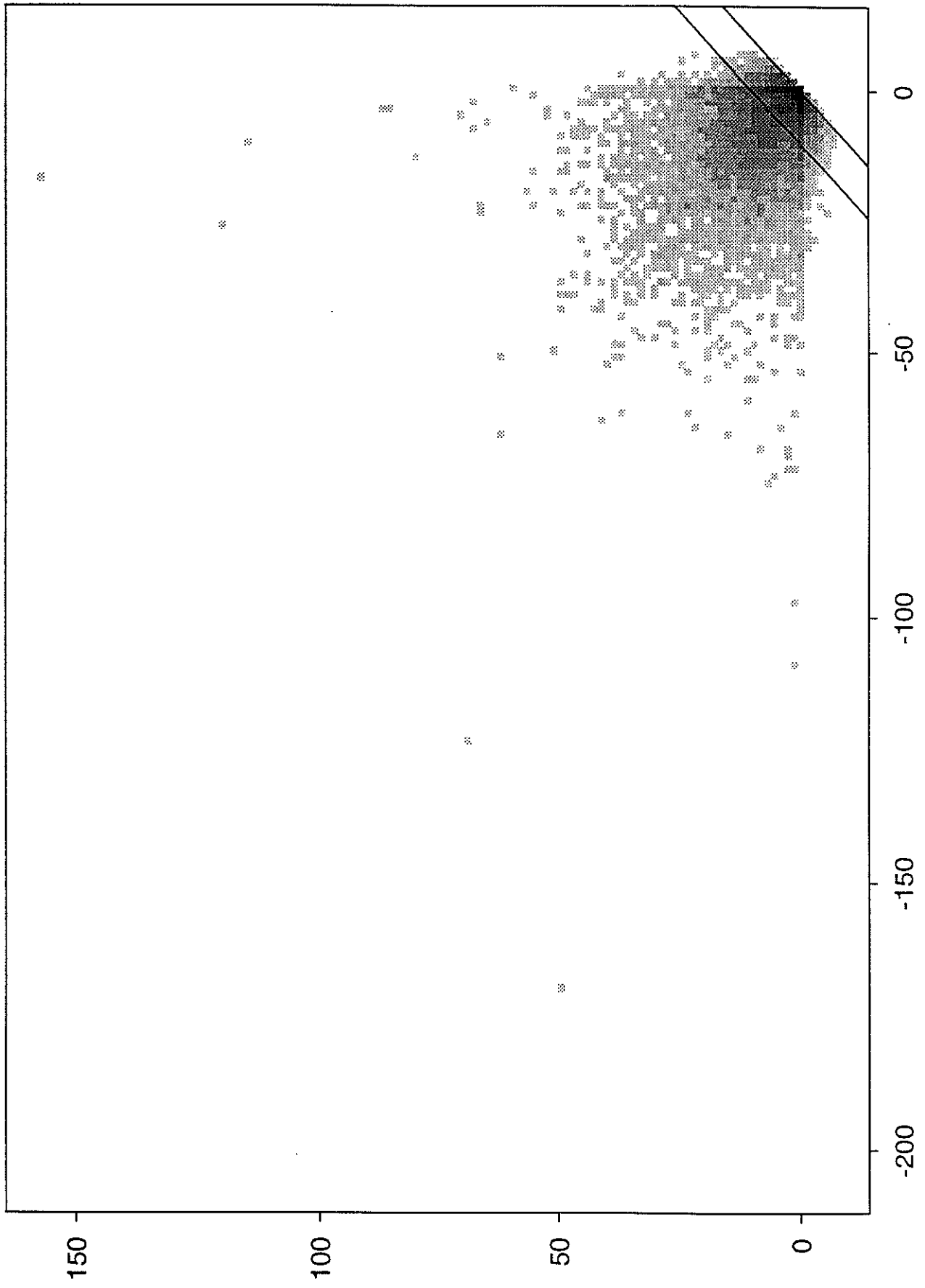


Figure 8: HMAX vs HMIN: HMAX-HMIN < 10

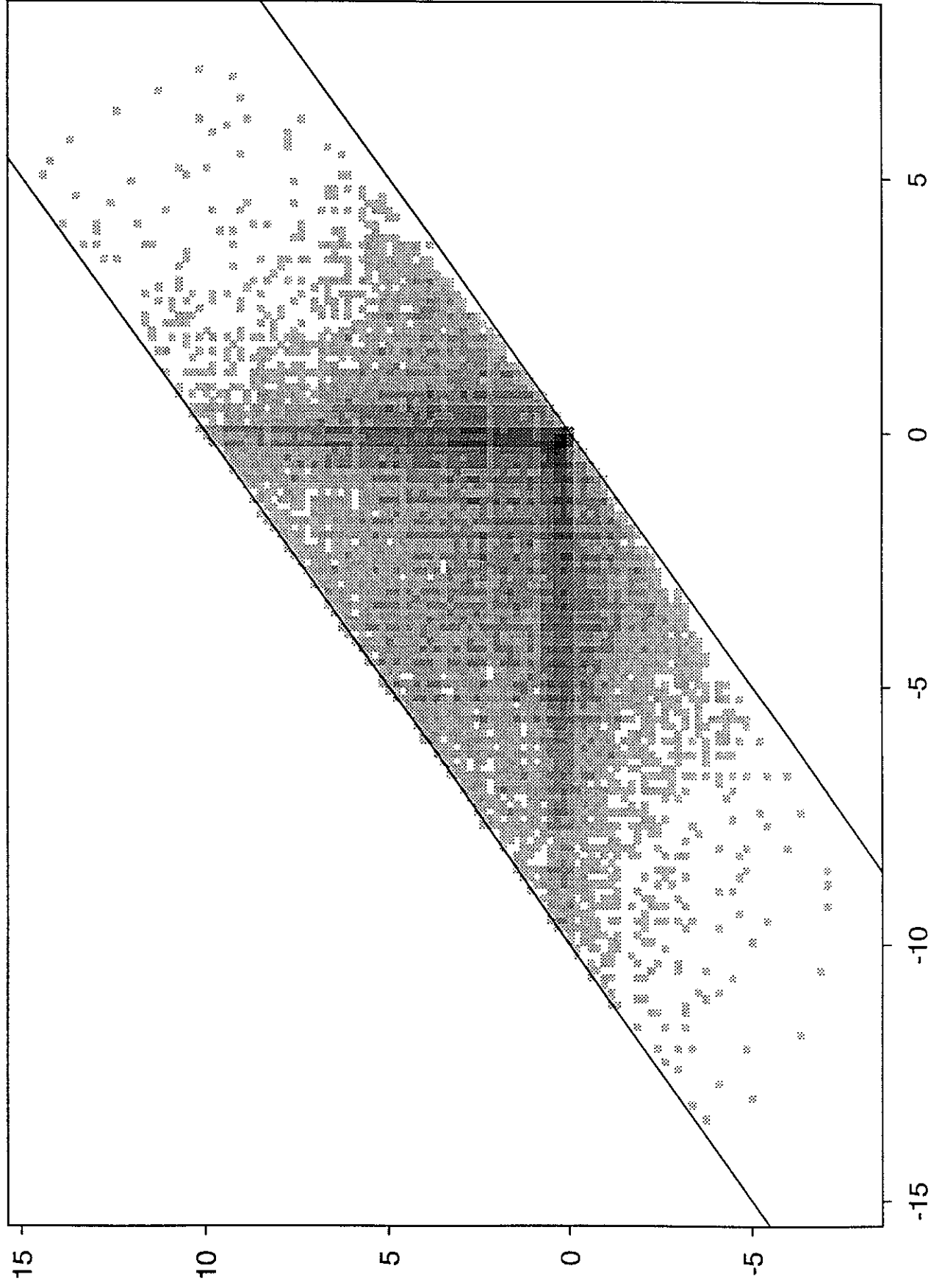


Figure 9: sorted AADT

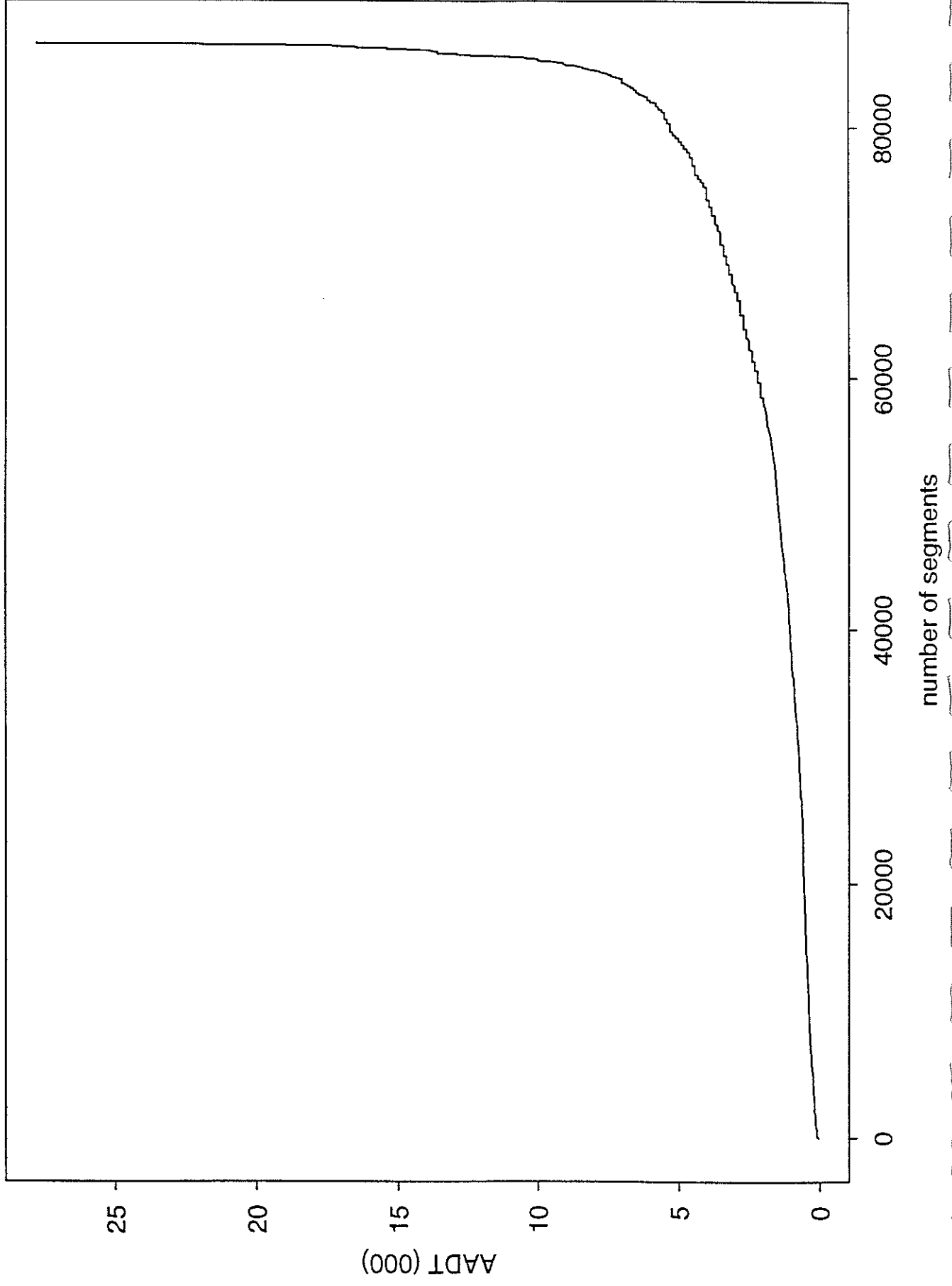


Figure 10: cumulative sum of sorted AADT

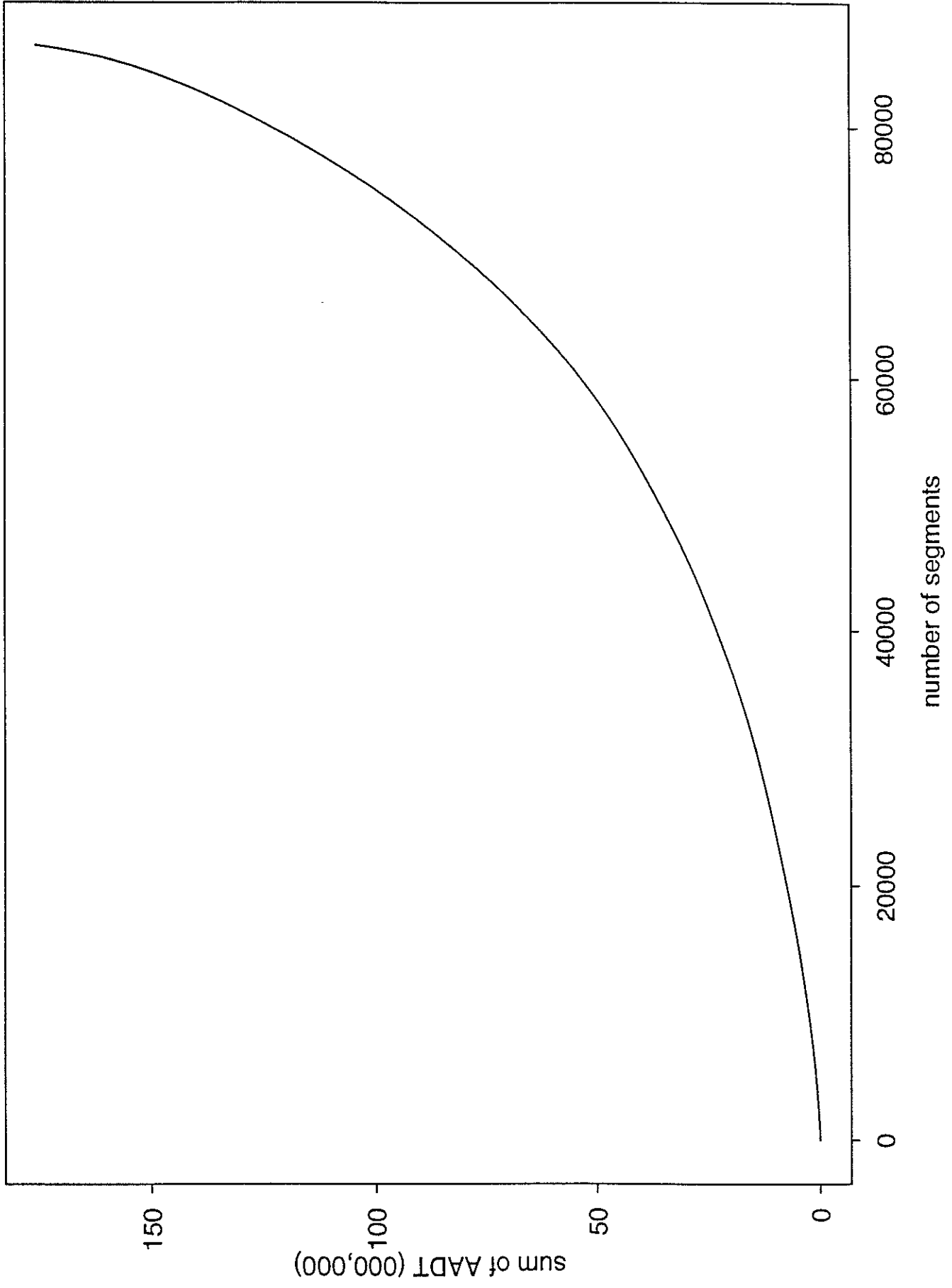


Figure 11: cumulative sum of sorted AADT vs AADT

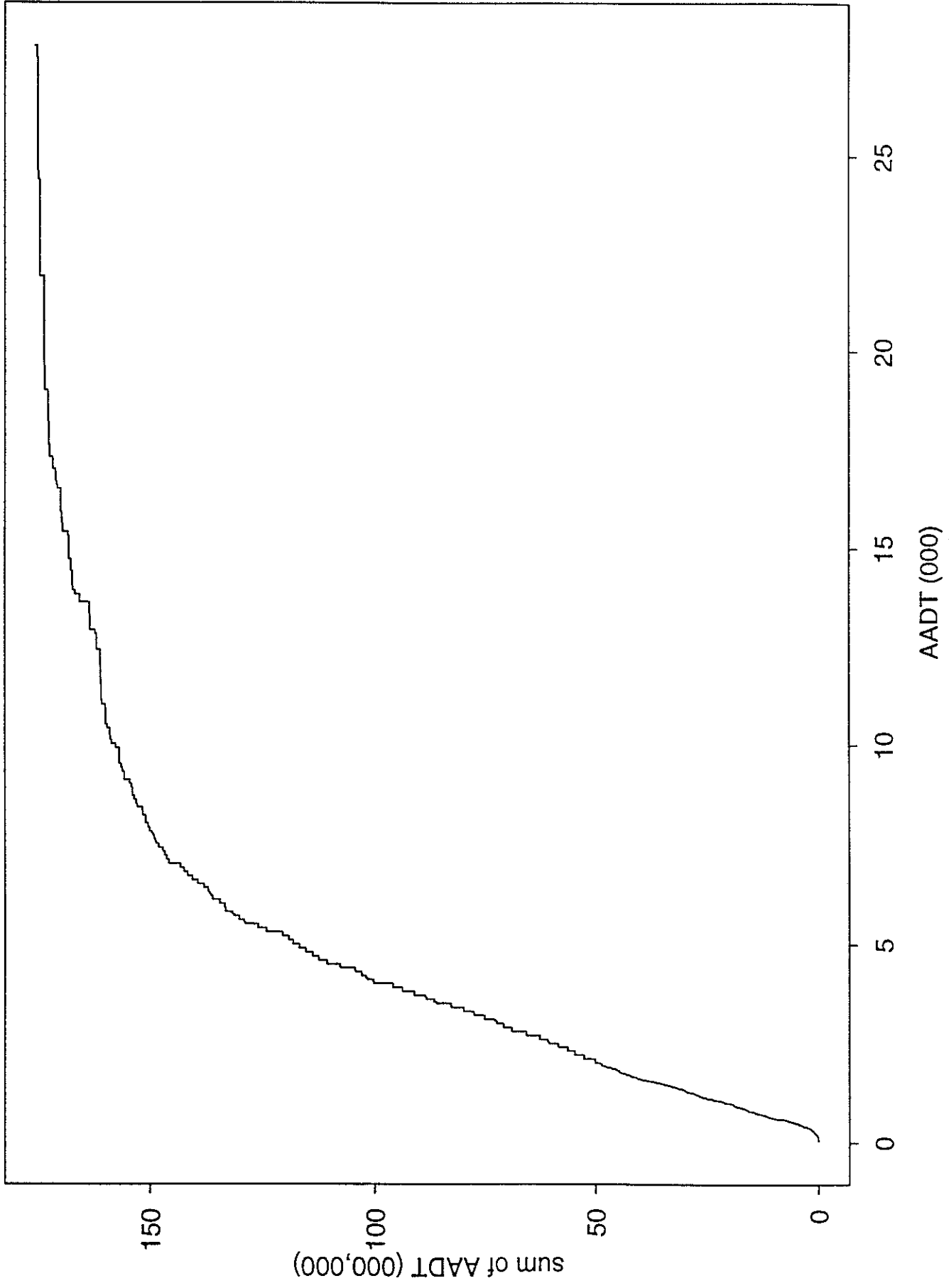


Figure 12: sum of accidents vs sum of AADT

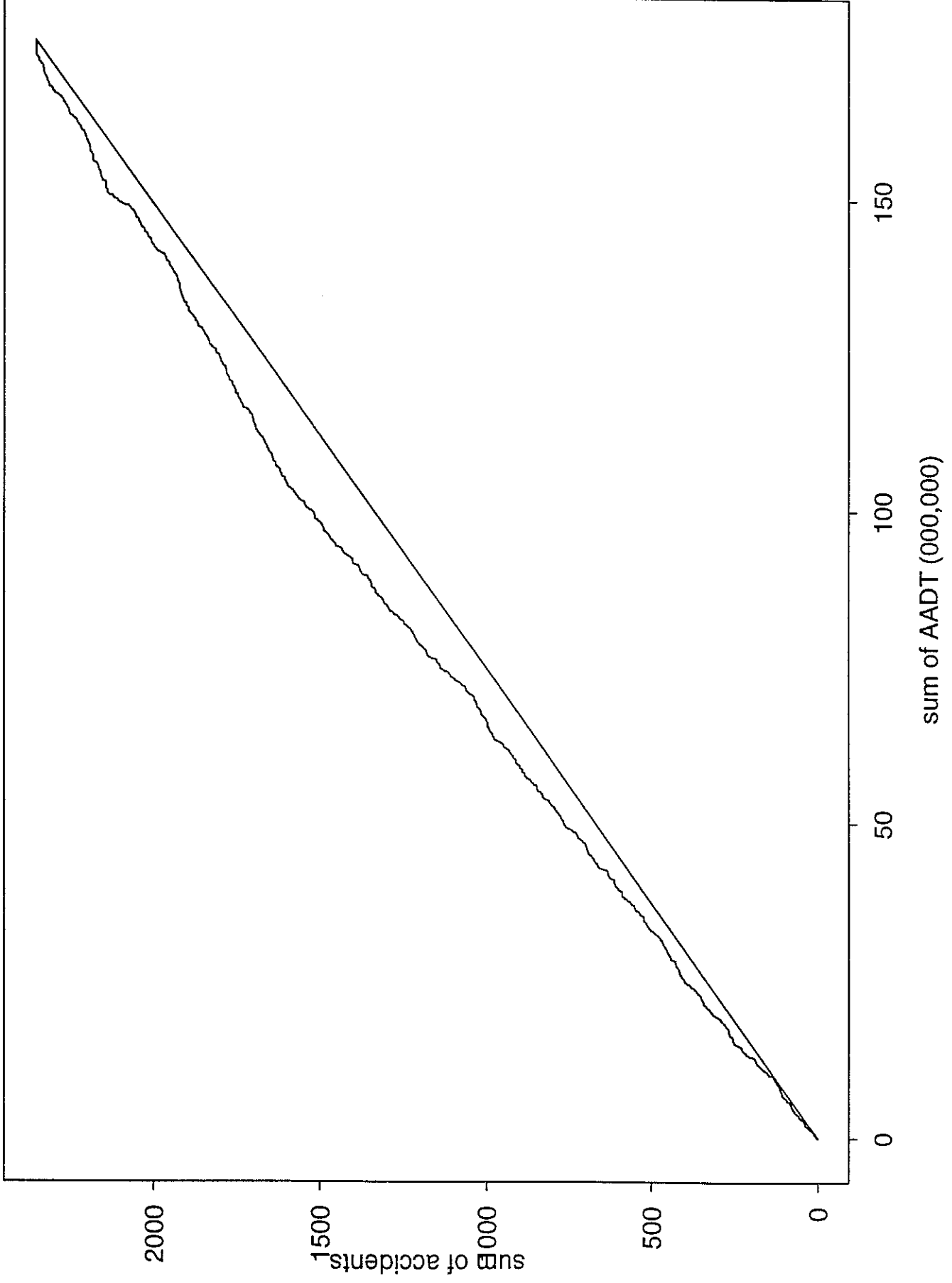


Figure 13: subset I - histograms of geometry data

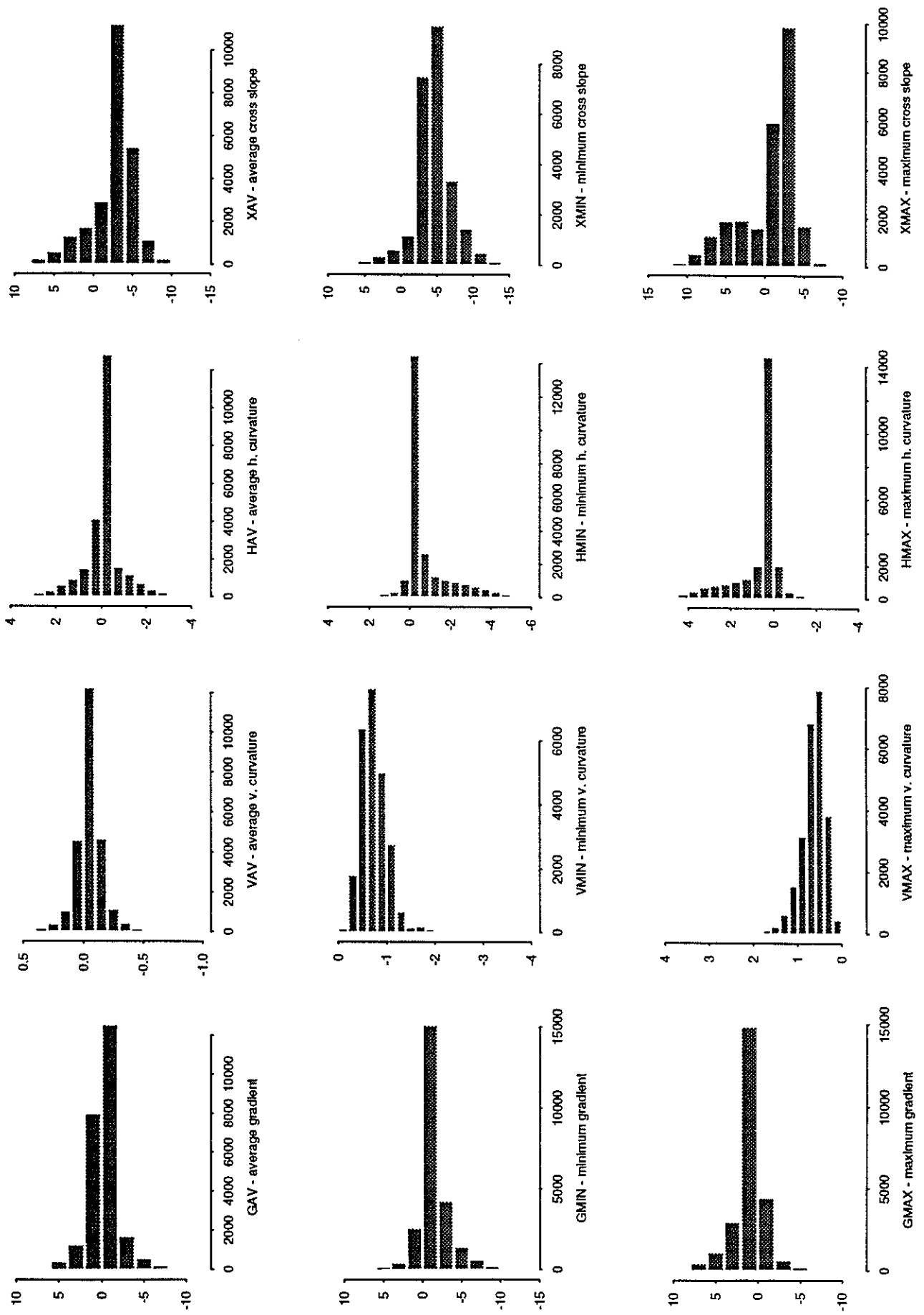




Figure 14: subset I - histograms of geometry data

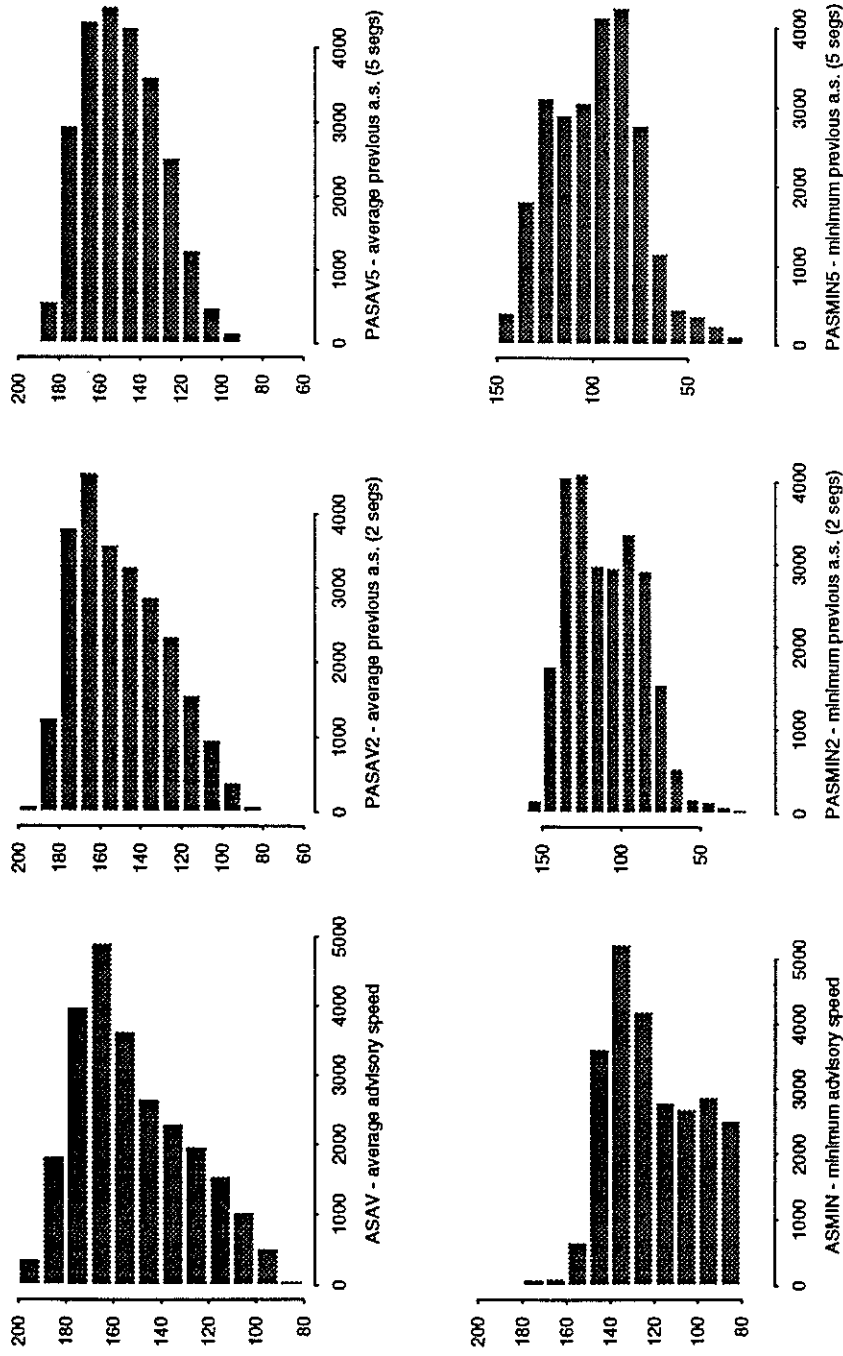


Figure 15: Subset I - histograms of other data

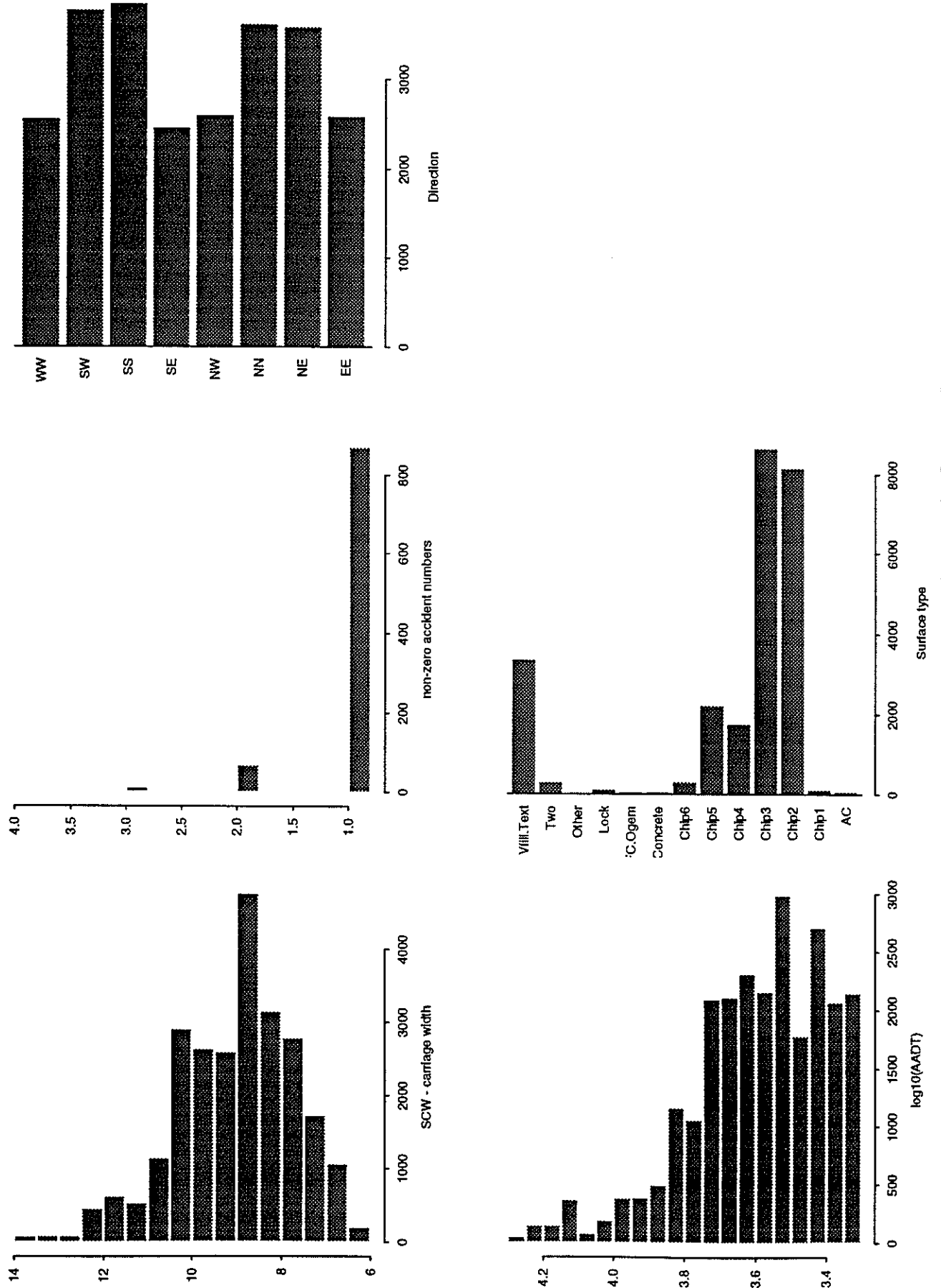


Figure 16: subset I - risk vs AADT

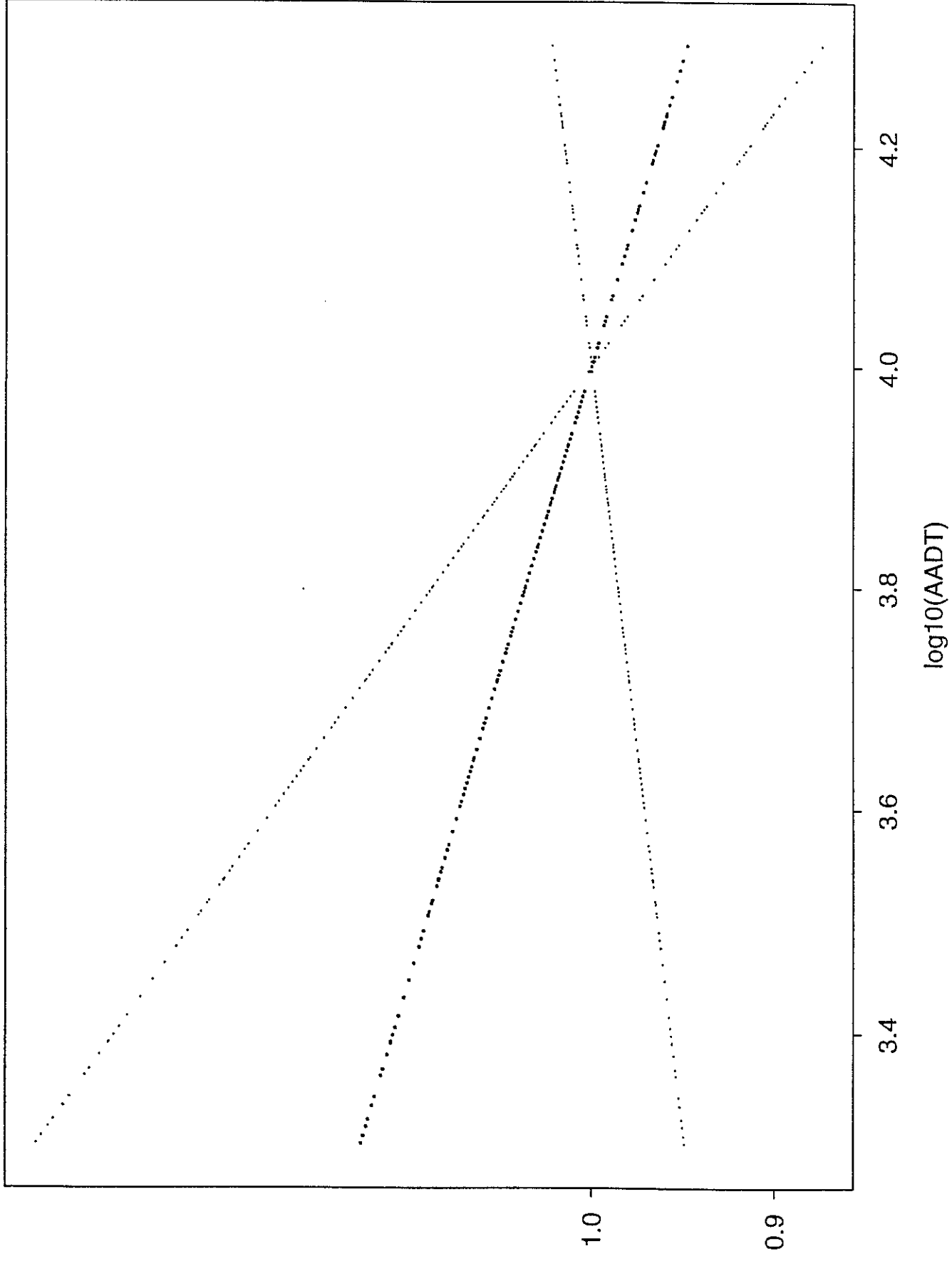


Figure 17: subset I - risk vs HAV

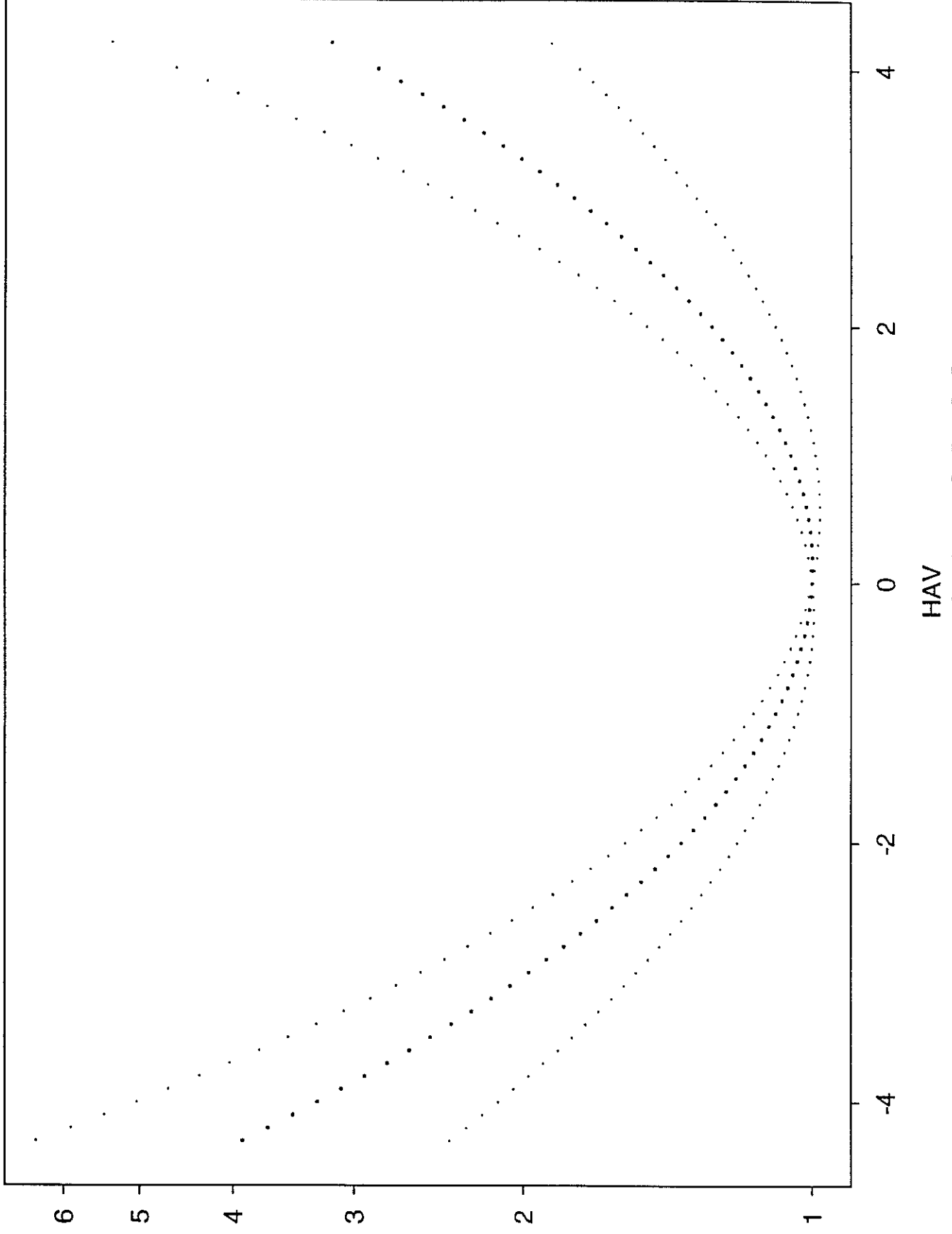


Figure 18: subset I - risk vs HDIFF

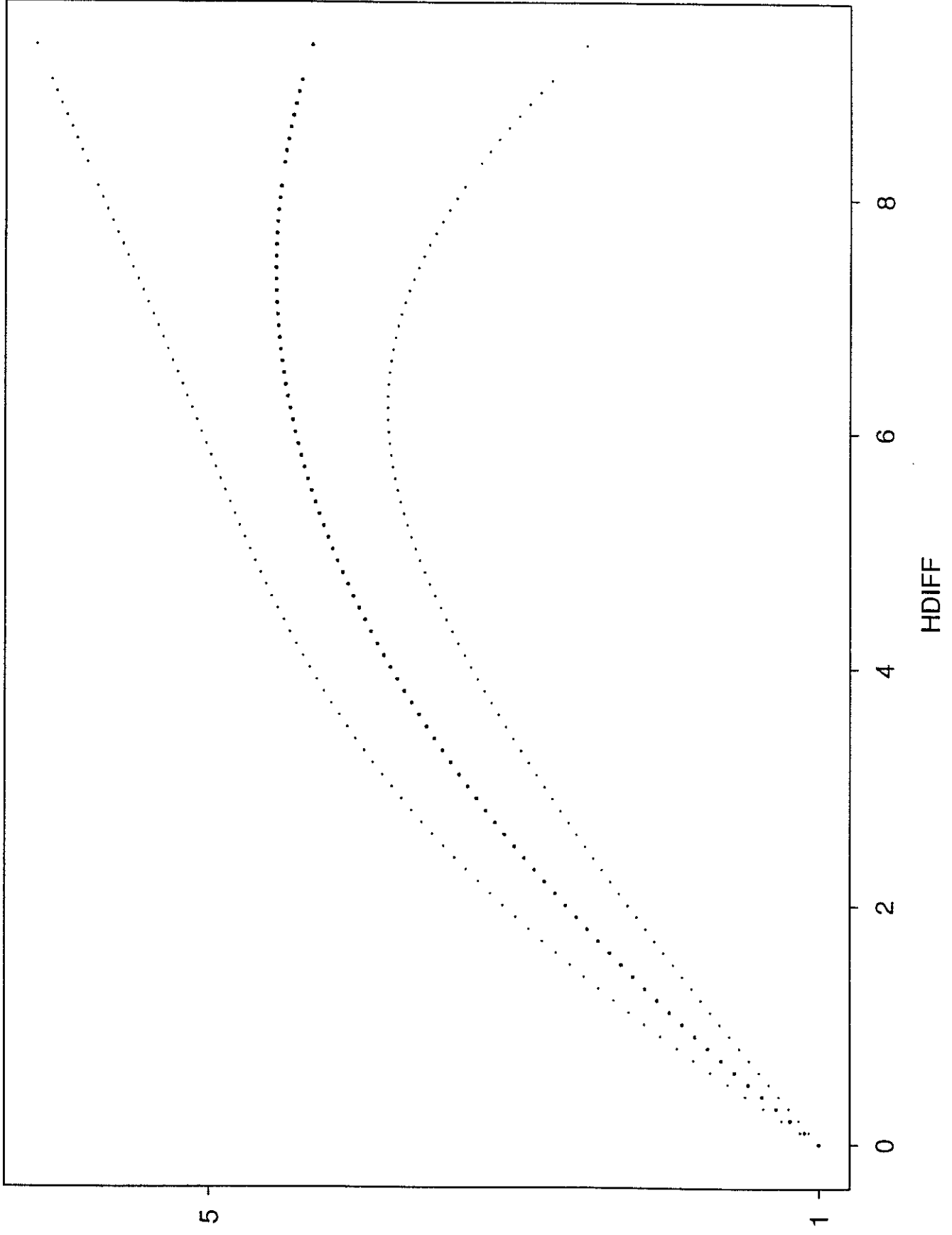


Figure 19: subset I - risk vs GAV

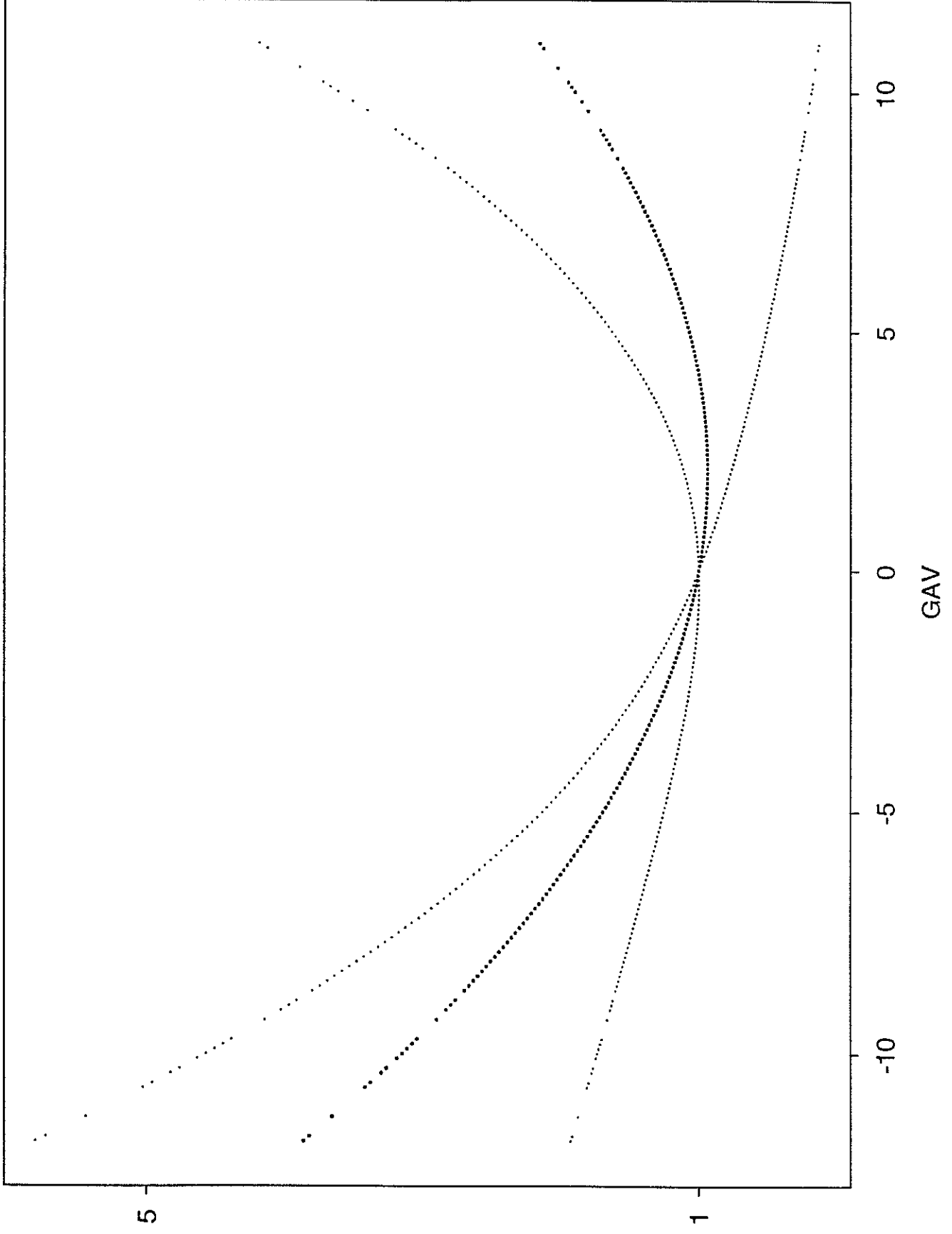


Figure 20: subset I - risk vs ASMIN and PASMIN2

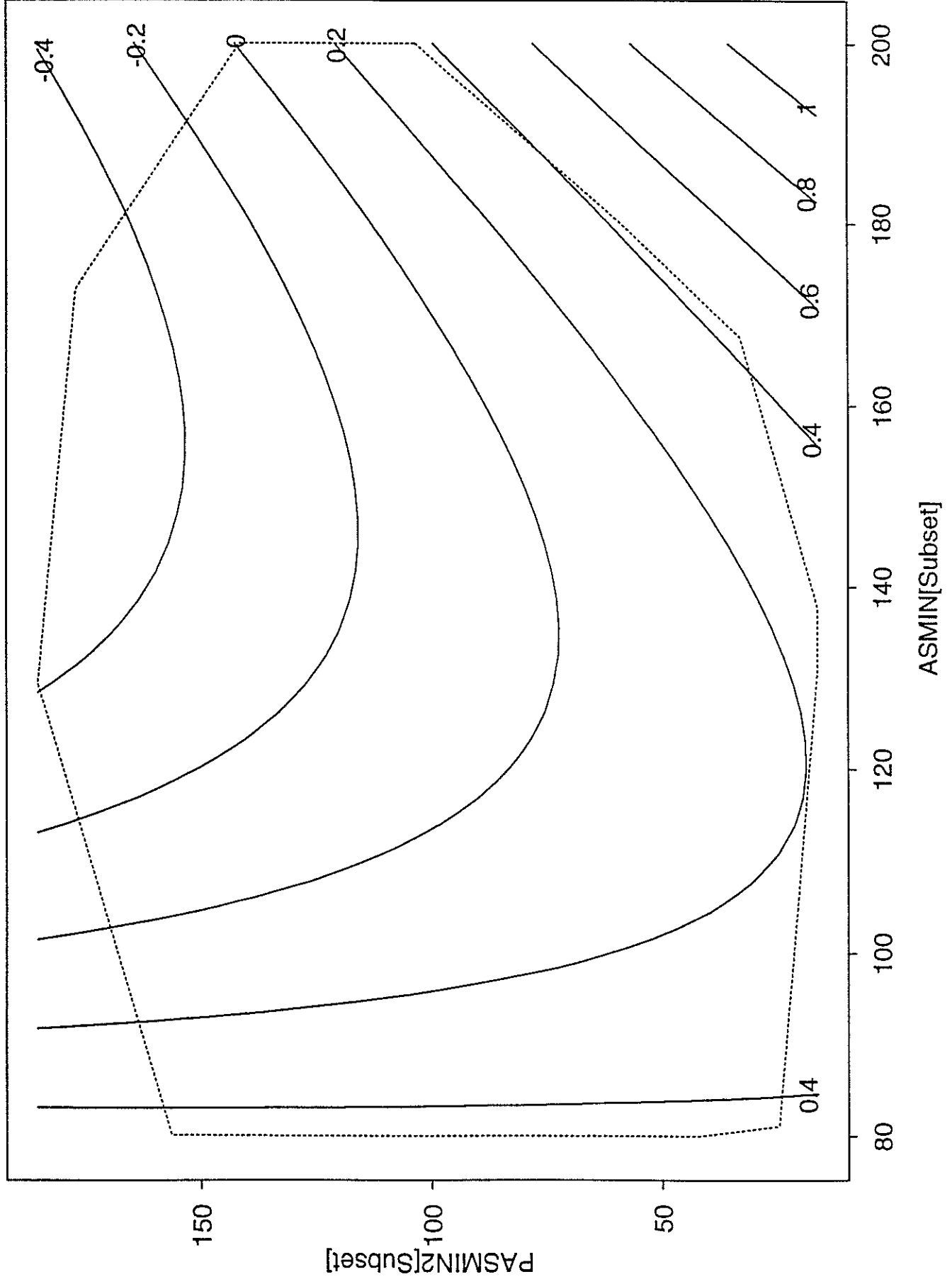


Figure 21: subset II - risk vs AADT

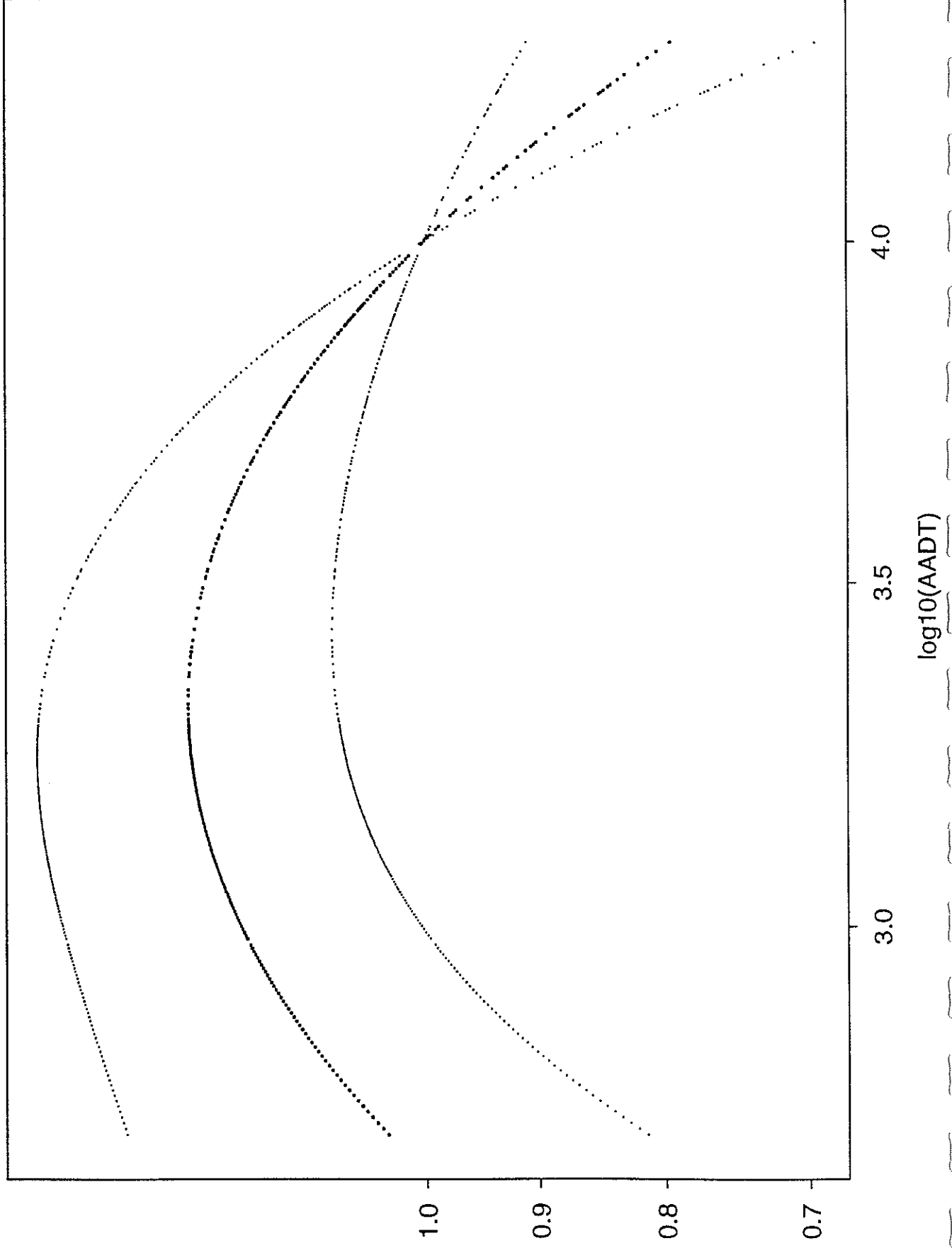




Figure 22: subset II - risk vs HAV

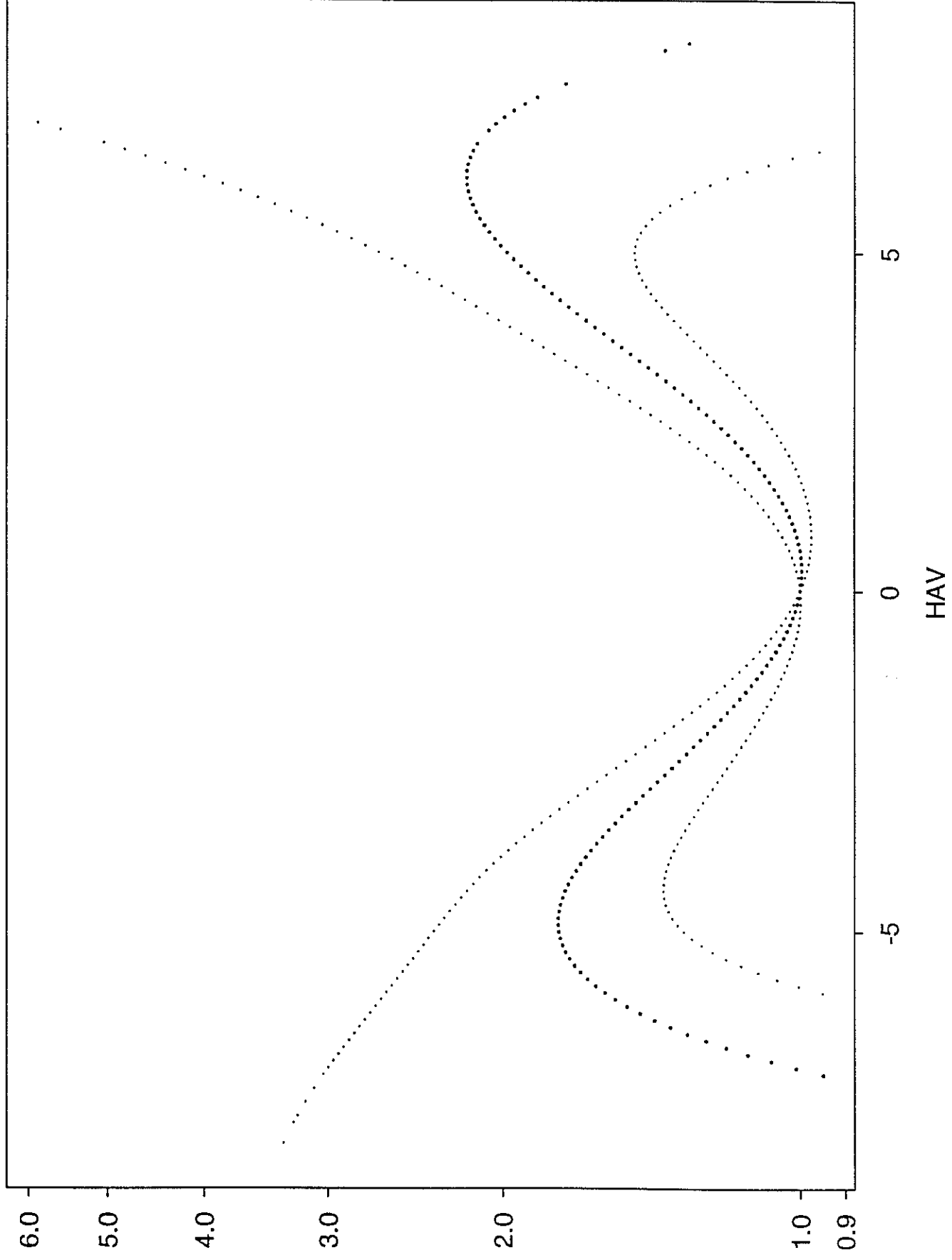


Figure 23: subset II - risk vs HDIFF

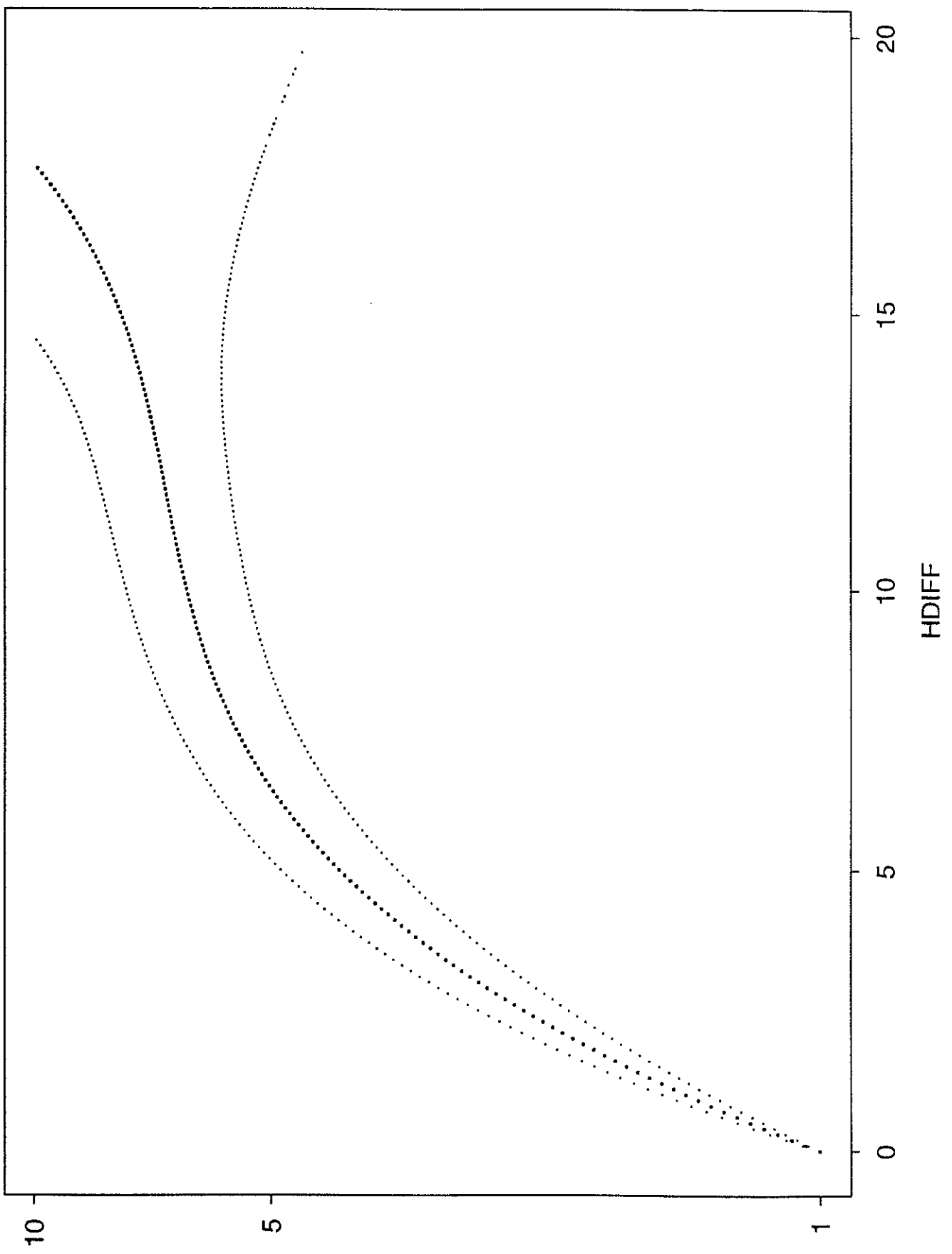


Figure 24: subset II - risk vs GAV

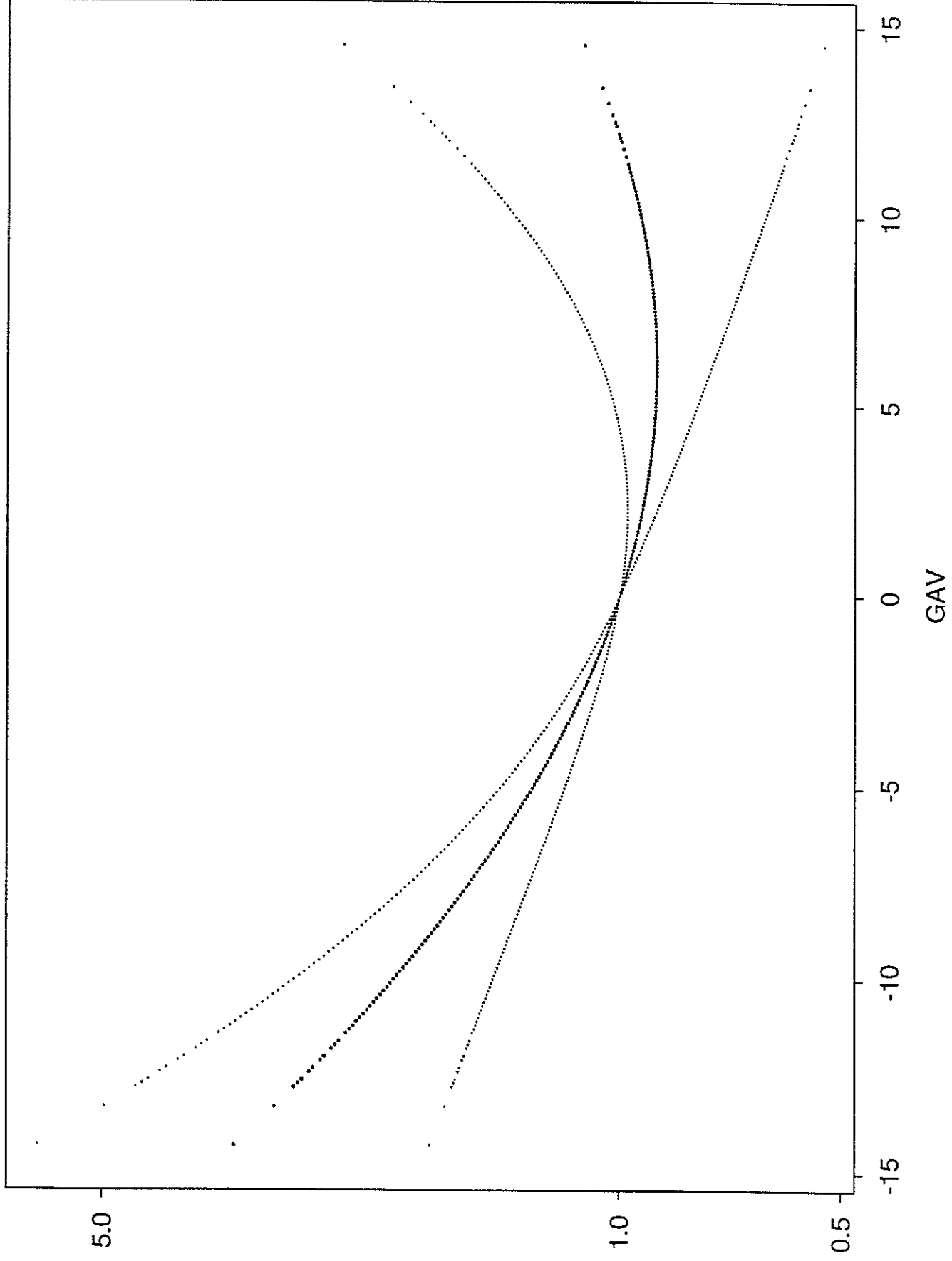


Figure 25: subset II - risk vs SCW

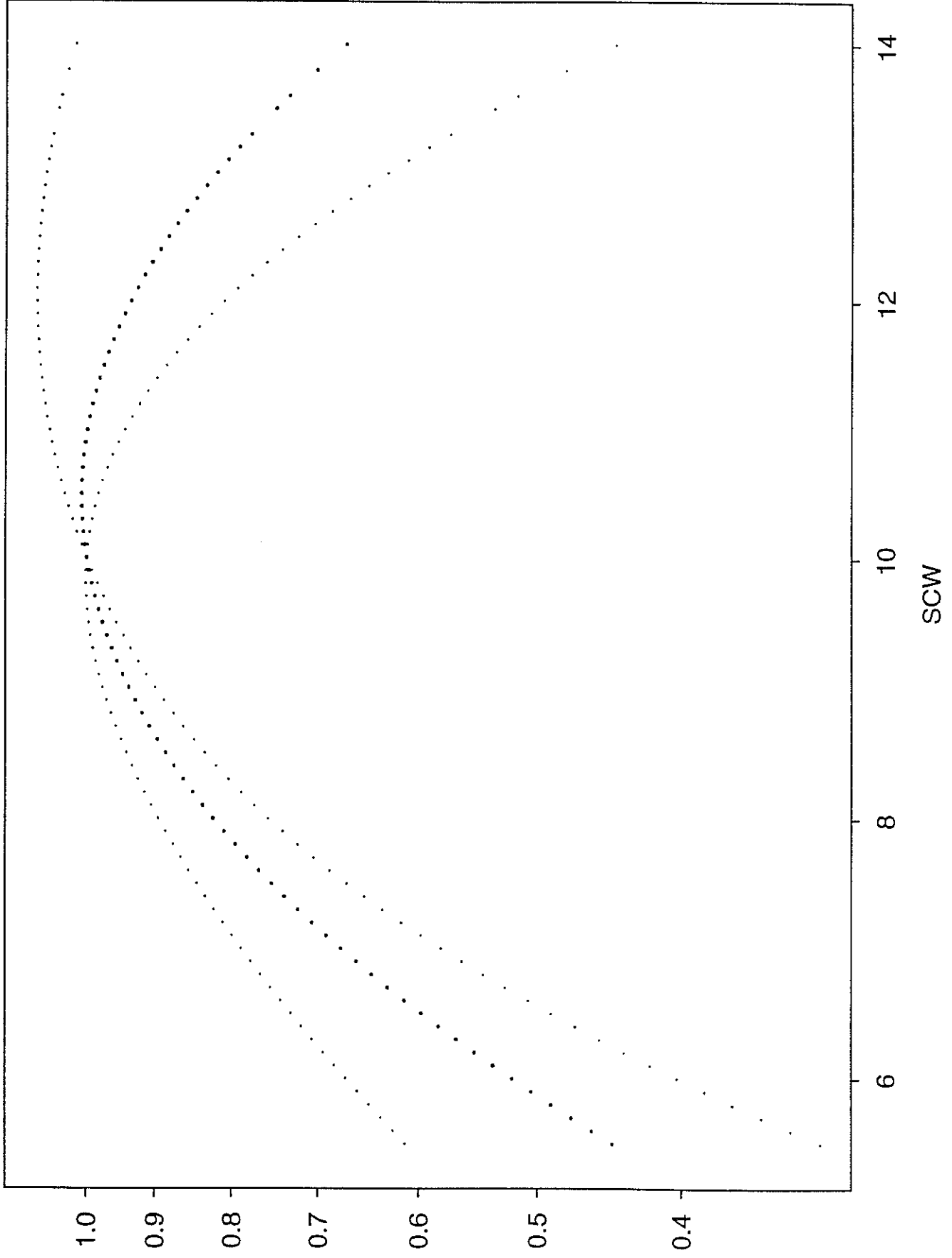


Figure 26: subset II - risk vs ASMIN and PASMINE2

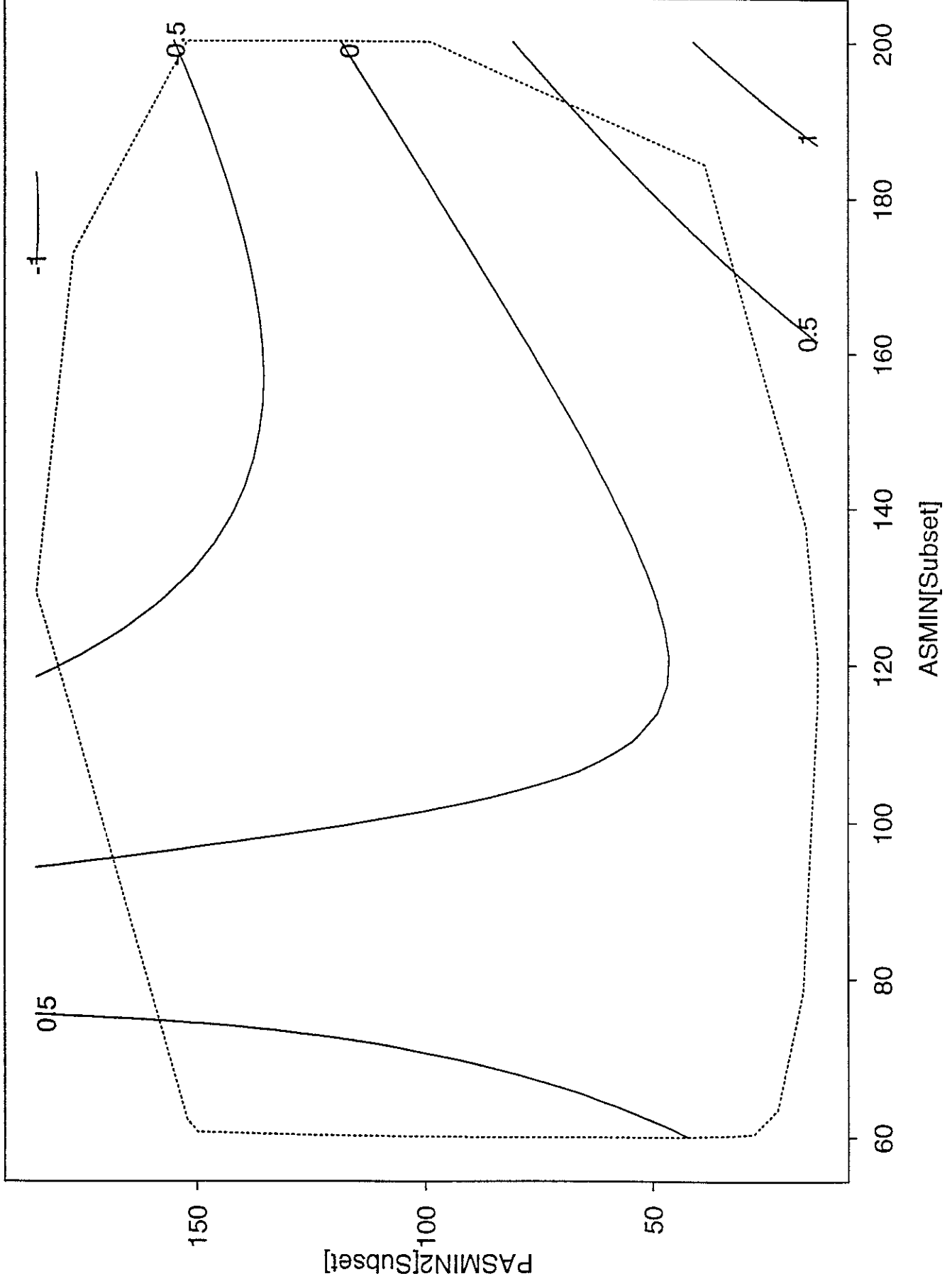


Figure 27: dry roads - risk vs ASMIN and PASMING2

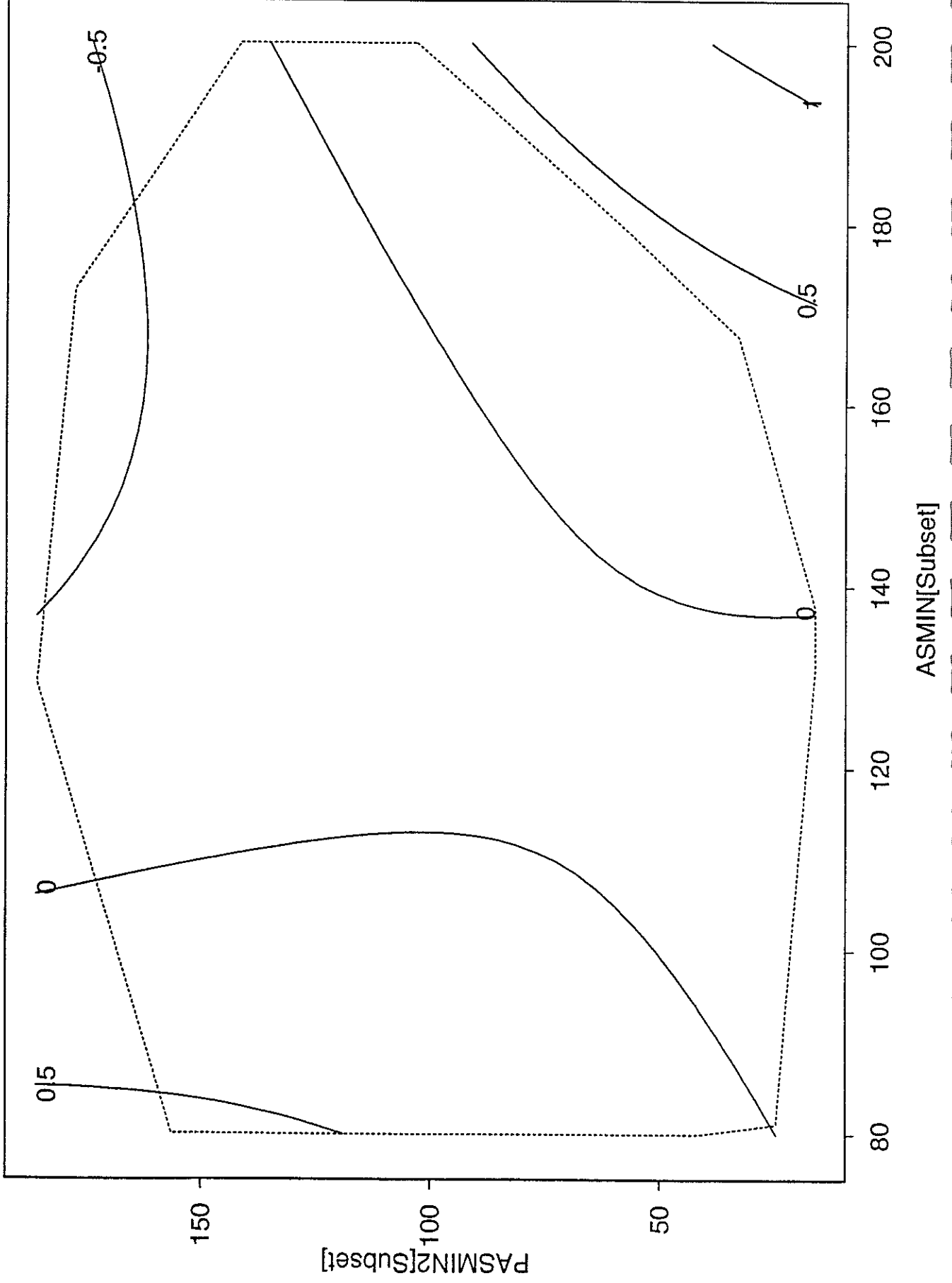


Figure 28: wet roads - risk vs ASMIN and PASMINE2

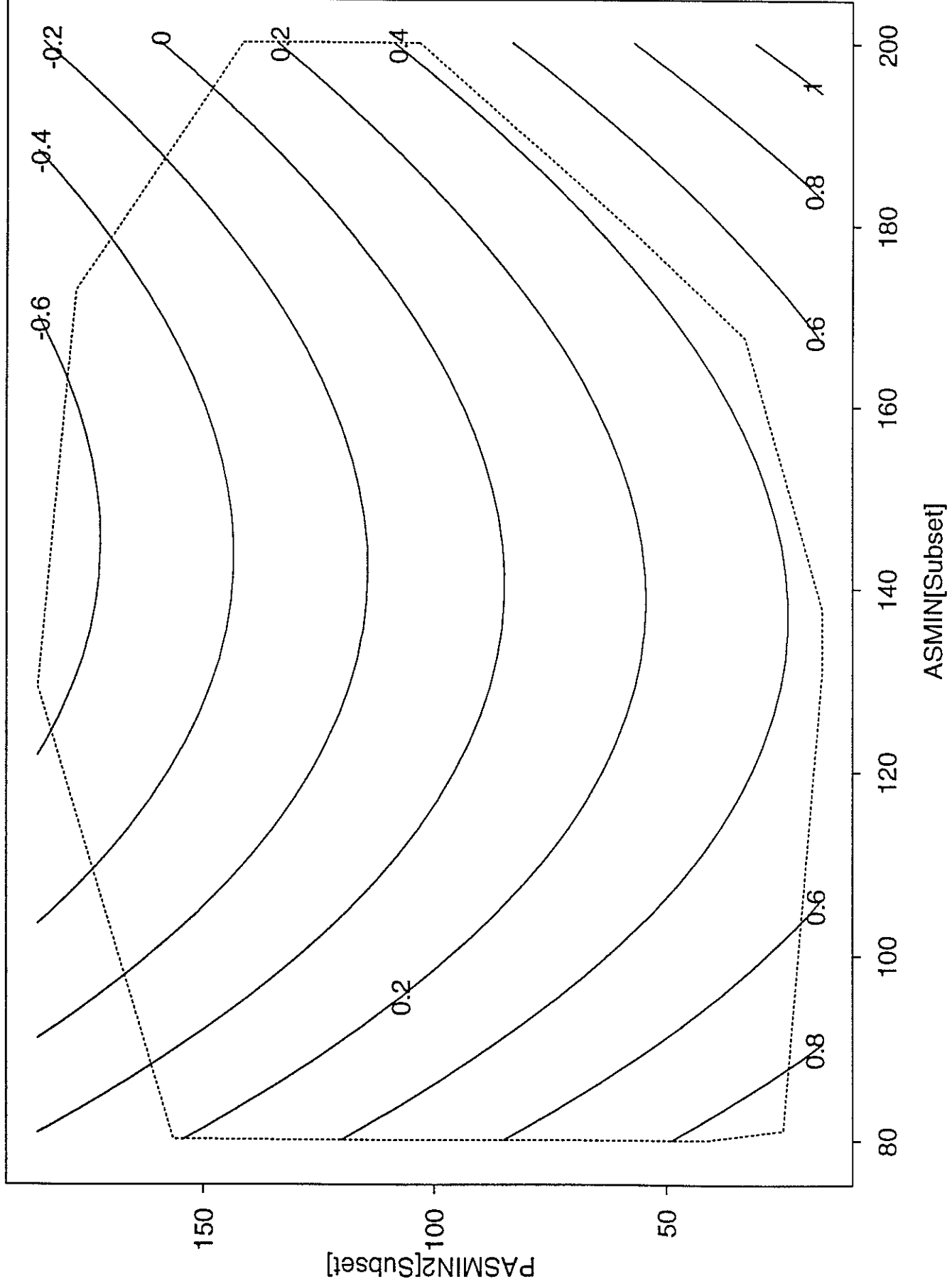


Figure 29: AB accidents - risk vs AADT

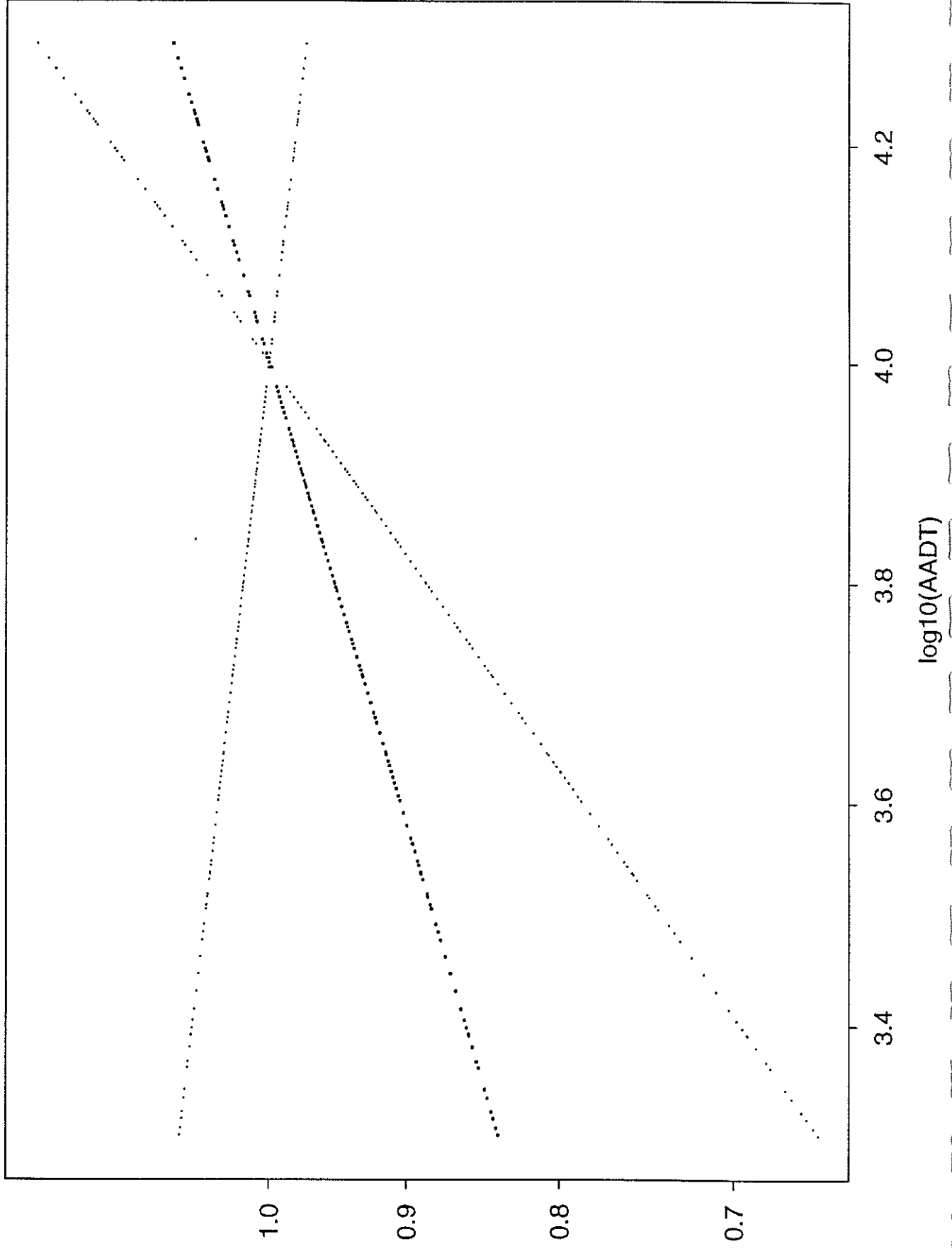




Figure 30: CD accidents - risk vs AADT

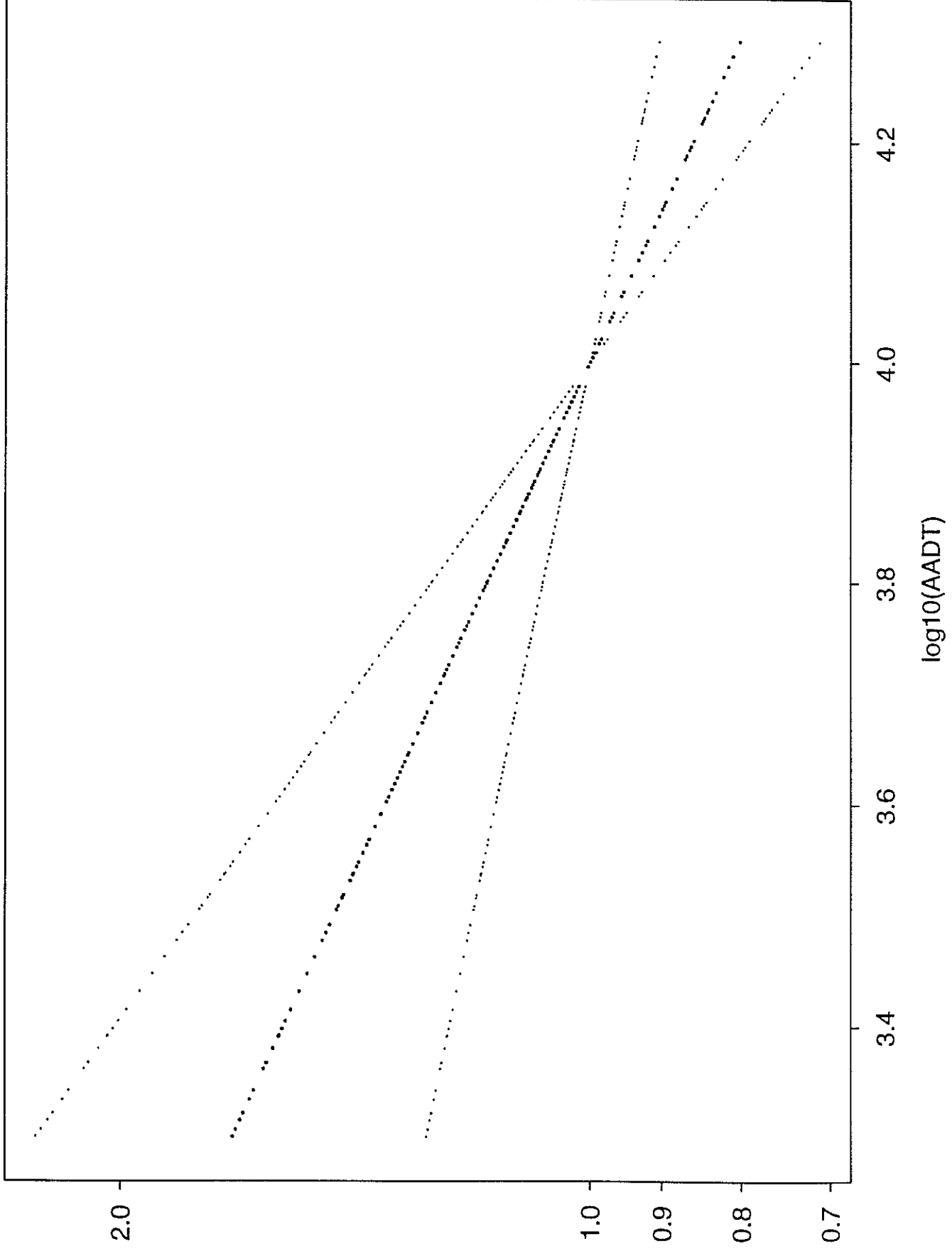


Figure 31: AB accidents - risk vs HAV

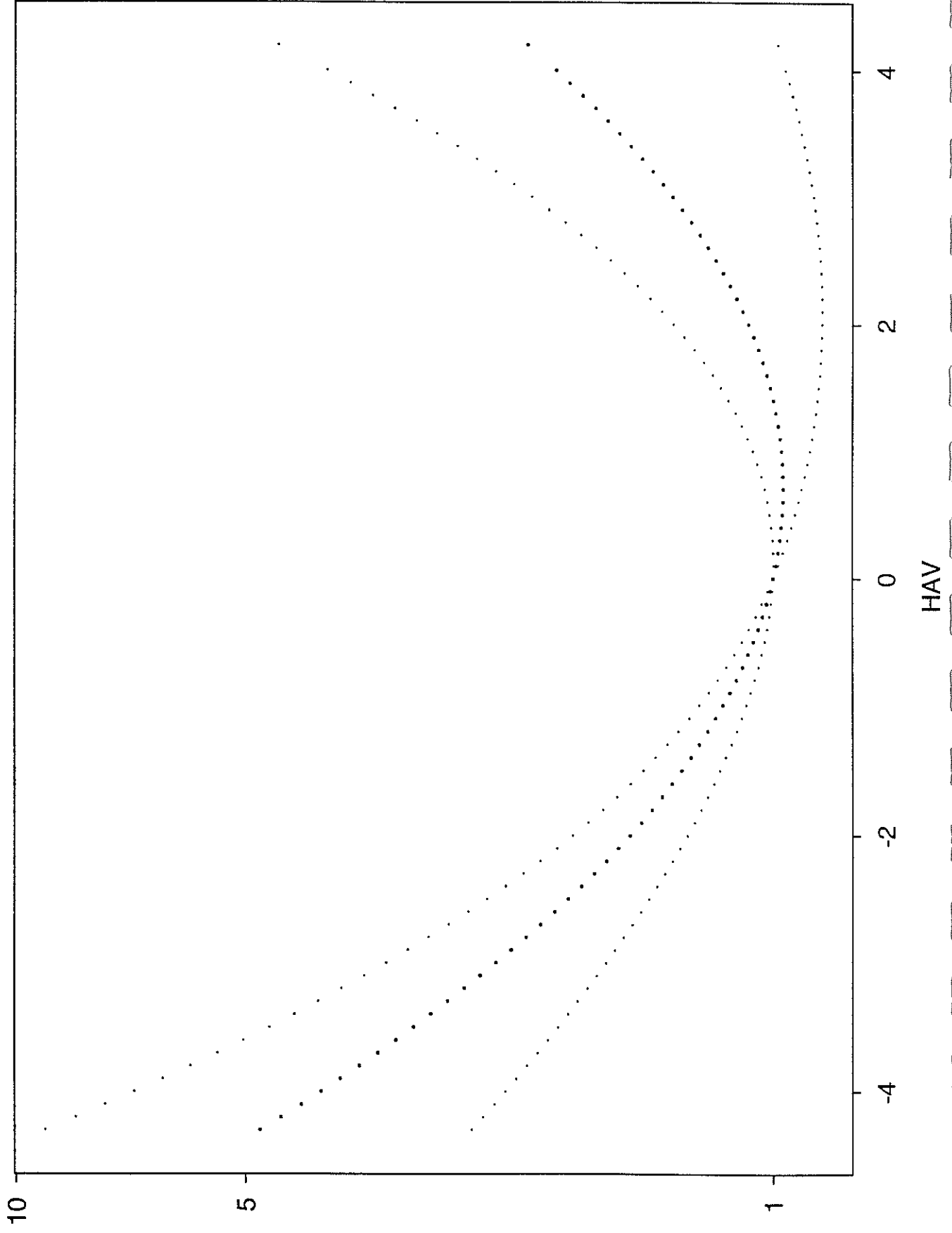


Figure 32: CD accidents - risk vs HAV

